

# POLITECNICO DI TORINO

Course of Master's degree in  
**AUTOMOTIVE ENGINEERING (INGEGNERIA DELL'AUTOVEICOLO)**

Thesis of Master's degree

## Co-casting of Al and Al-foam



Supervisor

Ing. Sara Ferraris

Prof. Paolo Matteis

Prof. Graziano Ubertalli

Candidate

Xing Weiyao

A.A. 2018-2019

## Abstract

In these years, the metal foam technology has been developed for a huge trend, therefore it is believed that the metal foam material will be next tremendous need in the market. Thanks to their peculiar properties (e.g. lightweight, energy absorbing ability) metal foams can be of interest in the realization of cars component and their use in substitution of hollow parts can be hypothesized to produce innovative functional metallic parts.

In this thesis, the Al foam and their use are focused in the casting process, as permanent functional cores. The topic is poorly explored in the scientific literature and in technological applications but can have important advantages such as weight reduction in comparison to dense components, the possibility to obtain «cavities» in casting objects, as well as impact energy, vibration absorption and acoustic insulation.

At first 3 different aluminum foams have been considered and characterized in the present thesis. They differ for density, pore shape and dimension. These foams have then been used as cores in casting experiments.

Foams and co-casted samples have been characterized by means of density measurement, optical microscopy (microstructure, pore, skin and walls dimensions, interfaces), Field Emission Scanning Electron Microscopy Equipped with Energy Dispersive Spectroscopy (FESEM-EDS) in order to investigate morphology and chemical composition, micro-hardness and compression tests to evaluate mechanical properties.

Finally a second set of foams with a more homogenous dense skin and different ceramic coatings have been characterized as possible improved cores for the future casting experiments.

# Chapter 1

## Closed cells Aluminum foams

### 1.1 Definition of Closed Cell Aluminum Foam

Aluminum foams can be defined as a cellular arrangement consisting of aluminum metal and some volume of gas-inserted pores. In closed cell foams (different from open cells ones) pores are separated by dense walls and are not interconnected. An example of closed cells aluminum foam is reported in *Figure 1*. Aluminum foam structure is durable and light, sturdier and stiffer with lower density and higher surface section to volume ratio compared to dense aluminum. Currently, this kind of new material is tremendous used in plenty various industry application.



*Figure 1: A closed cell foam sample[1]*

There are a few of Aluminum foams in the production, and closed cells foam is the usual one of them. Unlike other foams, closed cell Aluminum is much easier to control and to produce.

Earliest in 1960s, the concept of metal foam was created but until 1990s, it was actually used into mass production by Shinko wire company in Japan. 2 patents on sponge-like metal were issued to Benjamin Sosnik in 1948 and 1951 who applied mercury vapor to blow liquid aluminum.

The closed cells foam firstly is used for impact absorbent, like polymer foam used in bicycle helmet. Since the light and stiff features are most important keys for foam, it is used not only just for impact crash, but also as a lightweight structural material which retains fire-resistant and recycling potential. Due to its pores inside where air remains, its floatation is better than any other normal Aluminum.

## 1.2 Production Methods

Until now, there are many ways to produce cellular aluminum foam. Benjamin(2001) categorized the production methods simply as

- a) Production of foam from metal powder,
- b) Metal foam from melts using direct and indirect ways

in which these methods are classified on the basis of the state the metal is processed in.

### 1.2.1 Production of foam from metal powder

For mostly usage, Fraunhofer process is popularized. Foamed metals are produced by a powder metallurgical method developed and patented at Fraunhofer-Institute in Bremen.

The process can be briefly described as follows and schematized as in *Figure 2*.

1. Mix metal powder with the foaming agent
2. Compaction of metal powder mixing into a dense foamable precursor material
3. Making of precursor material by standard deformation techniques
4. Foaming of precursor material by heating it to its melting temperature

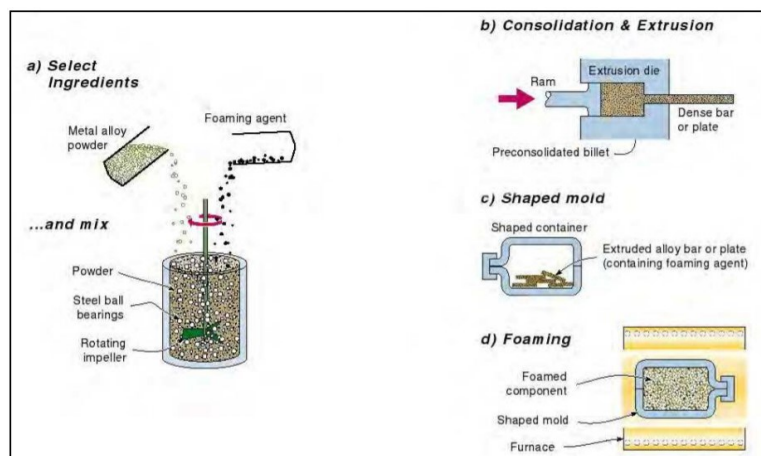


*Figure 2: Scheme of the production of metal foams from powders [2]*

For the powder method for foam production, the powder should be mixed with the foaming agent firstly, and then they are compacted together. Before it should be a semi-product with agents are distributed homogenously in the dense metal where no pores inside it, then translate it into the designed shape mold like sheets or rods. Finally, the mixed semi-product is heated above the melting temperature. The density can be controlled by adding different number of agents, and by this method, the porosity mostly is below 90%.

An example of the foam obtained by this method is reported in *Figure 3*.

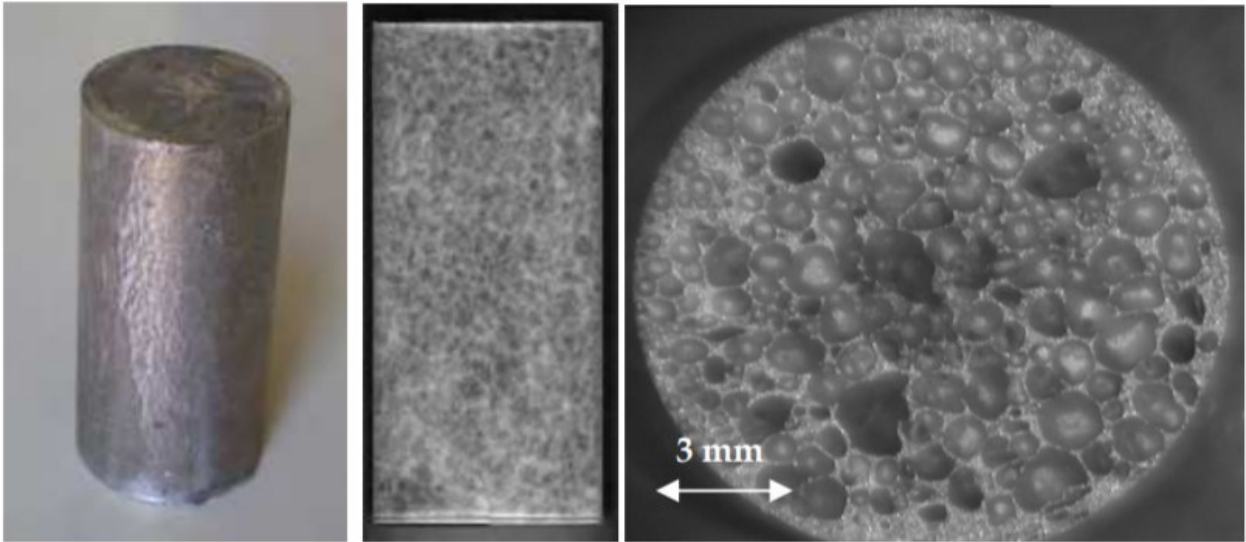


*Figure 3: (left) Images of a foam produced by the expansion of a melted PM precursor in a mold, (center) an X-ray radiograph of the foam structure and (right) a cross section of the foam showing the pore structure[2]*

### **1.2.2 Metal foam from melts using direct and indirect ways**

For this study, liquid metal foam processing is largely used so liquid state processing of metal is introduced in detail.

The closed cell foam needs air injection or blowing agent when produced.

Normally, when the gas is inserted into the molten metal or generated inside the metal, it is going to rise to the top surface since the large buoyancy force in the high-density molten liquid metal, but this can be avoided by changing the viscosity of liquid which can be achieved by adding some small ceramic powders like Silicon Carbide, Aluminum oxide or alloy to stabilize the liquid during the foaming process.

Two different ways achieved foaming are shown mainly: direct foaming and indirect foaming.

The direct foaming method starts from a specially prepared molten metal containing uniformly dispersed non-metallic particles to which gas bubbles are added to create foam. The gas is generated by external resource. According to the *Figure 4* of directing foaming, adding silicon carbide, aluminum oxide or magnesium oxide are used to increase the viscosity of the molten metal.

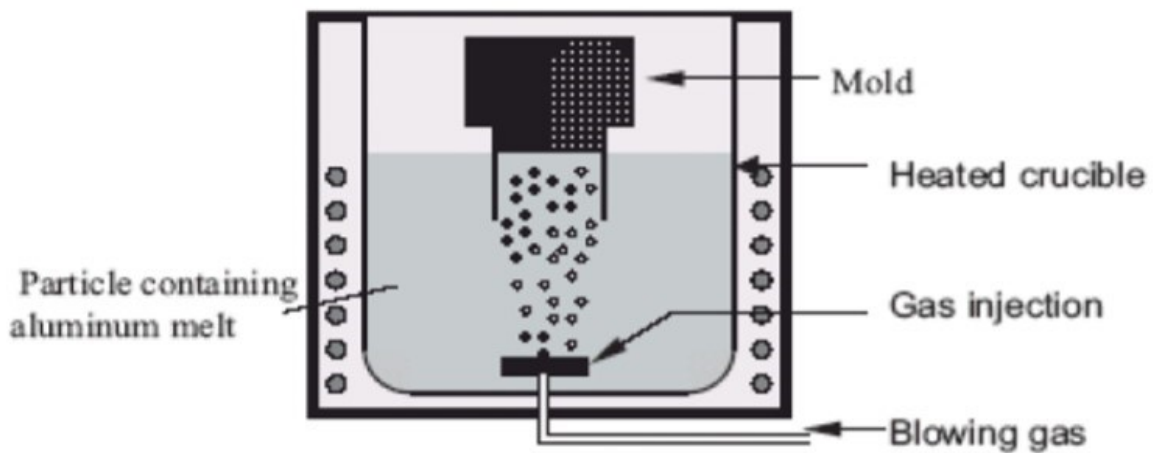


Figure 4: Simple explanation of direct foaming by Benjamin

The metal used for this is normally ordinary metal matrix composition which is also called-MMC[3] or A359 which is commercially used. First step is to prepare this kind of metal and second is to melt this MMC to liquid state. Like showed in the *Figure 5*, the gas-inserted is done by rotating a specially designed impeller or vibrating nozzles.

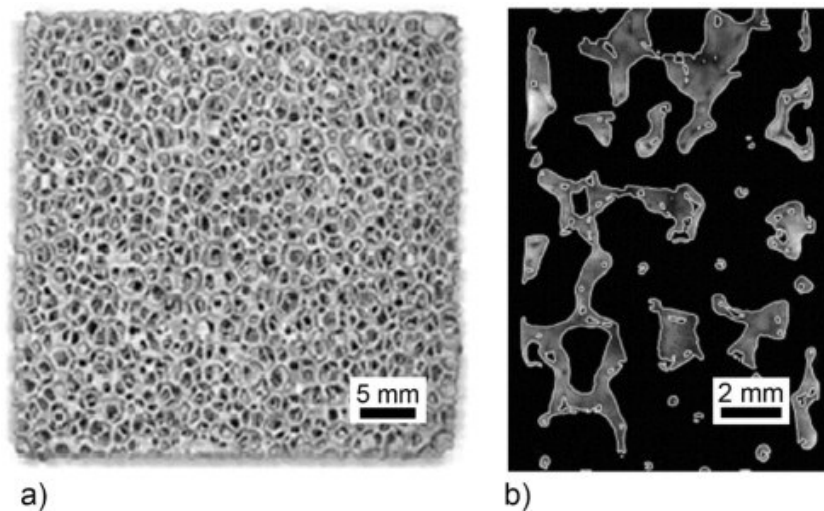


Figure 5: A MMC foam example [3]

As the process is on, the gas bubble will accumulate, and later inserted gas will push the previous gas-metal mixture to the top where this mixture turns into a fairly dry foam and liquid foam which has not been solidified drains out of the vessel. Now the foam is more or less stable thanks to the ceramics or alloy added before.

After this, the foam should be pulled out. Here a conveyor can be used on which solidification can be still occurred during transportation. It is must be attentional that applying suitable force and rotating speed to the conveyor while the metal foam should be cared enough since it is still half-solid half-liquid foam state and the pores generated are easily damaged or broken.

The final foam obtained could be as long as, as wide as wanted. Typically speaking, the thickness is approximately 10 cm. The porosity of aluminum foam which is made in this way range from 70% to 98%, also the density will last very different from 0.069 g/cm<sup>3</sup> to 0.54 g/cm<sup>3</sup>.

Average pore size can be as big as 75mm and down to minimum 3mm, also the thickness changes a big step among the pores. These characteristics parameters are tightly related to the injecting gas flow rate, the impeller rotating speed or nozzle vibration frequency and other parameters like temperature and pressure.

Moreover, the shearing force due to the conveyor belt also leads to a well-distributed cellular metal foam by pulling the semi-product in a vertical way instead of an oblique direction. The final foam can be kept as closed outer surface product or be cut into the shape required, but due to the high amount of ceramics used in the very first step, the machining process of this type of foamed metal will be quite difficult. To solve this problem, it is better not to add any stabilizing ceramics which is the main reason of hardness. In order to keep low viscosity not by adding ceramics, it should be kept a temperature closed to the melting temperature to make the metal and process stable, which caused a big industrial cost.

A schematization of the whole process is reported in *Figure 6*.

The advantage of this kind of processing method is that it can ensure the velocity of production and a continuous product will be obtained with any length wanted by the market request, and in the meanwhile the low-density property can be guaranteed. It is pronounced that the Canadian company Cymat can finish a production line with delivery of 1000 kg of foam within 1 hour in width up to 1.5m and thickness up to 15cm. So, this will be an effective way to produce a less expensive foam efficiently compared to others.

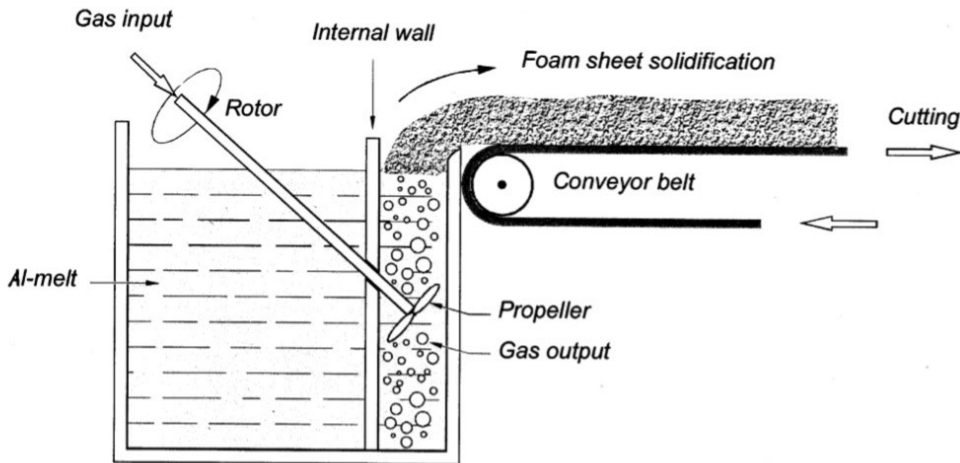


Figure 6: Direct foaming working principle

The indirect foaming method starts from a solid precursor which consists of a metallic matrix containing uniformly dispersed blowing agent particles, for Al-based alloys mostly titanium or zirconium hydride. The air-bubble is got by in-situ gas formation.

This sort of method can be explained by the *Figure 7* well knowingly.

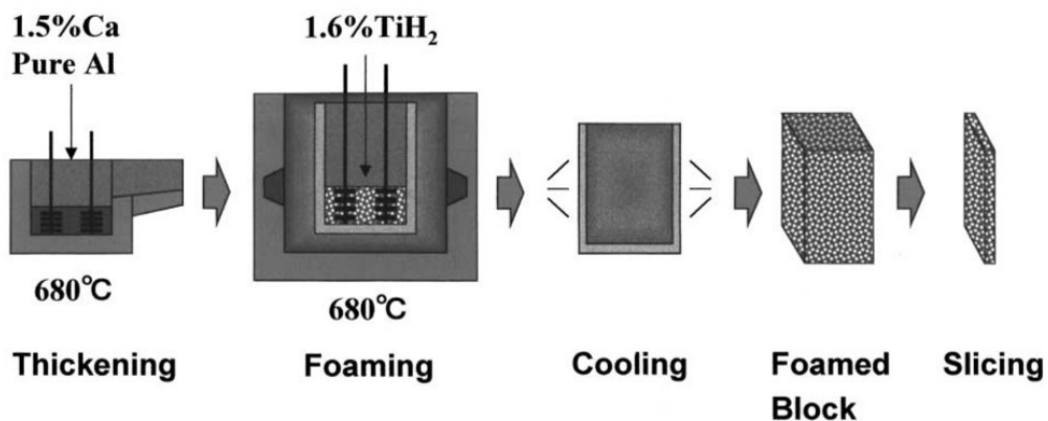


Figure 7: Indirect foaming working principle[4]

In this production process, the calcium is added into the vessel which contains molten aluminum at 680 degrees. Then the molten is stirred for a few minutes during which the viscosity increases thanks to the formation of calcium oxidation products like calcium oxide, calcium-aluminum oxide or maybe  $Al_4Ca$  that thicken the product as long as the processing. The trend lines of viscosity changing vs stirring time under different fractions of Calcium is showed in the *Figure 8* below.

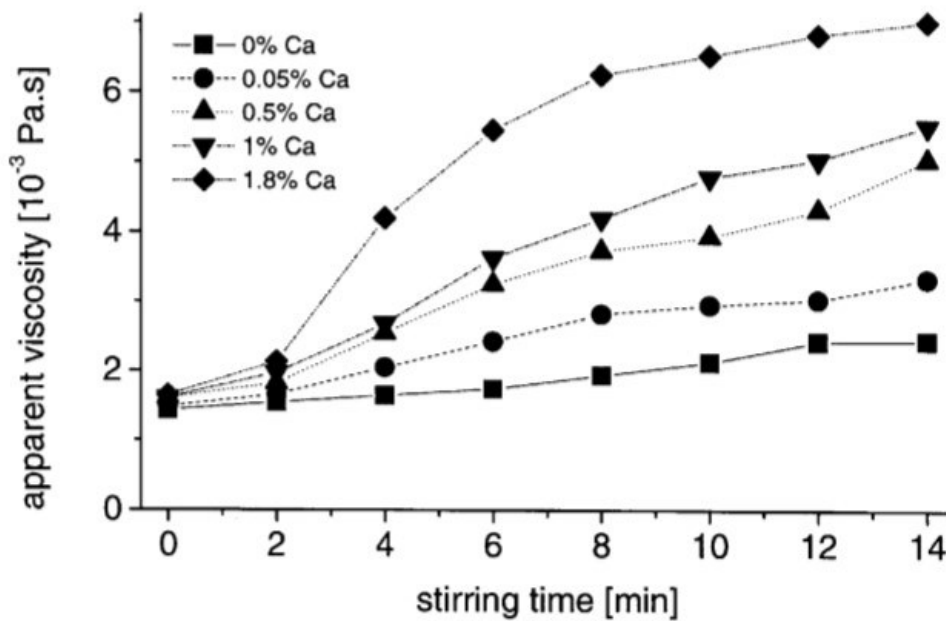


Figure 8: Viscosity vs stirring time under different wt% Calcium[4]

In the practical production, 1.5% weight of Calcium is added into the precursor and after desired viscosity is reached, titanium hydride  $TiH_2$  (Figure 9) is added which acts like a blowing agent. Since now, the process starts and gas bubbles are started generating. In a time while, the foam expands whole the vessel under a constant pressure. After cooling down below the melting temperature and solidification process finished, the liquid foam turns into a solid state and can be pulled out of the vessel by other progress. An example of the obtained foam is reported in Figure 10. In this way, the foam obtained is named as “Alporas” and this is a homogenous aluminum foam. In other studies, zirconium hydride is also recommended as a sort of blowing agent for producing gas bubbles. The temperature to add zirconium aluminum is a little different from the titanium hydride one with about 670 degrees.



Figure 9: Titanium Hydride  $TiH_2$  powder[5]

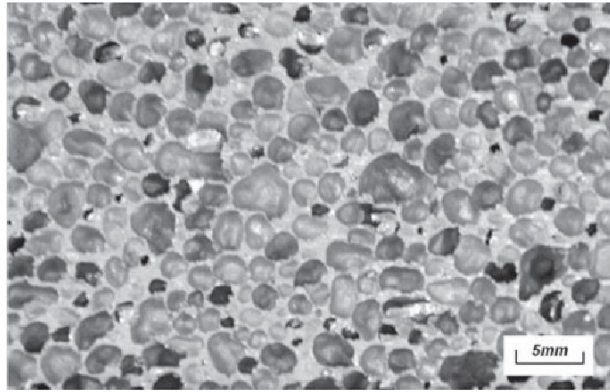


Figure 10: Macroscopic view of Alporas foam[6]

The typical shape of indirect foaming batch or vessel is 2050\*650\*450 mm by Shinko Wire company. The mass can be up to 160 kg while the density is as low as  $0.27 \text{ g/cm}^3$ . The density changes inside the foam block that is got, while in the top middle part it extends to the largest one. The machining like cutting process is easier than the foam under direct foaming method, since there is no adding ceramics during the process. But since this type of foam can only be produced batch by batch, it is not continuous as the direct method, the cost increases a lot. An example of a complex object obtained by this technique is reported in *Figure 11*.



Figure 11: A T-shape foam product[7]

Concluded comparison between direct and indirect foaming methods is reported in *Table 1*:

Direct foaming	Melt alloy		Indirect foaming	Prepare foamable precursor	
	Make alloy foamable			Remelt precursor	
	Create gas bubbles			Create foam	
	Collect foam			Solidify foam	
	Solidify foam				

Table 1: Conclusion of 2 methods for liquid metal foaming[4]

To a simple saying, direct foaming is to insert gas which is usually air into the molten and foamable metal, while indirect foaming is to add some bubble-created blowing agent into metal and wait for foam creating.

In Table 2 the main differences of product foams by 2 different methods are listed:

	<b>DIRECT FOAMING</b>	<b>INDIRECT FOAMING</b>
<b>NUMBER OF PORES</b>	Large range by inserting gas behavior	Large range by amount of blowing agent used
<b>AVERAGE SIZE</b>	3mm to 25mm	2mm to 10mm
<b>THICKNESS</b>	Average 10cm	5-200mm, standard 10mm
<b>INTERSECTIONS</b>	Well and long intersections	Nice intersections
<b>DEFECTS IN THE CELL-WALLS</b>	Worse since the bad process on the solidification of surface	Good behavior since foamed inside a vessel
<b>SIZE-PORE DISTRIBUTION</b>	Top coarctation bot poor	Homogenous
<b>SHAPE</b>	Regular shape with long length	Could be any shape depends on batch shape
<b>GEOMETRY OF PORE</b>	Irregular shape	Irregular shape

Table 2: Comparison of products between direct foaming and indirect foaming

### 1.3 Chemical Composition

Since Aluminum element is used to be foamed, Aluminum is the largest fraction in the above described metal foams. For the direct foaming method, the MMC is usually casting alloy AlSi<sub>10</sub>Mg (A359, an example of its microstructure is reported in *Figure 13*), or wrought alloys such as 1060 consisting of 99.6% Aluminum, 0.05% Copper, 0.35% max Iron, 0.03% max Magnesium, 0.25% max Silicon, 0.03% max Titanium, 0.05% max Vanadium and 0.05% max Zinc. And also wrought alloy 3003 or 6061 can be used largely. The typical compositions of the most used Al-alloys is reported in *Table 3*.

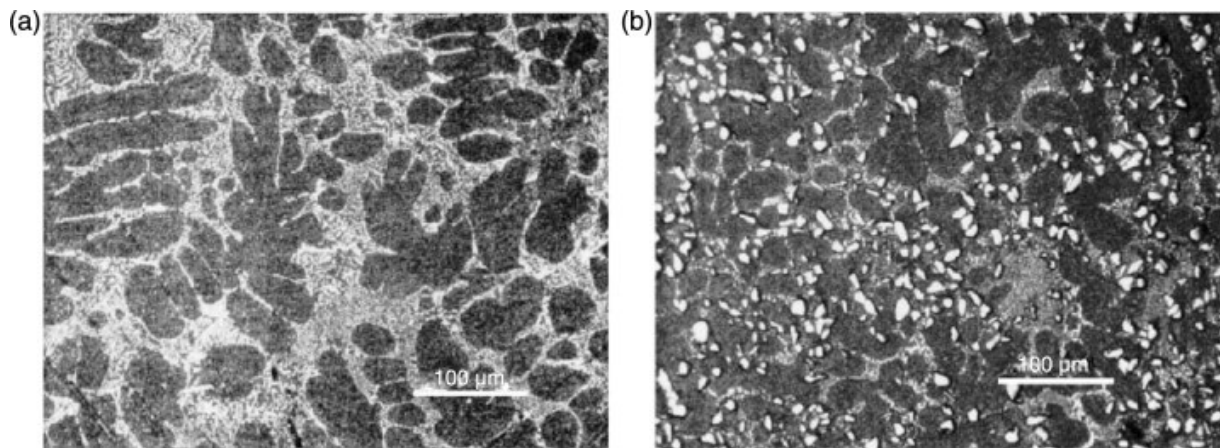


*Figure 12: Optical observation of metal A359[13]*

For the indirect foaming method, the metal used for foaming is more or less like the direct one, but since adding the different blowing agent into the liquid metal, different compositions will be obtained for the final product. Mostly element Titanium, Calcium and Magnesium can be found in the final foam product analyzed by FESEM. If zirconium hydride is used as blowing agent, also Zr and H will be checked in the last.

	<i>Alloy</i>	<i>A359</i>	<i>1060</i>	<i>3003</i>	<i>6061</i>
<i>Composition</i>	Aluminum	87.55-89.55%	99.6% min	96.8-99%	95.85-98.56%
	Copper	0.05% max	0.05% max	0.05-0.20%	0.15-0.4%
	Iron	0.55% max	0.35% max	0.7% max	0.7% max
	Manganese	0.45% max	0.03% max	1.0-1.5%	0.15% max
	Silicon	9.0-11.0%	0.25% max	0.6% max	0.4-0.81%
	Zinc	0.10% max	0.05% max	0.1% max	0.25% max
	Titanium	0.15% max	0.03% max	Residual	0.15% max

Magnesium	0.2-0.45%	0.03% max	0.15% max	0.8-1.2%
Vanadium		0.05% max		
Nickel	0.05% max	Residual 0.15% max	0.15% max	Residual 0.15% max
Lead	0.05% max			
Tin	0.05% max			

Table 3: Different composition of each aluminum alloy

To make the details of different sort of Aluminum foam from different company, the Aluminum foams are distinguished in 3 types: Cymat, Alulight and Alporas. For Cymat Aluminum foam, the Aluminum alloy A356 Stabilized Aluminum Foam(SAF) is used, while for Alulight foam, there are 2 materials can be used: AlSi12(EN AB-44300 or EN AB-44500) [8] and AlMg1Si0.6[9] . For the last Alporas, the composition is very simple: 97% Aluminum with 1.5% Ca and 1.5% TiH<sub>2</sub> [10].

The typical compositions of the above cited commercial aluminum foams are reported in Table 3

	Al alloy	Cymat	Alulight	Alporas	
		A356	AlSi12(Fe)(b)	Almg1Si0.6(6013-T4)	Al
Composition	Aluminum	92.061-92.547%	84.02-87.47%	94.8-97.8%	97%
	Copper	0.002-0.003%	0.18%	0.6-1.1%	
	Iron	0.086-0.108%	0.45-0.9%	0.5% max	
	Manganese	0.003-0.005%	0.55%	0.2-0.8%	
	Silicon	6.97-7.38%	10.5-13.5%	0.6-1.0%	
	Zinc	0.006-0.009%	0.3%	0.25 max	
	Titanium		0.15%	0.1% max	1.5%

Magnesium	0.381-0.425%	0.40%	0.8-1.2%
Vanadium		Residuals 0.15% max	Residuals 0.15% max
Nickel	0.004-0.007%		
Lead			
Tin	0.001-0.002%		
Calcium			

Table 4: Typical compositions of cited aluminum foams

## 1.4 Foam Properties

In most parts of properties, the foam by indirect foaming method acts better than the one by direct foaming, but also later is lower costly than the previous one.

The parameters that influence the structure-sensitive properties of cellular metals are(ordered by their importance):

- Intrinsic properties (open or closed cells)
- Relative density to original metal
- Type of cellular structure (open or closed cells)
- Irregularity in mass distribution
- The cell size and size distribution (including exceptional shapes)

The peculiar properties of foams, compared to dense metal are:

a) Lower density ( $0.069 \text{ g/cm}^3$  to  $0.54 \text{ g/cm}^3$ )

b) High ductility with lower cost.

Others basic mechanical properties are summarized in *Table 4*:

Property, symbol [units]	Cymat	Alulight	Alporas
Material	Al-SiC	Al	Al
Relative density, $\rho/\rho_0$	0.02–0.2	0.1–0.35	0.08–0.1
Structure	Closed cell	Closed cell	Closed cell
Young's modulus, $E$ [GPa]	0.02–2.0	1.7–12	0.4–1.0
Poisson's ratio, $\nu$	0.31–0.34	0.31–.34	0.31–0.34
Compressive strength, $\sigma_{pl}$ [MPa]	0.04–7.0	1.9–14.0	1.3–1.7
Tensile elastic limit, $\sigma_y$ [MPa]	0.04–7.0	2.0–20	1.6–1.8
Tensile strength, $\sigma_{UTS}$ [MPa]	0.05–8.5	2.2–30	1.6–1.9
Endurance limit, $\sigma_e^c$ [MPa]	0.02–3.6	0.95–13	0.9–1.0
Densification strain, $\epsilon_D$	0.6–0.9	0.4–0.8	0.7–0.82
Tensile ductility, $\epsilon_{UTS}$	0.01–0.02	0.002–0.04	0.01–0.06
Fracture toughness, $K_{IC}^c$ [MPa.m <sup>1/2</sup> ]	0.03–0.5	0.3–1.6	0.1–0.9
Thermal conductivity, $\lambda$ [W/m·K]	0.3–10	3.0–35	3.5–4.5
Resistivity, $R$ [ $10^{-8}\Omega\cdot\text{m}$ ]	90–3000	20–200	210–250

*Table 5: Basic properties of foam[11]*

The most important 2 differences between foam and dense metal are the energy absorption and sound absorption.

The foam has much better impact behavior than dense metal due to its special cellular structure and this is can be used in automotive or building constructions.

The average values of impact energy absorption per unit volume for ALPORAS foam during deformation of 55% under the static load:  $1.0 \text{ MJ/m}^3$ , and for the dynamic load is  $1.51 \text{ MJ/m}^3$ . As can be seen absorption is 50% higher for the dynamic loading compared with the static load. [11]

For any pore-like materials, sound will always be vanished when entering these materials due to the propagation principle of sound wave. It is also happened for aluminum foam. Foam is not like sound insulation sponge that kind of nice sound absorption, but it is still better than the normal dense metal and it can be worked in some cases like reducing the noise occurred between engine and chassis.

ALPORAS Aluminum foam is widely used for the sound absorption. It is found that the dissipation is lead mainly via viscous losses mechanism according to the cracked-array-model. There are 2 ways to improve this: hole drilling and compression[10]. It is because to involve the cavity resonator mechanism will decrease the cracks. But due to the experiments, the combinations of two methods doesn't lead to a significant increase of sound absorption.

Then density and sample thickness are to the sight. The absorption ability increases with decreasing of density. It is because the sound wave enters into the foam easier than before. Also, optimal thickness of absorber was experimentally estimated to be 10 mm with maximum absorption coefficient 60%. Lower or higher sample thickness do not increase the absorption according to the experiment fact.

## Chapter 2

### Aluminum foams in casting technologies

#### 2.1 Production methods to foams in casting technologies

The use of Aluminum foams in casting technology is actually a promising solution for the realization of permanent functional cores with interesting properties (e.g impact, vibration and sound absorption). However it is still poorly explored in the scientific literature. Some examples are reported in the following.

In different experiments, Al 99.5(ALPORAS) ,AlMgSi1(Alulight) and AlSi10(Cymat) are used for producing foam cores. Aluminum foam cores can be produced by heating in a furnace or by the injection into the mold. The method chosen depends on the designed shape of the final product. If the final shape is complex, it is better to choose injecting the metal foam into the mold. But in both different methods, the process is based on gas-released particles decomposition in semi-solid state of metal. The process procedure is listed in the *Figure 13*:

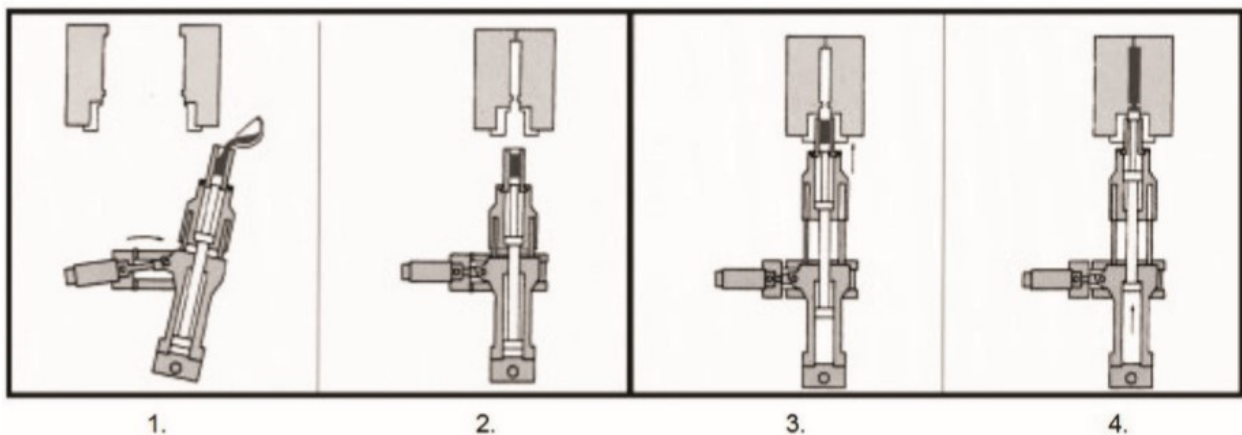


*Figure 13: Gas-released particles decomposition in semi-solid state of metal[11]*

The 1<sup>st</sup> step is to charge the cylinder by semi-solid metal which is heated by precursor. 2<sup>nd</sup> thing to do is to position the injecting unit and closing of the die. 3<sup>rd</sup> to do is dock the cylinder to the die. The 4<sup>th</sup> step which is also the last step is to inject the metal melt by moving the piston.

According to the study, two ways are shown to achieve the application of foam core in the casting: the first is that casting metal around a foam core, while the second is that casting a product with a foam core. The aim to obtain a porous foam core surrounded by a dense shell, as schematized in *Figure 14*.

The difference between these two ways is that in the first application, foam core replaces the traditional sand or solid core to produce the desired shape of product, while in the second application, the inside of metal from dense original metal to metal foam is changed.

Usually sand core or solid core for casting are used, while the cavity can be any designed shape : simple or complex.

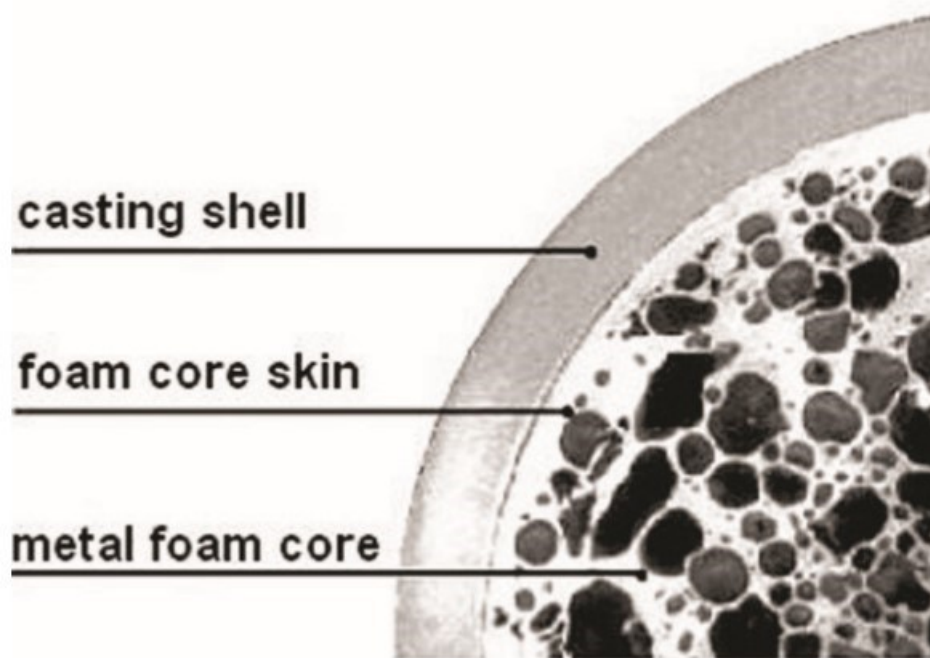


Figure 14: Cross-section of segment of casting product with the aluminum foam core[11]

In the present climate, replacing sand core or solid core with foam core is becoming more and more attractive. The reason and the advantage are that the foam core can be removed or stayed inside the product after casting process and it can contribute to the property of original casting product. If the foam core is maintained inside the product, it will increase the strength and stiffness of the product thanks to the special property of foam itself and without worrying its weight rising since the foam core has the lower density compared to the material used inside the cavity- which is usually normal dense metal like Aluminum or Magnesium. Other benefits are the growth of ability for energy-absorbent, sound cancellation and vibration damping of the final casting product. Also, the heat transfer insulation will improve the casting final product basic property.

If the foam is removed after final casting, the process is still better than the removing of sand core or solid core. In the traditional process, the sand core will leave some uncleanable sand inside the casting product while the solid core will damage the casting product when they are removed in the last. But foam core doesn't have this problem, since the foam core is coated by ceramics like zirconia or alumina for specific application, when it is removed there will be nothing left and it will not damage the casting product thanks to the coating process since the coating surface is always as smooth as possible. Recent research also finds that some penetration and infiltration occur at the gate area of the cavity because of the heat transfer from the molten metal to the foam core, and coating of foam core avoids this problem as well as possible. Moreover Al foam can be easily recycled avoiding the need of sand treatment.

On the other hand, until now, some companies have started the step on the production with foam core study. For instance, LKR Ranshofen, Austria has made a prototype of engine mounting bracket for BMW automotive company (Figure 15). The prototype is made of

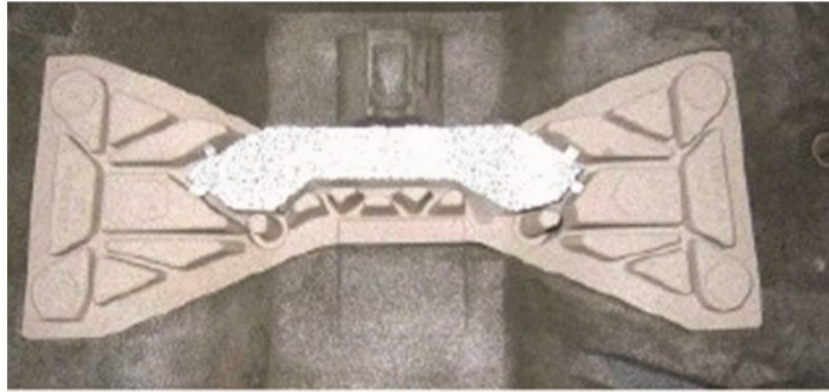
foam core and a cast shell with 25 cm long and can support the whole weight of the automobile engine. The working principle is that the foam core mounting bracket absorbs the mechanical vibrations from the engine and converts it into heat -which is released to the atmosphere in the last- by friction inside the material. Another goodness is the safety requirement is enhanced since the stiffness of foam core is higher than the dense metal.



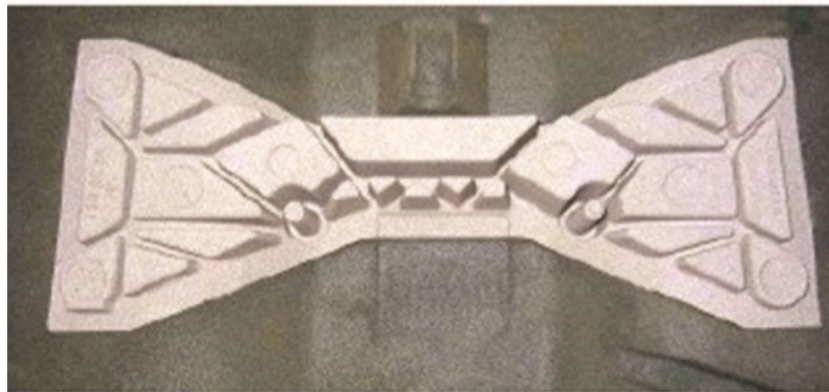
*Figure 15: Prototype of a BMW engine mounting bracket[11]*

In the PhD dissertation of Balazs Kovacs[11] for the purpose of an experiment one car crossmember was produced containing a permanent casting core of aluminum foam. The aim of this experiment was to demonstrate that the usage of the aluminum foam core for the casting crossmember provides better sound attenuation with superior mechanical properties. Earlier type of crossmember was produced with ribs. According to the dimensions of the previous model a new crossmember casting mold with aluminum foam core was designed.

The casting mold is made of silica casting sand with a furan resin. The mold cavity for the shell around the core is 5 mm wide for the reason of simpler pouring and flowing of molten metal. The weight of the casting product with metal foam core is about 2 kg and it is more or less 30% heavier than the previous one without the core[11]. The increase of dynamic stiffness, which occurs on the basis of the weight increase, must also be observed.



a)



b)

Figure 16: Comparison of two different molds: a) casting mold with a permanent foam core; b) casting mold with rib reinforcements on the casting products[11]

## 2.2 Main criticism problems

### 2.2.1 Main criticism of casting process with foam core

The obtainment of a casting product with a foam core presents, several criticisms occurred:

#### a) The local melting of the core surface

When the melt flows and fills the mold, the penetration and infiltration will happen at the gate of the cavity since the molten metal transfers the heat to the core and further damages the surface.

Strategy to overcome:

Applying a coating process around the foam core surface by ceramics or alloy.

#### b) Local surface friction damage is appeared

Without the coating, the foam core has the possibility to damage the casting because the mechanical friction between the core surface and casting surface. It happens even the coating layer is not enough thick.

Strategy to overcome:

To make the coating of the core as thick as possible. Experimentally it shows that with a thickness of over 350  $\mu\text{m}$ , the damage will be vanished, and foam damage is defined by global compression strength.

#### c) Deformation of the foam core

The deformation can happen during the high temperature pouring of the shell around the core since the heat transfer from molten metal to the core acts along the casting process.

Strategy to overcome:

By controlling the solidification and pressure during the casting will avoid the deformation problem. The core will be protected from damage and deformation if the solidification of molten metal occurs at the contact between the core and melts and the solidification of casting shell begins at the maximum pressure of the molten metal.

#### d) Die casting problem

To produce the core by die casting (an example is reported in *Figure 17*), there are main two phases to do. The first is to fill the die with melts, the second is to apply very high dwell pressure to balance the shrinkage. The problem happens at the first step, since we need to fill the die as fast as possible, but the high speed makes a high peak pressure at the end of phase which can damage the foam core.

Strategy to overcome:

To avoid the peak pressure, we use a real-time controlling die casting machine to control the casting velocity and the casting pressure at each step of the casting process.

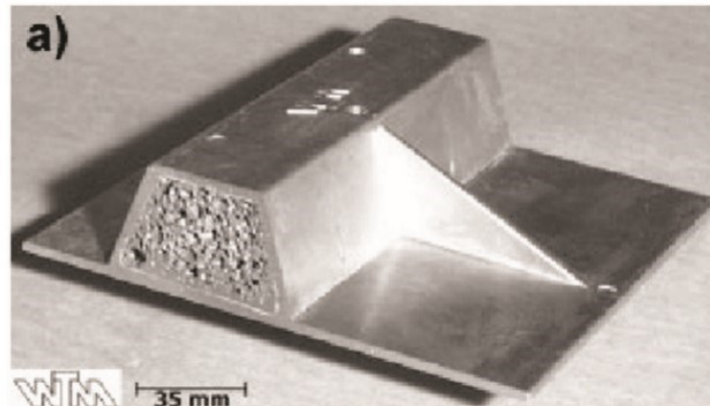


Figure 17: Test sample with Aluminum foam by die casting[11]

In the obtainment of a casting with foam core, another criticism is the attachment the core to the cavity. A suitable attachment system is applied. It must keep the position of the core during the casting process and remain the desired distance between the core and inner surface of cavity. The special distance will decide the thickness of casting shell. One possible solution is to design a long shaped spacer placed at the corner of the core. The spacer should be long enough so that the transferring force from core to cavity will be even and uniform. The location and arrangement of the spacer are also important since they determine the flow activity of the melt around the core. If they are good, the flow of melt will be smooth without attenuation or barriers.

### 2.2.2 Main criticisms related to the final casting shell-foam core component

Another issue is related to the bonding between the dense shell and foam core

Frequently no bonding between the core and the shell can be observed. The possible answer according to Branko Bauer is that the continuous aluminum oxide layer, present on the surface of the foam core, prevents the core surface from reaction with the molten metal. In the practical using, we need there are some bindings to improve the property of the whole product including foam core and shell. To solve this, we have two possible solutions:

a) Mechanical bonding by using flow of liquid metal into the outer foam structure supported by intentional weakening of the surface skin. But in this way, there is a drawback: it will increase the weight of casting and the bonding only occurs locally which is difficult to control.

b) Metallurgical bonding by coating the cores. With a suitable metallic coating a metallurgical bonding can be achieved, but the drawback is this kind of bonding can not meet the requirements of components properties since if coatings has bonded with foam core, it will affect the foam core characteristics.

## Chapter 3

### Materials and Methods

#### 3.1 Samples

Three different aluminum foams (Cymat type) were considered as possible cores for aluminum casting(*Figure 18*). The difference among these foams is the average density.

The foams were characterized as such and after insertion in aluminum casting.

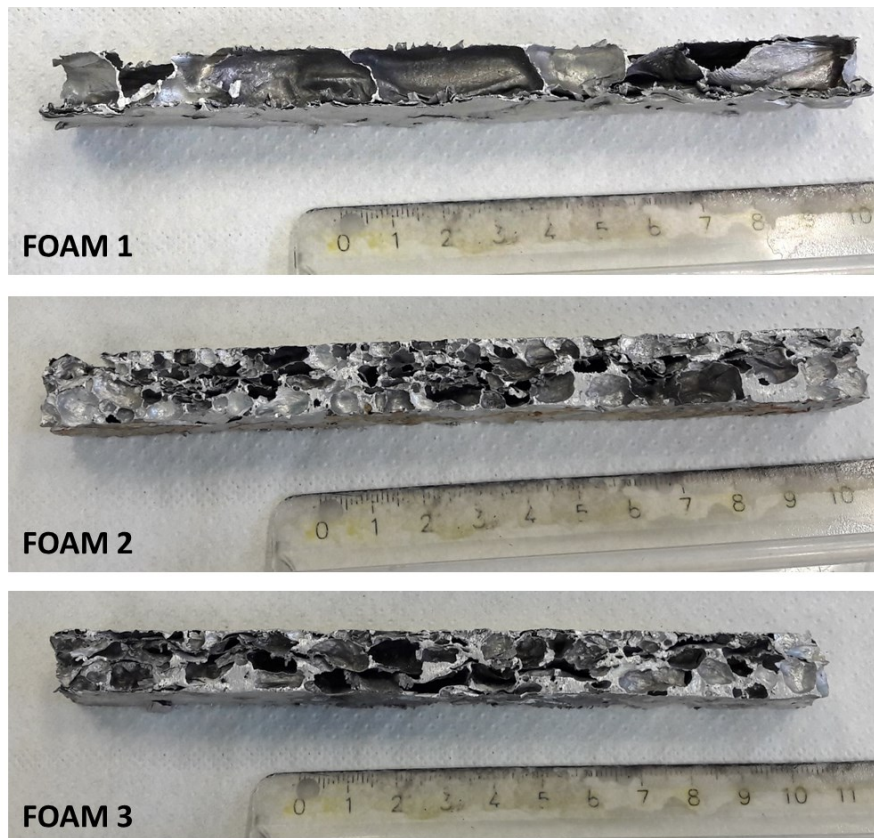


*Figure 18: 3 different Aluminum foams(Cymat type), used in the experimental work.*

The surface of the foams presents a thin dense skin which is not homogenous, but presents some cracks. The pore dimension in Foam 1 is clearly bigger than that in Foam 2 and 3. The quantitative results will be uploaded in chapter 4.

The above described foams have been used as cores in casting experiments, as shown in *Figure 19*.

**FOAM 1**



**FOAM 3**



**FOAM 2**



*Figure 19: Insertion of foam cores in casting experiments*

Each type aluminum casting sample has 4 different zones: 2 dense metal zone and 2 zones with foam inside. The foam material used in the experiment is Cymat aluminum foam. The samples figures are *Figure 20, 21 and 22*.

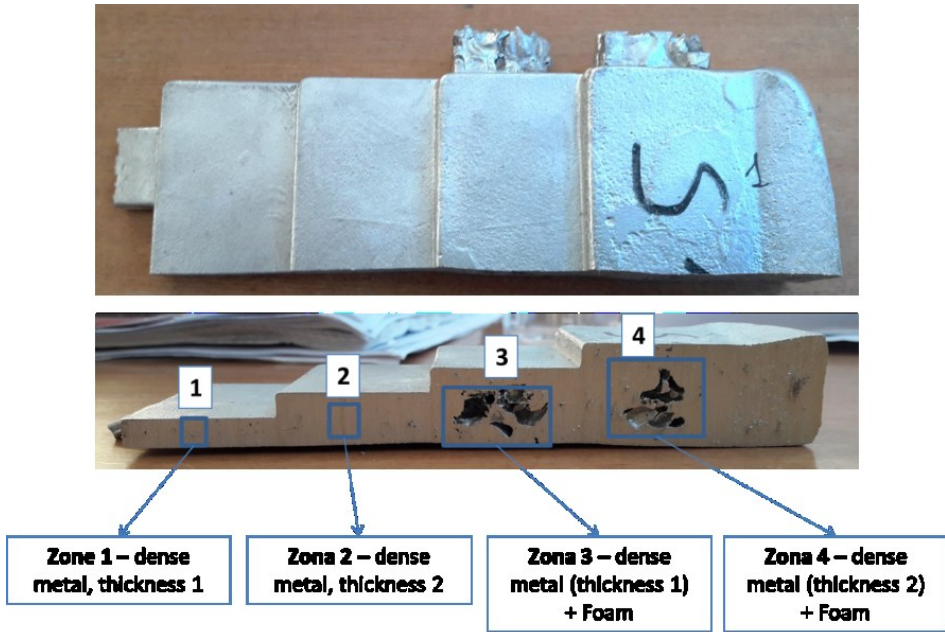


Figure 20: Foam in casting S1

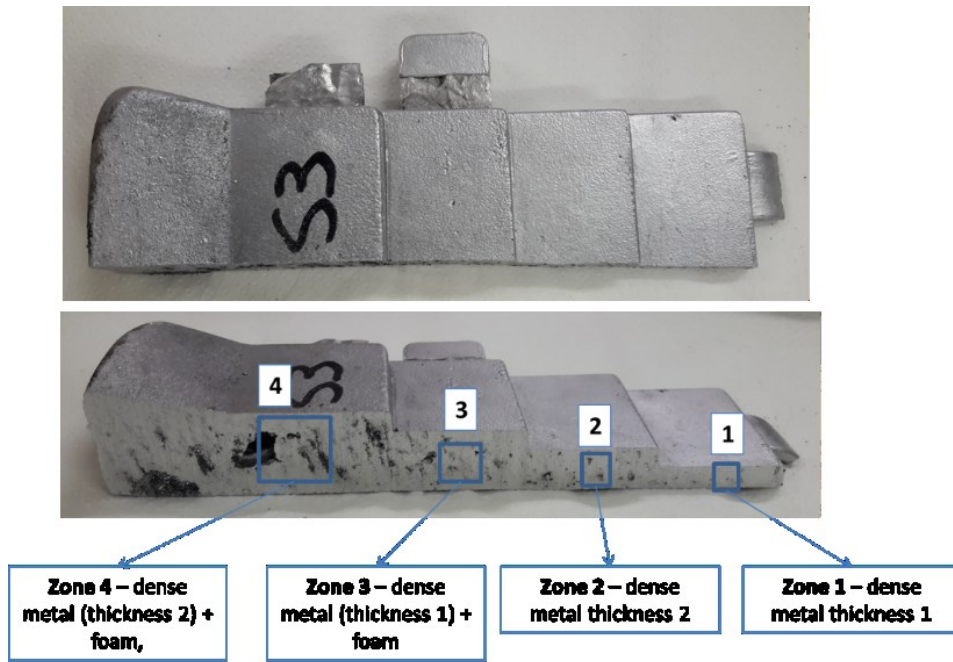


Figure 21: Foam in casting S3

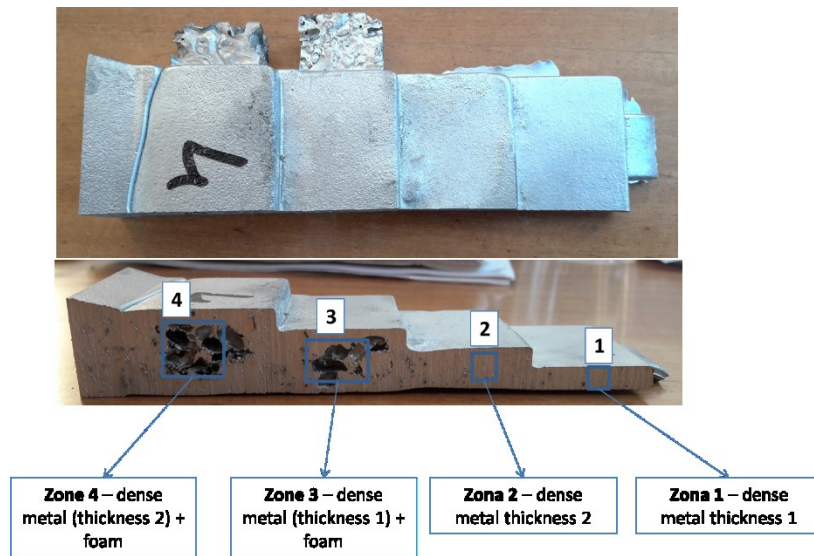


Figure 22: Foam in casting S4

Another set of samples analyzed in the thesis is constituted by three foam inserts with different coatings to be used as possible cores in casting experiments. They are foam core (IFAM-FOAMINAL type, *Figure 23*) without coating, foam core with zirconia coating and foam core with alumina coating from left to right respectively.



Figure 23: 3 different coated foam cores

From the *Figure 23*, it is obviously that the uncoated foam is showing the metal color, while the other 2 coated foams are much brighter. There is a little blue color on the alumina coating which is analyzed later to be painting mistake during transportation. The experiments done have avoided this zone.

### 3.2 Samples cutting

Small samples (few centimeters each) have been obtained from foams panes and cast products by means of an automatic cutting machine equipped with an alumina blade[*Figure 24,Figure 25*].

In the experiments, the cutting machine is used in foams, foam in casting and uncoated foams. Moreover, the foams in casting have been crosscut in the last to research the residual porosity which is used to compare the porosity of foams in casting in order to study how the foam affects the solidification.



*Figure 24: ATA Cutting machine*

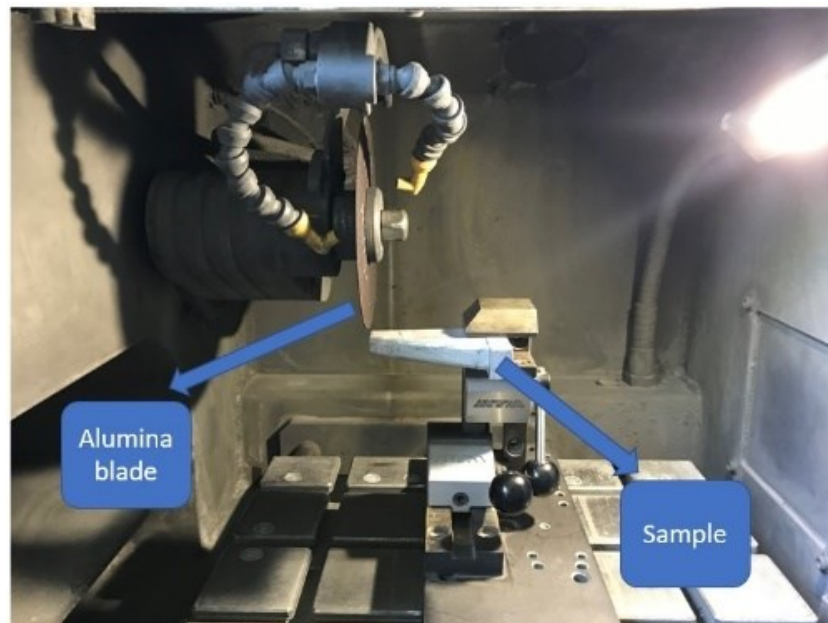


*Figure 25: Details inside the cutting machine*

As far as cast objects are concerned a sample representative for each zone has been obtained(as previously indicated in *Figures 20-22*):

- Dense zone 1 with thickness 1
- Dense zone 2 with thickness 2

- Zone 3 with foam insert thickness 1
- Zone 4 with foam insert thickness 2

Firstly, the sample is cut more or less 2 cm<sup>3</sup> each in order to be mounted in the resin to be polished. Then for each sample, the zones 3 and 4 have been crosscut in the last as told before.

### 3.3 Resin mounting and surface polishing

In order to prepare sections for metallographic observations samples have been mounted in resin (two examples are shown in *Figure 26, 27*) 1S1, 2S1, 3S1, 4S1, 2S4, 4S4, foam1, foam2, foam3, uncoated foam, alumina coated foam and zirconia coated foam. Since foams are porous a first amount of resin has been inserted in the die then the sample has been introduced to allow pore filling with resin and the whole sample was covered with resin and let harden overnight.

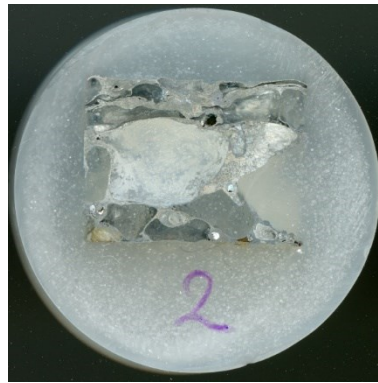


*Figure 26: A scan example figure about a sample foam mounted in white resin*



*Figure 27: A scan example figure about a sample foam mounted in black resin*

Samples have been polished with SiC abrasive papers (60-2500 grit) on a polishing machine with water flow. Low number paper means more abrasive of the paper. From number 60 to 120, the abrasive paper is used to remove the trace cycles that were left in cutting process and to expose the metal which is sunk in the resin. Then the higher number abrasive papers are used to polish the metal surface.

The final polishing was performed with Alumina suspension (0.05  $\mu\text{m}$  particle size) diluted in water without lubricant. This step needs a special plate like a towel. It is used to protect the aluminum from cracks and stretches. But sometimes alumina is a little abrasive and the sample cannot achieve a mirror polishing. In this case, the diamond suspension with different particle size from 0.05-0.01 $\mu\text{m}$  can be applied which will get a better result.

At the end of the polishing process samples were washed in distilled water in an ultrasonic bath and dried with compressed air. The resin sample is covered by a wiper paper and stored inside a dried plastic bag which has the name label on the surface of bag.

### 3.4 Optical microscopy

Optical microscopy(*Figure 28, 29*) has been used for the measurements of foam dense skin and pore walls thickness, measurements of pore dimensions, investigation of foams and casting objects microstructure, foam-dense aluminum interface and porosity evaluation.



*Figure 28: Optical microscope machine item ID: Reichert Jung MEF3*

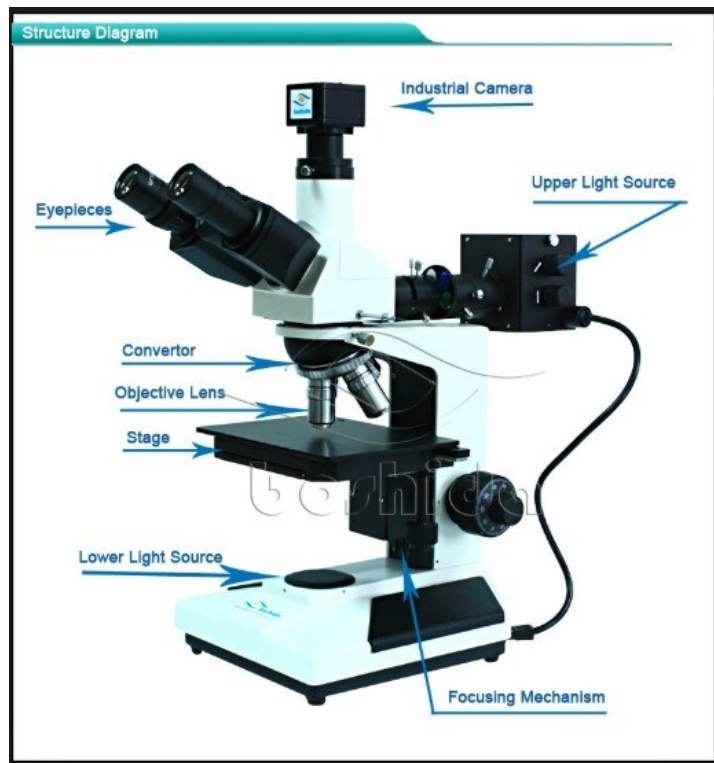
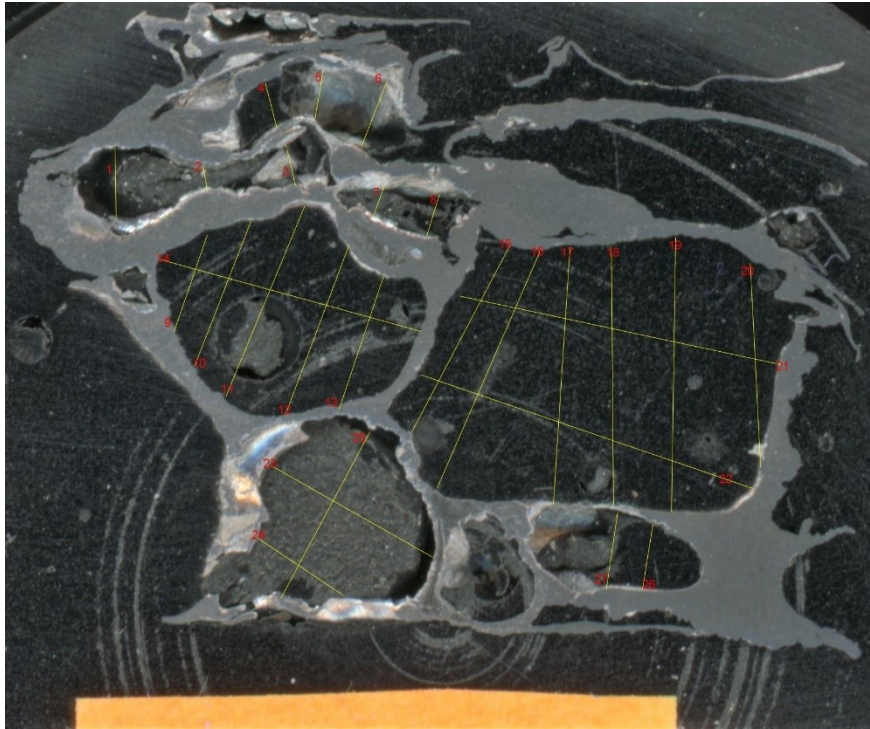


Figure 29: Optical microscope[12]

The sample is put on the stage and the light resource is turned until image is caught on the screen. Changing different objective lens can achieve different magnification of image. Using the focusing roll to get a clear picture on the screen, snap the image and save it.

### 3.4.1 Measurement of pore dimensions, skin and wall thickness

The pore dimensions measurements and skin/wall thickness measurements are totally different. The pore dimensions need the image that is obtained under macroscopy or a scanner. The resin sample name is labeled by a stick, since the dimension of stick is known, so it can be measured the length when the sample is scanned.



*Figure 30: An example of pore dimensions measurements*

The lengths obtained with Image-J software, and then use the measurement tools in Image-J, it is simply to get the values of dimensions.

An example of the measuring route for pore dimension is reported in *Figure 30*.

Meanwhile, for the skin/wall thickness, it is needed the microscopy with coefficient 0.8 and magnification of 20 (2X objective lens \* 10X eyepiece lens). With the help of scale tool in Image-J, it is easily to get the unit length of each figure snapped. The use the measurement tool in Image-J, the values of skin/wall thickness can be obtained.

Examples of the measuring routes for skin and pore wall thickness are reported in *Figures 31 and 32* respectively.

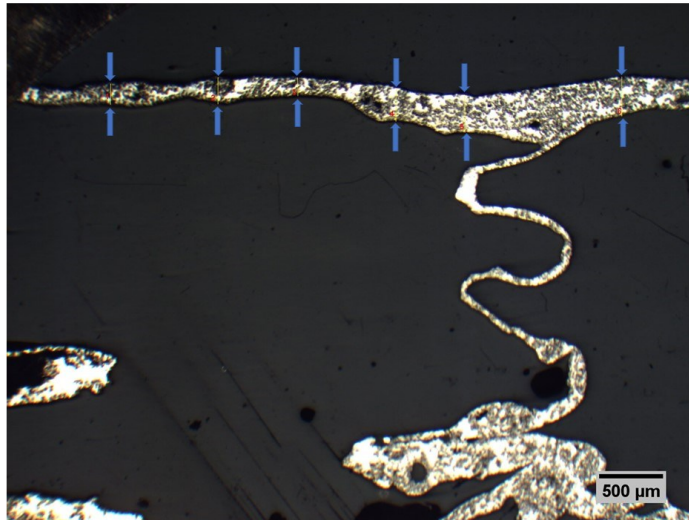


*Figure 31: An example of skin thickness measurements. The blue arrows are added to indicate measurements positions.*

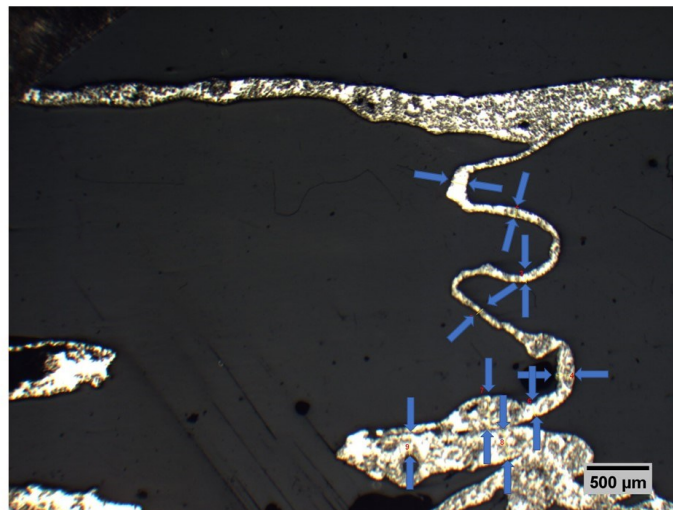


*Figure 32: An example of wall thickness measurements. The blue arrows are added to indicate measurements positions.*

Inside the figure, the blue arrows indicate the positions of measurements. Like before shown in pore dimension, the measurement tool in Image-J can easily export a excel file with values measured.

Also, the coating thickness is very important in the foam casting technology. It can be achieved by same magnification and coefficient. The skin thickness measurements standard is to measure from the outer surface to the nearest pore surface.

An example of measurements on IFAM foams is reported in *Figure 33*.

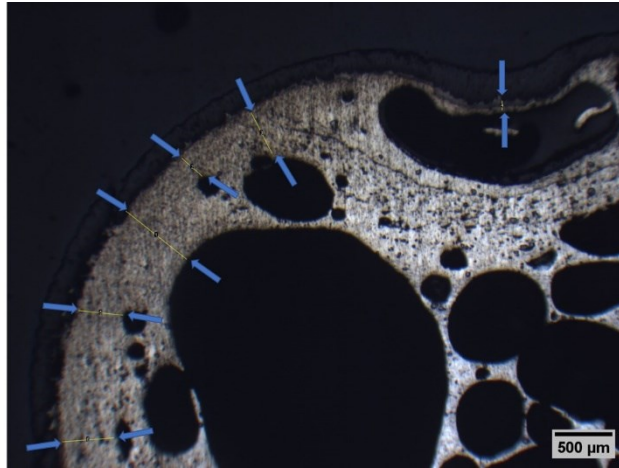


Figure 33: An example of coating foam skin thickness measurements

### 3.4.2 SDAS measurements

Secondary Dendrite Arm Spacing (SDAS) is the distance between the secondary dendrites arms.

Secondary dendrite arm spacing (SDAS) is a microstructural analysis which can be quantitatively related with cooling rates. It was measured by locating at least five consecutive secondary dendrite arms and measuring the spacing between them. The length of the line (black line showed in *Figure 34*) across the secondary dendrite arms (red lines shows in *Figure 34*) was determined by using the image pixels to micron conversion within the software Image-J. Once the length of the line and the number of dendrites the line crossed were determined, the SDAS value,  $\lambda_2$ , was calculated using Equation, where L is the length of the line and n is the number of intercepted dendrites.

$$\lambda_2 = \frac{L}{(n - 1)}$$

In this experiment, SDAS measurements are used to calculated inside the foams in casting, especially in zones 3 and 4 since SDAS values can indicate the relationship with cooling rate directly which is also the rate of solidification. The normal principle according to the literature[14], when the thickness of the dense metal decreases, the cooling rate will be slow and the SDAS values will be small. And in the other dense metal zones, the solidification is mainly working inside dense metal.

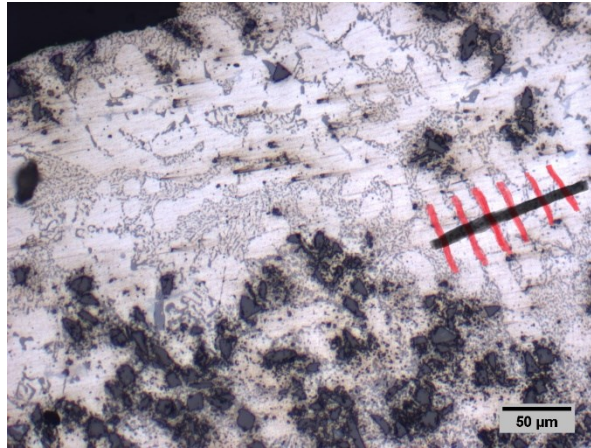


*Figure 34: An example of SDAS measurement with 6 consecutive dendrite arms*

In order to estimate the SDAS in casting objects 8-12 images at 200X magnification were collected.

### **3.5 estimation of porosity**

In order to estimate the global porosity of the samples macro-images collected by means of a scanner have been used. Like shown in *Figure 35*:

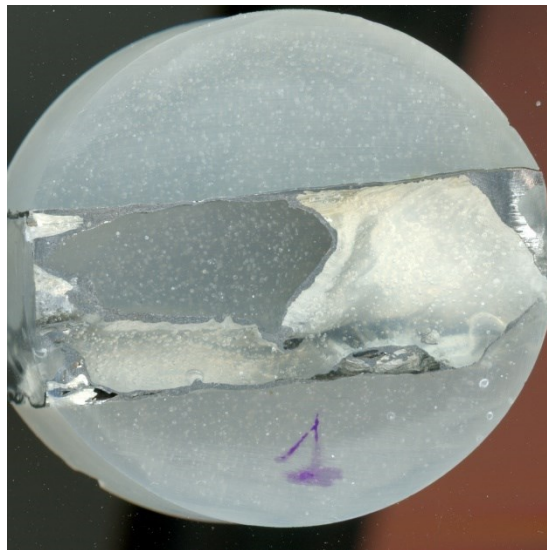


*Figure 35: Prepare a scan macroscopic image of sample*

The Gimp software is used to cut the image with smart scissors(*Figure 36*):

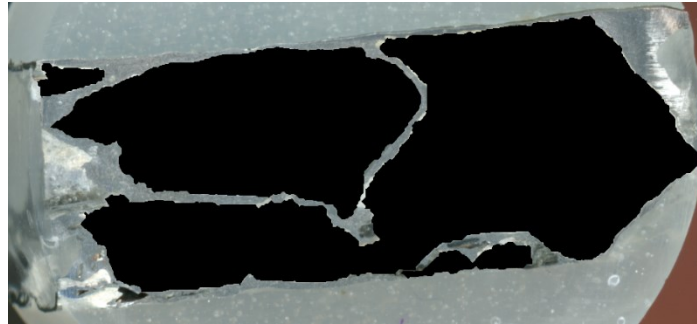


Figure 36: Image obtained from Gimp software

Then back to Image-J software, binary image is made(Figure 37):

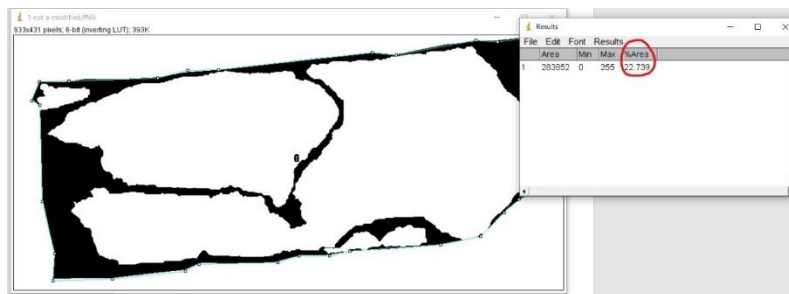


Figure 37: Binary image obtained by Image-J and anit-void fraction measurement

To note that, when binary image is made, the measurement tool in Image-J will calculate the binary area percentage, then it should use 100 minus this value to get the real porosity. The calculated values in the last will be 1 decimal number in percentage.

### 3.6 Field Emission Scanning Electron Microscopy equipped with Energy Dispersive Spectroscopy(FESEM-EDS)



Figure 38: SEM machine: Zeiss merlin

An electron beam is focused into a small probe and is across the surface of a specimen in scanning electron microscopy (SEM). Several interactions in the sample that result in the emission of electrons or photons occur while the electrons penetrate the surface. These emitted signals can be collected with the appropriate detector to yield valuable information about the material. The first result of observation in the SEM is the topography of the sample or named 'Top view' of the sample. The resolution is determined by beam diameter. *Figure 38 and 39* reports the FESEM used and an example of functioning scheme, respectively.

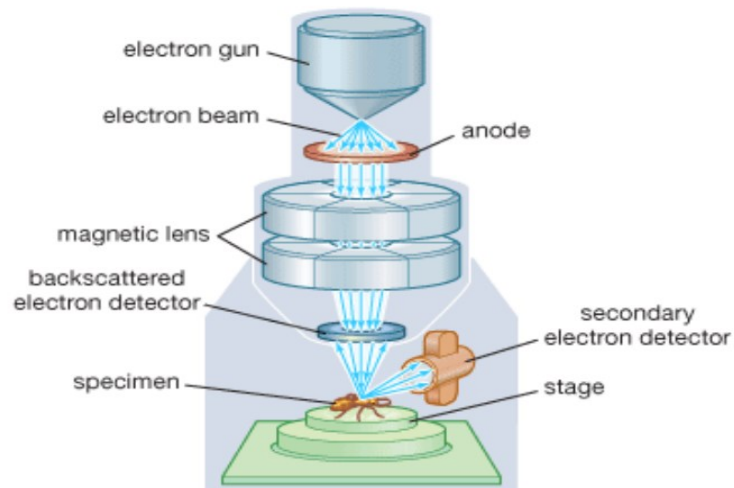


Figure 39: Normal SEM scheme

FESEM-EDS analysis have been performed in order to have indication on:

- The chemical composition of the foam used
- The chemical composition of the coatings on the tested foams
- The morphology of foams and coatings at high magnification

The Zeiss Merlin SEM machine has got the functions of obtaining EDS and SEM analyzes at the same time due to X-ray spectrometer. After achieving electron images with SEM, it is also possible to have element mapping with point analysis and area analysis.

When the desired electron image is obtained for a point or an area, it is possible to have the chemical analysis for seeing all the particular elements and their relative proportions on selected point.

Quantitative analysis entails measuring line intensities for each element in the sample and for the same elements in calibration standards of known composition . By scanning the beam in a television-like raster and displaying the intensity of a selected X-ray line, element distribution images or 'maps' can be produced.

### 3.7 Compression test

Compression test is used to characterize the foam compressive resistance and to study its energy absorption property. In this experiment, Cymat foam 1, 2 and 3 are used. The appearance of samples used for the test is reported in *Figure 40, 41 and 42*:

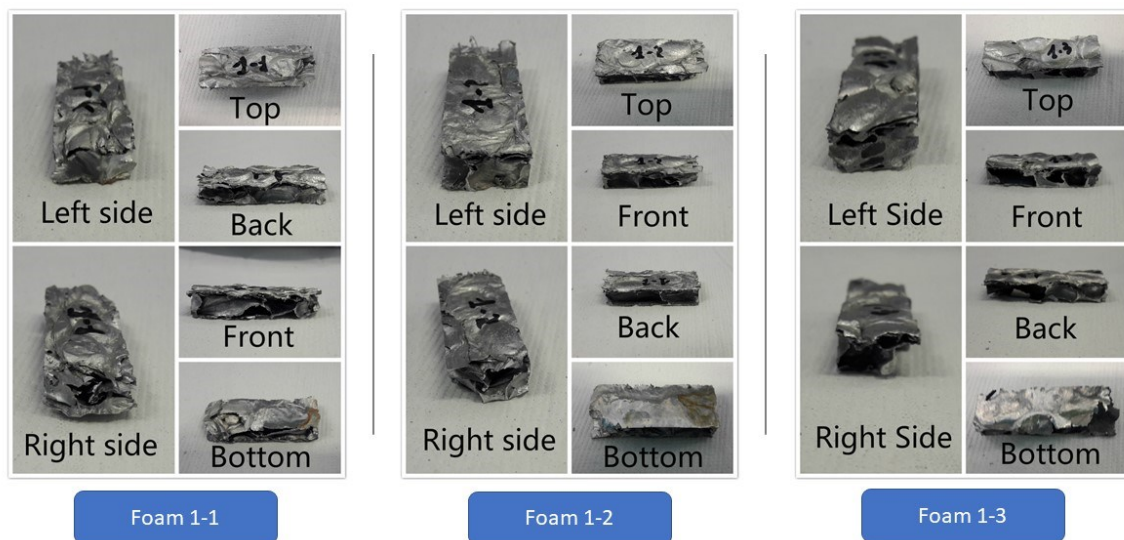


*Figure 40: Foam 1 section views before the compression test*

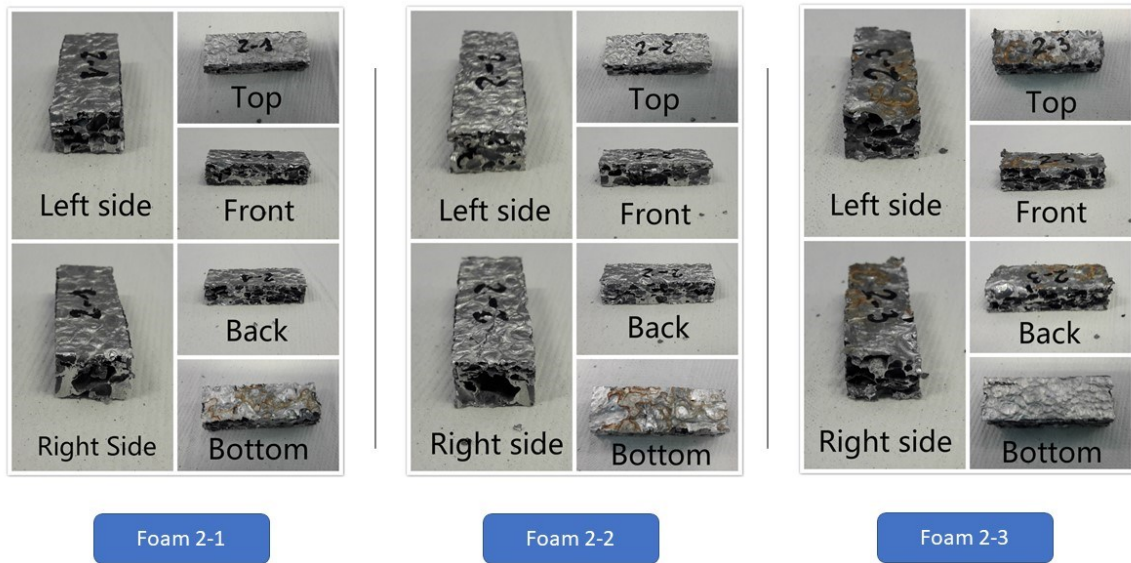


Figure 41: Foam 2 section views before compression test

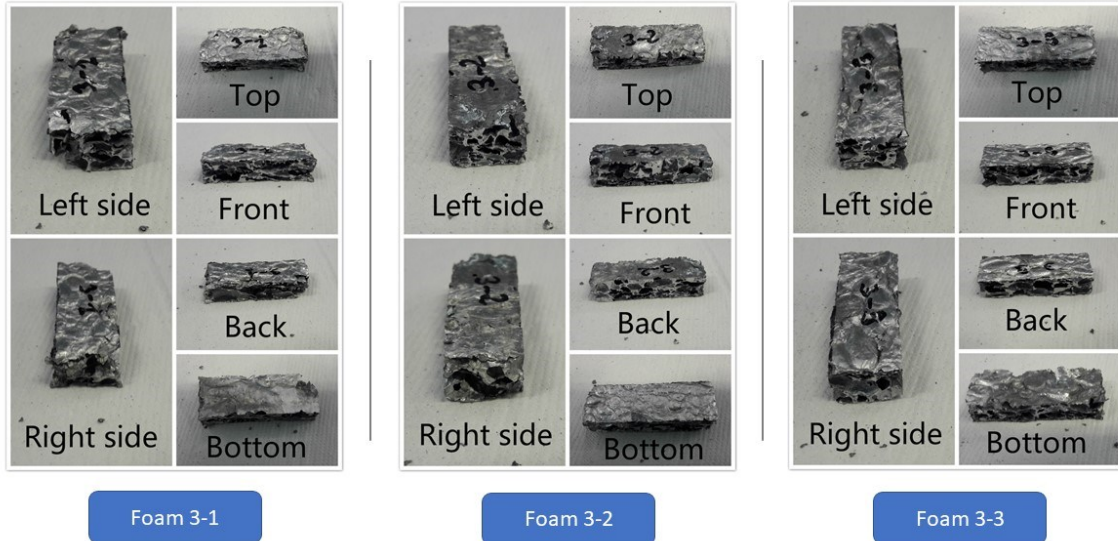
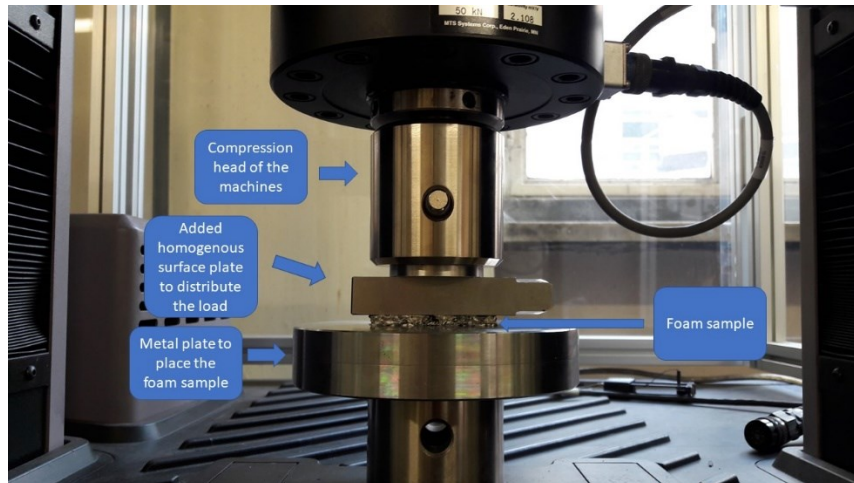


Figure 42: Foam 3 section views before compression test

Considering the experimental setups reported in the scientific literature and in international standards (Table 6) the compression tests in the present work were set as follows: speed is set to 1 mm/min with max load under 25KN. The samples are cut with the length 7\* times of its own pore dimension, in order to avoid edge effects. Considering the high variability of pore dimensions in the materials used in the present thesis the samples dimension was set

as 6 times the pore dimension of Foam 1 (bigger pores) In this case, there are 3 samples for each type of foam, so the total number experiments are 9.

In the compression test machine, there will be added a plate (shown in *Figure 43*) with homogenous surface between the compression head and the foam sample. This plate is to distribute the compression load in order to get a linear horizon load on the foam.



*Figure 43: Compression test machine*

The sample cut is due to the compression test standard in the *Table 6*:

Sample dimensions/shape	Applied load [KN]	Loading rate [mm/min]	Foam type	Reference
Square or circular cross-sections < 10000 mm <sup>2</sup> Foams with continuous surface, facing area >= 625 mm <sup>2</sup> . Discontinuous surfaces: assure the testing of at least 60 cells (cell size <300, cross section area >=625 mm <sup>2</sup> ; cell size 3-6 mm, cross section area >=2500 mm <sup>2</sup> , cell size 6-9 mm, cross section area >=5625 mm <sup>2</sup> )	Pre-loading 45N Loading load specimen until failure or until the measured LVDT/compress meter deflection equals 2% of initial core thickness	Speed testing should be selected in order to assure failure within 3-6 min Standard head displacement 0.5 mm/min		ASTM C365/C365M-16 Standard test methods for flatwise compressive properties of sandwich cores

<p>Cubic specimens</p> <p>Edge size at least 7 time the cell size. Different specimen dimension depending on the foam type/availability</p>	<p>50 KN load cell</p>	<p>0.6 mm/min (up to 10% strain) and then 3 mm/min</p>	<p>Alporas, Alulight, Alcan, IFAM</p>	<p>E. Andreews, W. Sanders, LJ Gibson, Compressive and tensile behavior of aluminum foams, Materials Science and Engineering A 270 (1999) 113-124</p>
<p>Cylindrical specimens: 2.36 cm diameter and 2.54 length (Alporas), : 0.95 cm diameter and 1.90 length (Duocel). Sample diameter at least 7 times the cell size</p>		<p><math>10^{-4} - 10^{-3} \text{ s}^{-1}</math></p>	<p>Alporas, Duocel</p>	<p>KA Dannemann, J Lankford, High strain rate compression of closed-cell aluminum foams, Materials Science and engineering A 293 (2000) 157-164</p>

*Table 6: Literature references for compression tests on aluminum foams*

## Chapter 4

### Results and discussion

In chapter 4, in case of showing results clearly, this part is divided into different aspects by typologies: foams, foams in casting and coated foams.

#### 4.1 Foams

##### 4.1.1 Macroscopic appearance of Foam 1, 2 and 3

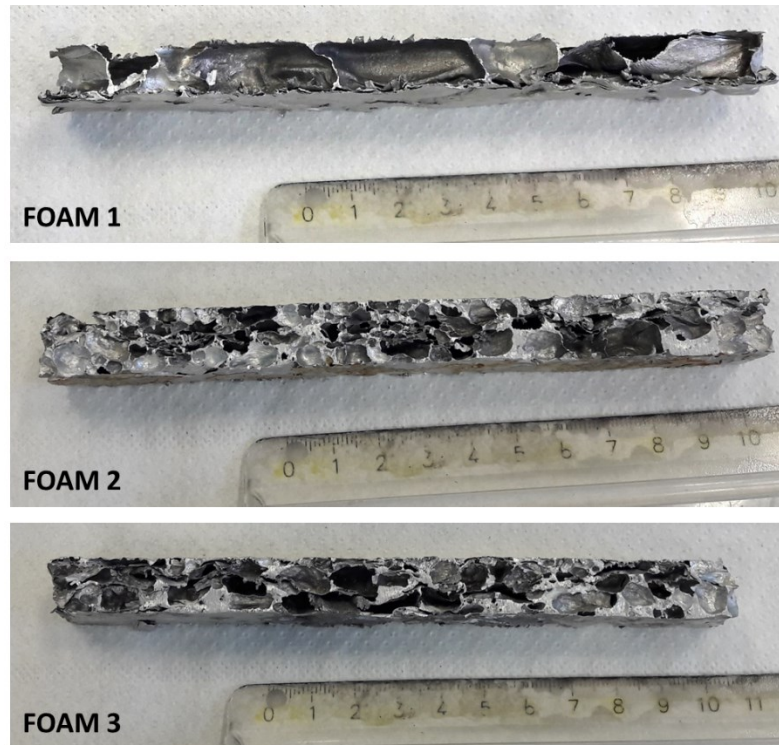


*Figure 44: Macroscopic appearance of the foams*

In *Figure 44*, the macroscopic appearance of the foams is reported. It can be observed that Foam 1 presents larger pores and highest porosity degree. Pores are smaller on Foams 2 and 3, and also the degree of porosity is lower. Quantitative pore dimension and porosity will be measured in chapter 4.2.

##### 4.1.2 Microstructure analysis

In *Figure 45*, *46* and *47* the optical microscope images of the three foams (200x magnification, without etching) are reported.

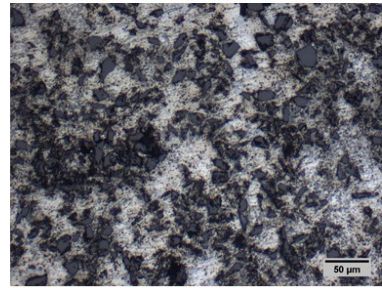
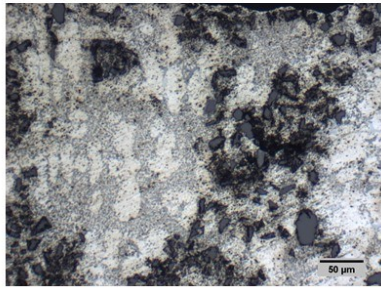
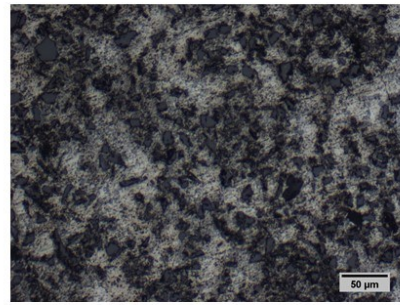
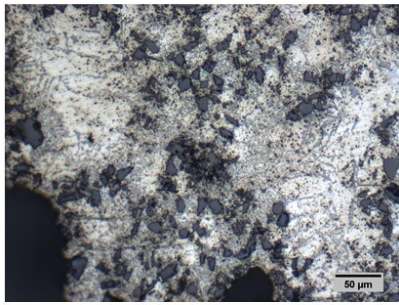


Figure 45: Foam 1-optical images 200x, no etching

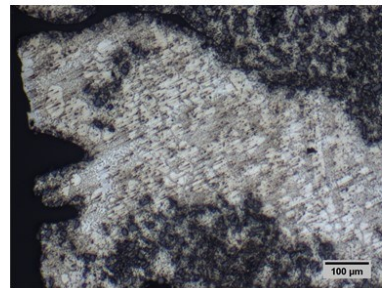
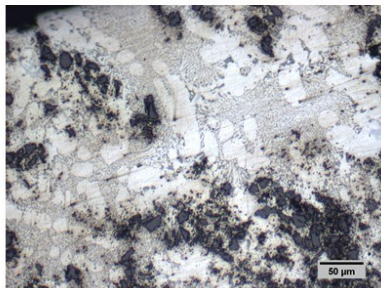
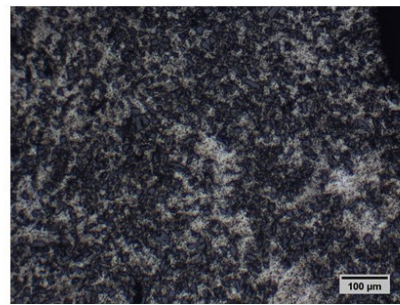
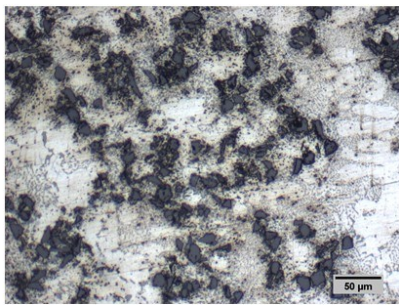
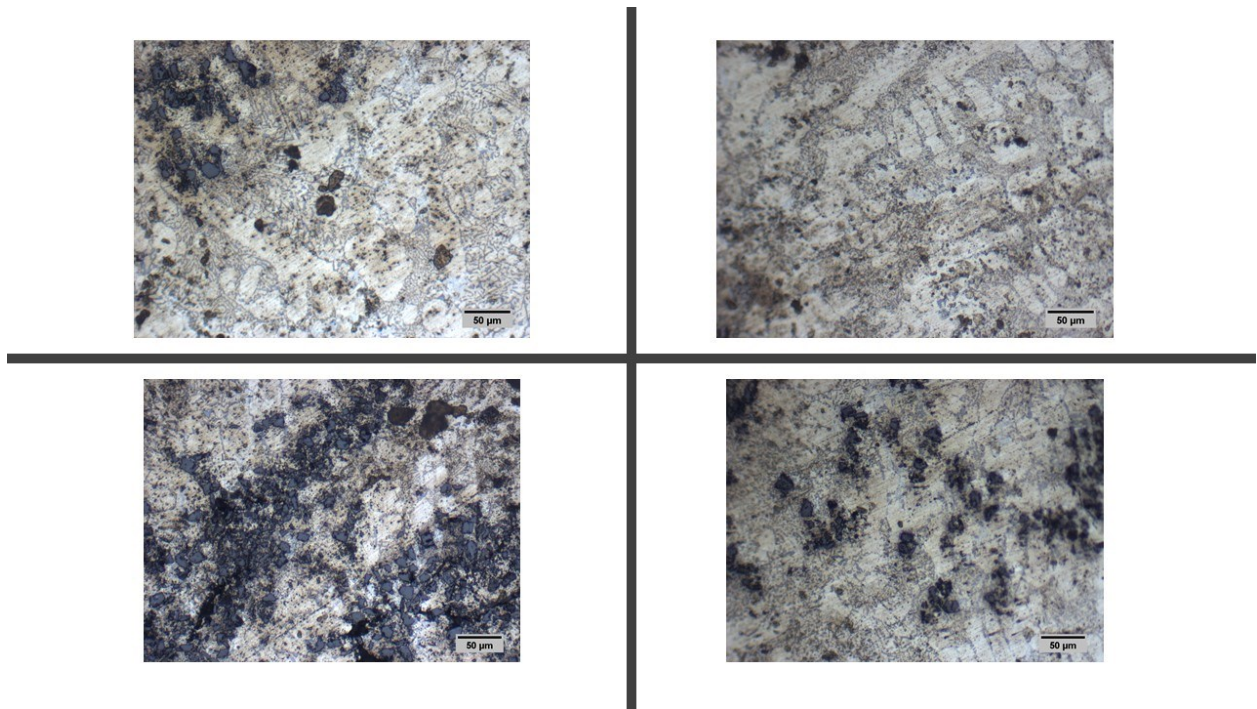


Figure 46: Foam 2-optical images 200x, no etching



*Figure 47: Foam 3-optical images 200x, no etching*

For all the foams three different structures can be evidenced: a clear zone with dendritic structure, which can be associated with an Al rich phase, inter-dendritic zones, attributable to the aluminum-silicon eutectic structure and a lot of dark particles. The small black particles can be the silicon carbide particles used for the stabilization of the foam in the Cymat type foams.

#### **4.1.3 Skin and wall thickness**

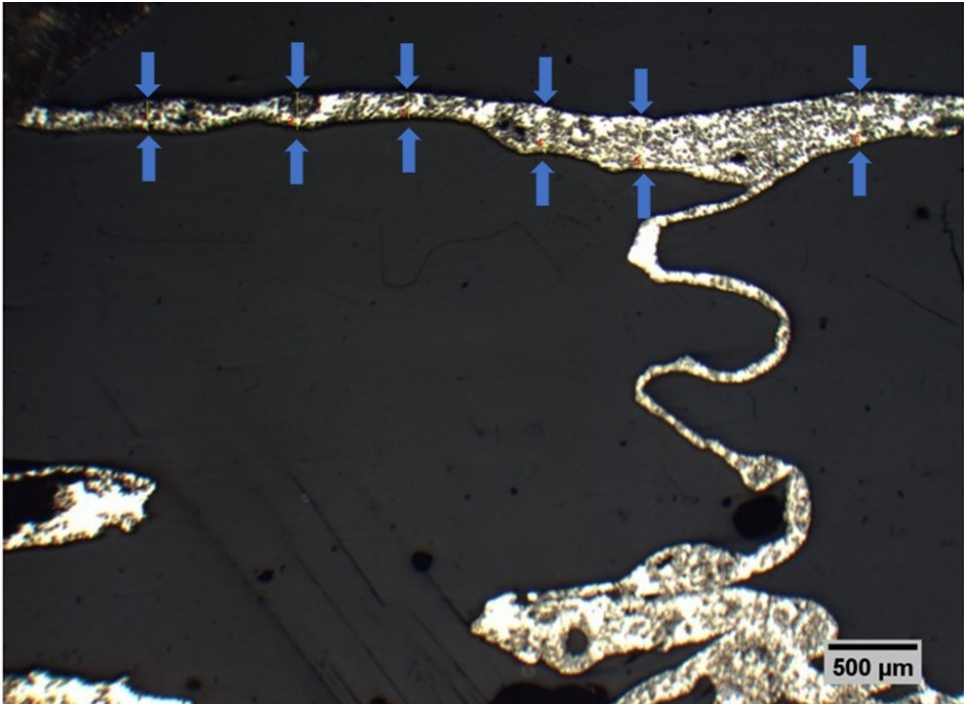
To measure the skin and wall thickness, the microscopy is set to 20X magnification with 0.8 efficiency. In this case, the skin and interconnection walls are most clear and easiest to be observed.

Attention here has to be highlighted: in the zone of connection between skin and wall, the part cannot be counted in either skin aspect or wall aspect.

Examples of the determination of skin thickness are reported in *Figure 48, 50 and 52* for the three foams. Moreover examples of the wall thickness measurements are shown in *Figure 49, 51 and 53* for the three foams.

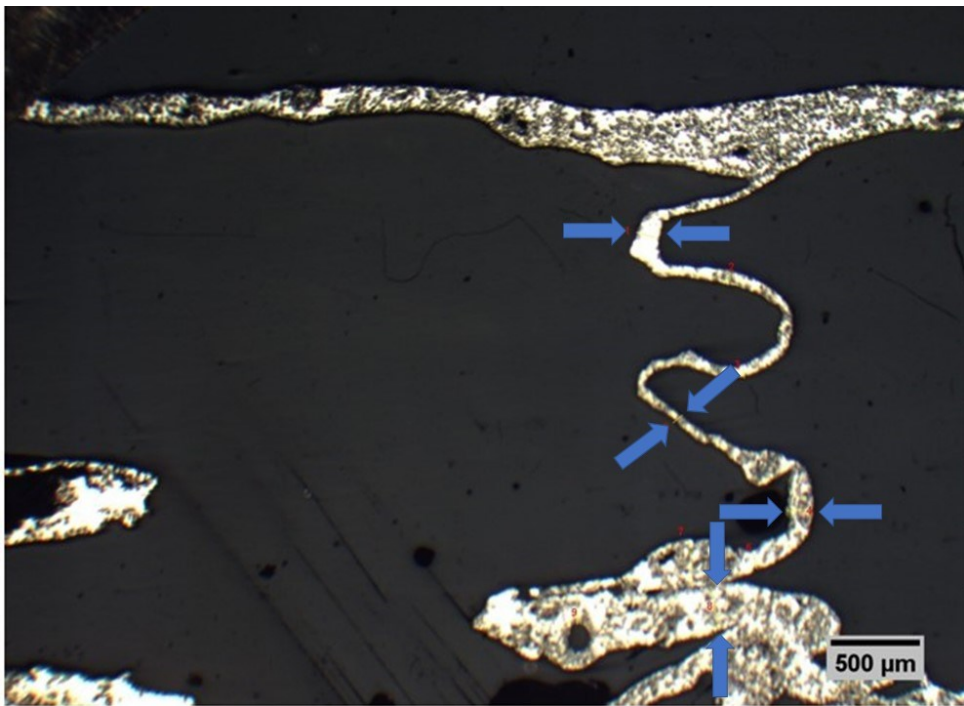
After collecting the values of skin and wall thickness for each foam, a normal distribution can be established by Excel.

*Figures 54 and 55* reports the normal distributions calculated for the skin and wall thickness respectively.



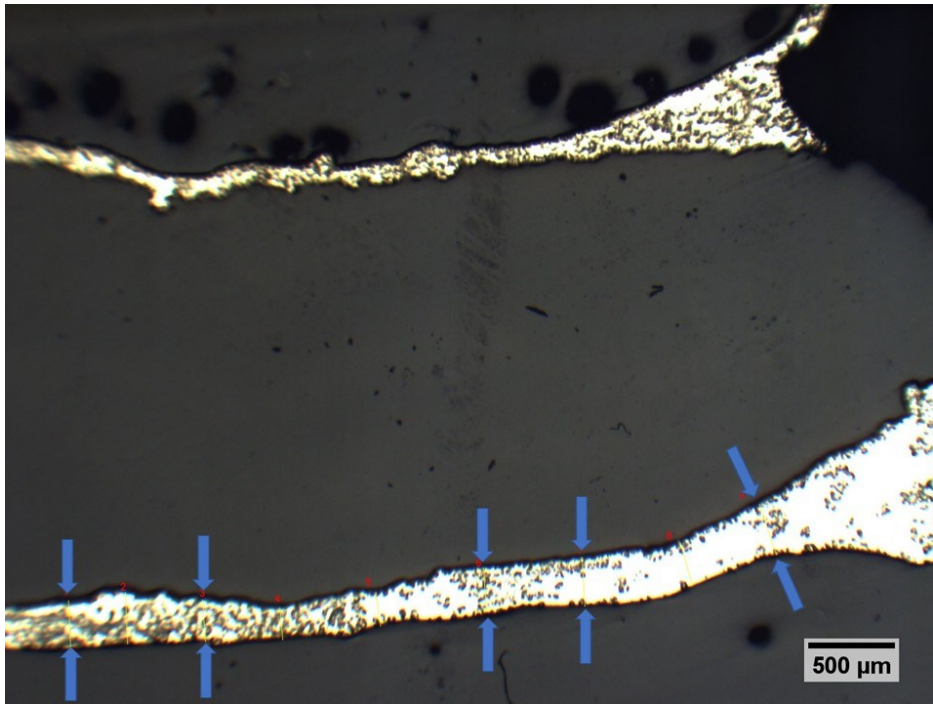
	Length	Unit
1	315.347	μm
2	369.479	μm
3	207.256	μm
4	256.796	μm
5	126.207	μm
6	85.586	μm
7	189.189	μm
	Average	
	221.4086	μm

Figure 48: An example of skin thickness measurements of Foam 1



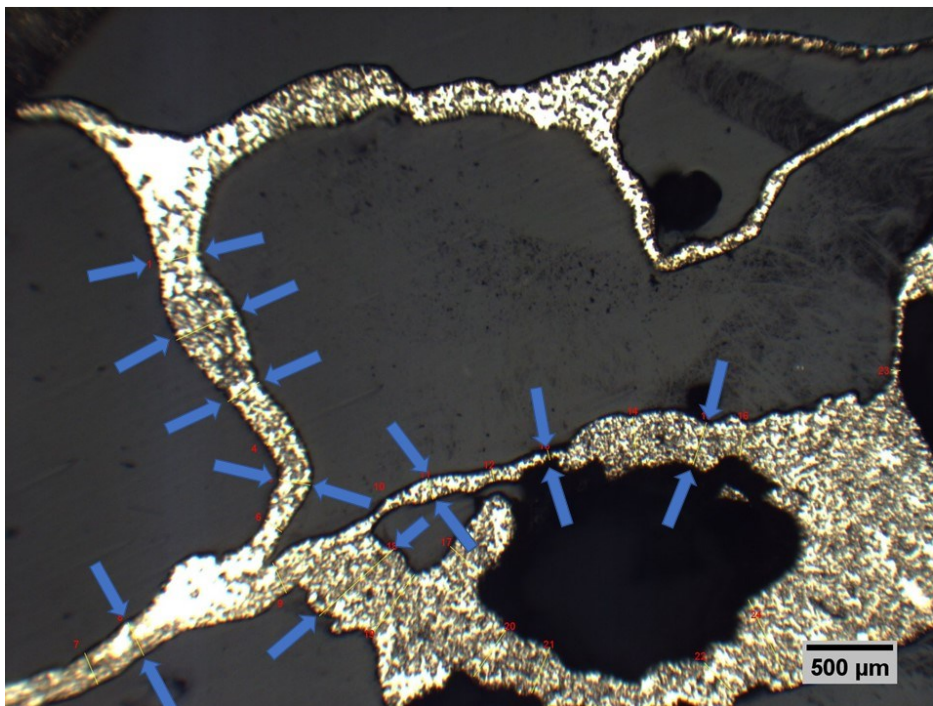
	Length	Unit
1	131.173	μm
2	68.906	μm
3	73.328	μm
4	135.809	μm
5	66.964	μm
6	101.626	μm
7	263.86	μm
8	247.176	μm
9	165.575	μm
	Average	
	139.3797	μm

Figure 49: An example of Foam 1 wall thickness



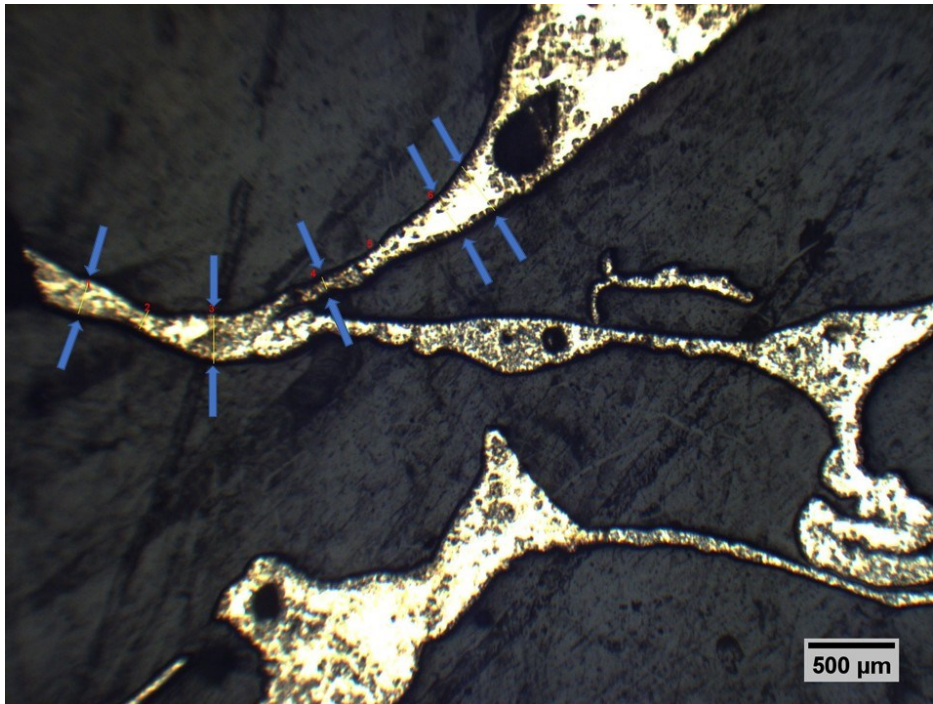
No.	Length	Unit
1	279.606	μm
2	297.604	μm
3	239.418	μm
4	185.562	μm
5	200.032	μm
6	257.388	μm
7	284.355	μm
8	253.696	μm
9	304.845	μm
	Average	
	255.834	μm

Figure 50: An example of Foam 2 skin thickness



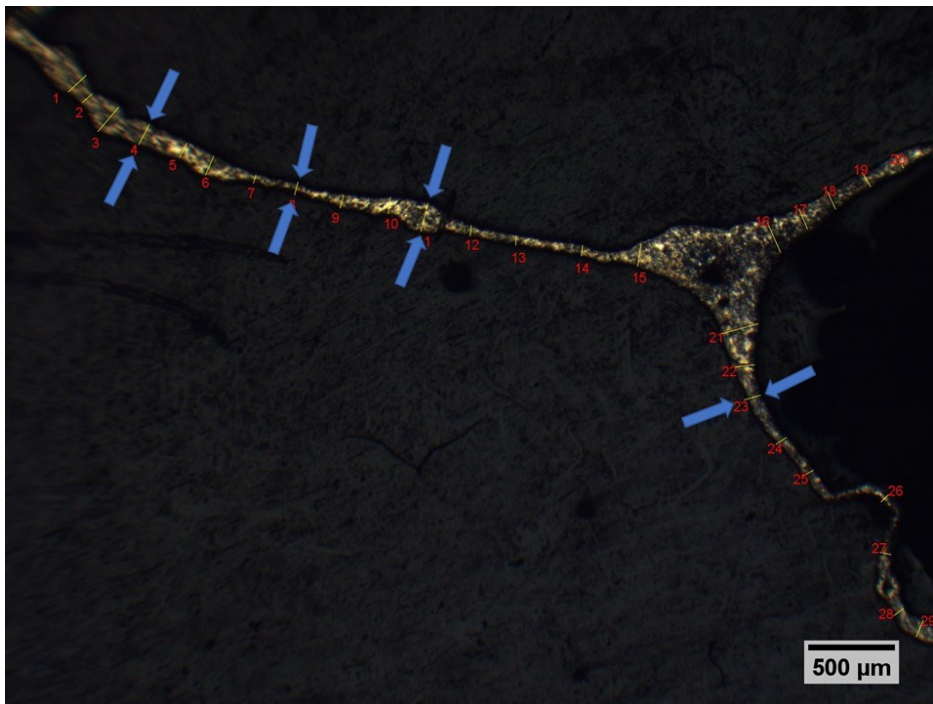
No.	Length	Unit
1	233.887	μm
2	382.883	μm
3	212.477	μm
4	182.419	μm
5	182.918	μm
6	116.248	μm
7	195.778	μm
8	209.544	μm
9	187.519	μm
10	58.732	μm
11	122.536	μm
12	77.76	μm
13	60.098	μm
14	280.584	μm
15	255.012	μm
16	177.743	μm
17	229.686	μm
18	580.575	μm
19	419.959	μm
20	333.607	μm
21	281.054	μm
22	245.444	μm
23	54.241	μm
24	568.086	μm
	Average	
	235.3663	μm

Figure 51: An example of Foam 2 wall thickness measurements



No.	Length	Unit
1	189.457	μm
2	120.869	μm
3	274.775	μm
4	72.772	μm
5	98.791	μm
6	213.667	μm
7	315.315	μm
	Average	
	183.6637	μm

Figure 52: An example of Foam 3 skin thickness measurements



No.	Length	Unit
1	138,637	μm
2	71,825	μm
3	186,883	μm
4	129,969	μm
5	90,651	μm
6	118,002	μm
7	49,190	μm
8	77,039	μm
9	77,039	μm
10	95,555	μm
11	167,153	μm
12	61,185	μm
13	54,054	μm
14	61,185	μm
15	129,969	μm
16	184,547	μm
17	124,221	μm
18	111,844	μm
19	93,868	μm
20	75,543	μm
21	231,117	μm
22	122,370	μm
23	98,380	μm
24	73,085	μm
25	69,565	μm
26	57,333	μm
27	62,294	μm
28	67,568	μm
29	102,916	μm
	Average	
	102,862	μm

Figure 53: An example Foam 3 wall thickness measurements

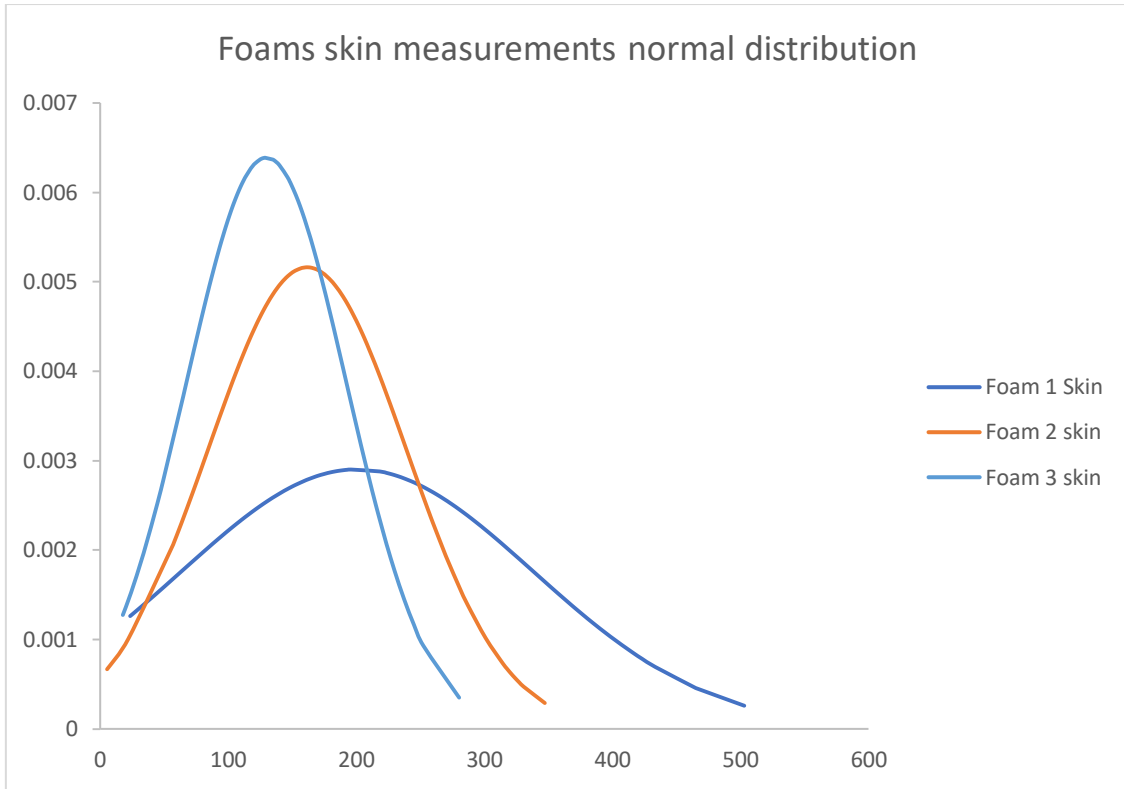


Figure 54: Foams skin comparison curve

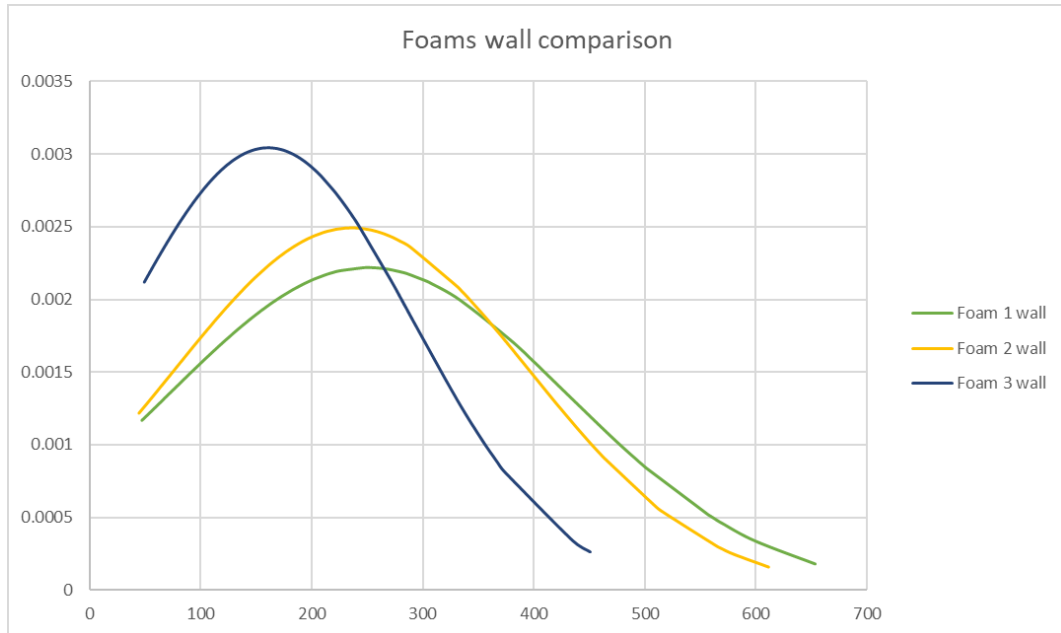


Figure 55: Foams wall comparison

It can be observed in the normal distribution curve, the thickness range of the Foam 1 is the largest among samples and like it is said before, in rich Al zone the dendritic structure can be evidenced. On the contrary, on some thin skin or wall inside the foam, there will be more particles which are clarified to be SiC particles.

In the last, a comparison table with mean and standard deviation can be made to explain difference clearly:

<b>Foams</b>	<b>Skin Thickness (<math>\mu\text{m}</math>, mean <math>\pm</math> stdev)</b>	<b>Wall Thickness (<math>\mu\text{m}</math>, mean <math>\pm</math> stdev)</b>
<b>Foam 1</b>	200.8 $\pm$ 137.4	250.6 $\pm$ 179.7
<b>Foam 2</b>	161.6 $\pm$ 77.2	235.9 $\pm$ 160.0
<b>Foam 3</b>	129.8 $\pm$ 62.4	115.8 $\pm$ 46.6

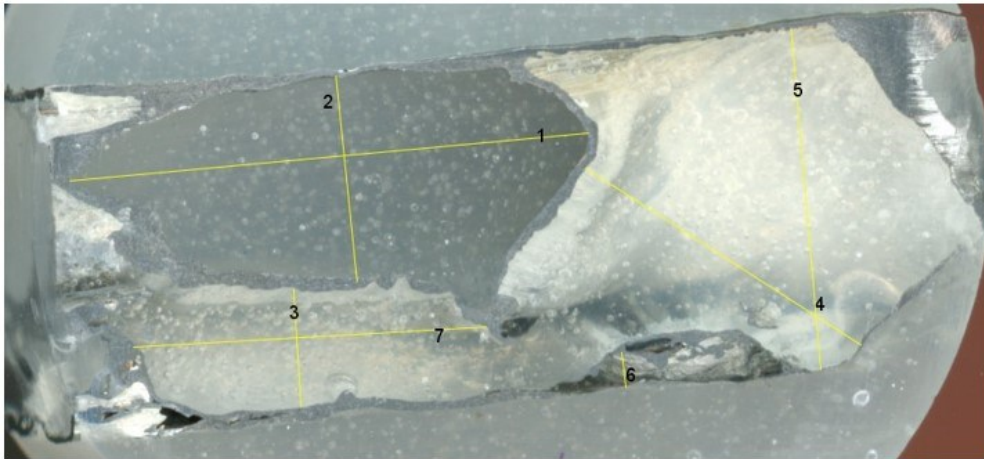
*Table 7: Comparison table of 3 foams thickness*

Due to the inhomogeneity of the materials the data present an elevated dispersion, globally there are no significant differences in the wall and skin thickness among the three foams, the maximum values are higher for the Foam 1 which presents also the highest data dispersion.

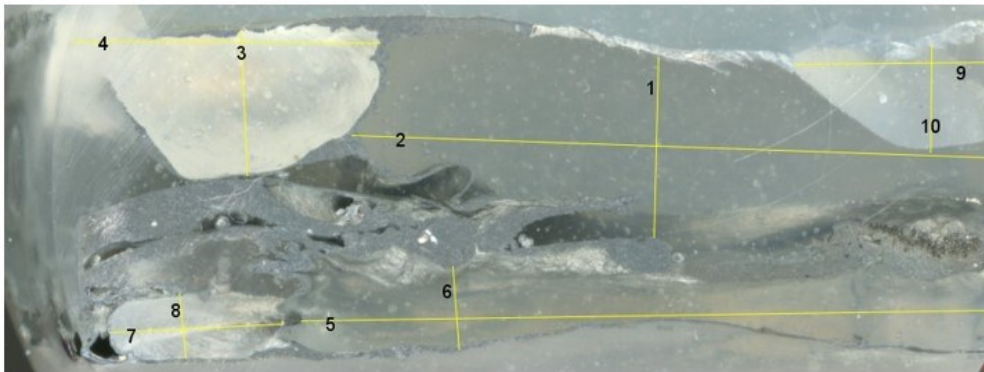
#### **4.1.4 Pore dimension and porosity**

**Pore dimension** is the main measurement of a pore inside foam. It represents the magnitude of a pore and then the main characteristic of a foam can be determined.

*Figures 56-60* reports examples of pore dimensions measurements on the scan images of the different foams. While the mean values obtained from the whole measurements are compared in *Table 8*.

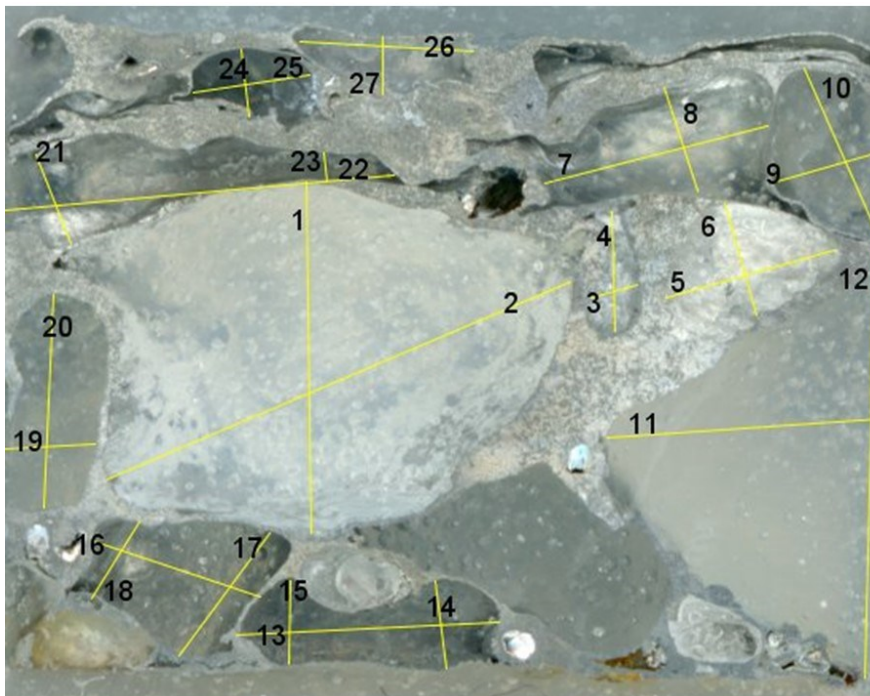


No.	Length	Unit
1	16.077	mm
2	6.315	mm
3	3.495	mm
4	10.132	mm
5	10.779	mm
6	1.016	mm
7	10.672	mm



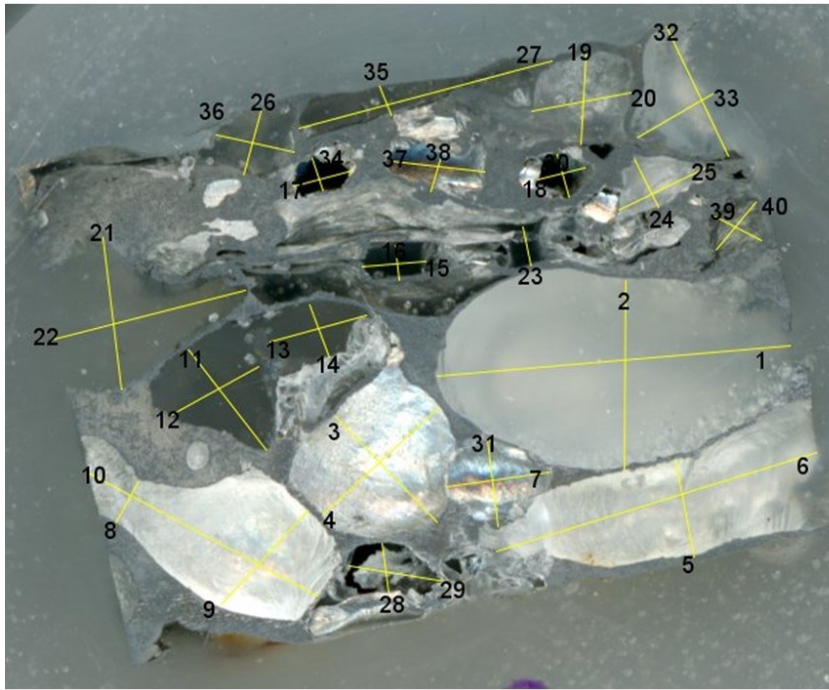
No.	Length	Unit
1	5.552	mm
2	19.817	mm
3	4.504	mm
4	9.591	mm
5	21.35	mm
6	2.569	mm
7	5.289	mm
8	2.013	mm
9	6.109	mm
10	3.285	mm

Figure 56: Foam 1 pore dimension results for 2 sides(up for A side, bot for B side)



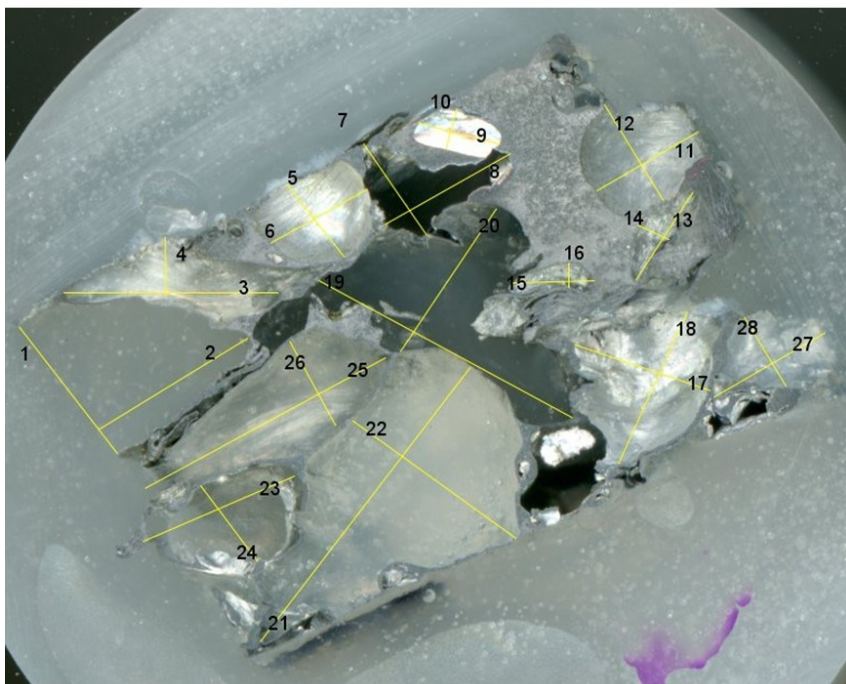
No.	Length	Unit
1	7.281	mm
2	10.421	mm
3	0.997	mm
4	2.472	mm
5	3.629	mm
6	2.398	mm
7	4.762	mm
8	2.25	mm
9	2.398	mm
10	3.746	mm
11	5.746	mm
12	8.964	mm
13	5.442	mm
14	1.827	mm
15	1.713	mm
16	3.646	mm
17	3.156	mm
18	1.865	mm
19	1.848	mm
20	4.419	mm
21	1.982	mm
22	8.071	mm
23	0.597	mm
24	1.393	mm
25	2.432	mm
26	3.596	mm
27	1.186	mm

Figure 57: Foam 2 pore dimension(A side)



No.	Length	Unit	No.	Length	Unit
1	8.89	mm	21	3.829	mm
2	4.726	mm	22	4.946	mm
3	3.67	mm	23	0.979	mm
4	3.953	mm	24	1.265	mm
5	2.424	mm	25	2.424	mm
6	8.405	mm	26	1.643	mm
7	2.603	mm	27	6.565	mm
8	1.168	mm	28	1.234	mm
9	3.204	mm	29	2.478	mm
10	6.491	mm	30	1.099	mm
11	3.18	mm	31	2.197	mm
12	2.529	mm	32	3.592	mm
13	2.501	mm	33	2.177	mm
14	1.412	mm	34	0.836	mm
15	1.592	mm	35	0.786	mm
16	0.865	mm	36	1.997	mm
17	1.539	mm	37	2.361	mm
18	1.226	mm	38	1.035	mm
19	2.284	mm	39	1.301	mm
20	2.521	mm	40	1.549	mm

Figure 58: Foam 2 pore dimension(B side)



No.	Length	Unit
1	4.744	mm
2	5.192	mm
3	6.365	mm
4	1.745	mm
5	2.76	mm
6	3.254	mm
7	3.298	mm
8	3.968	mm
9	2.624	mm
10	1.207	mm
11	3.475	mm
12	3.336	mm
13	3.083	mm
14	0.997	mm
15	2.392	mm
16	0.711	mm
17	4.23	mm
18	4.931	mm
19	8.558	mm
20	5.099	mm
21	10.255	mm
22	5.972	mm
23	4.891	mm
24	2.792	mm
25	8.373	mm
26	2.834	mm
27	3.807	mm
28	2.377	mm

Figure 59: Foam 3 pore dimension(A side)

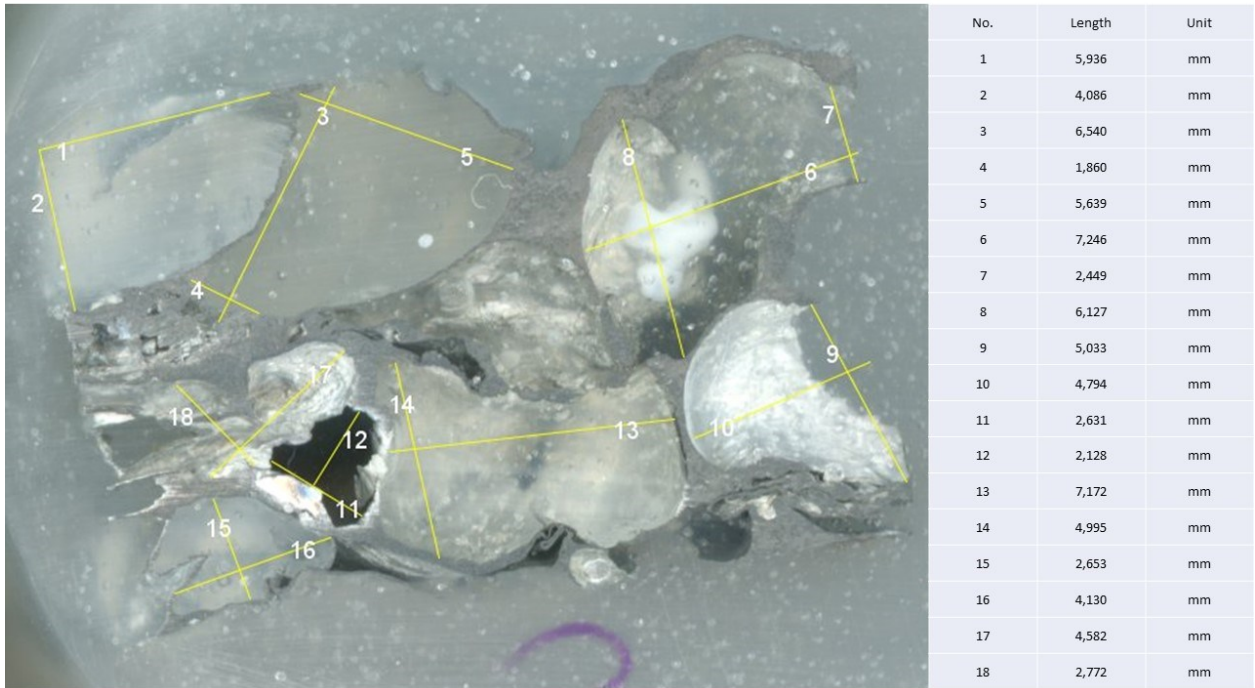


Figure 60: Foam 3 pore dimension(B side)

Foams	Pore dimension (mm)
Foam 1	8.2±5.9
Foam 2	3.1±2.2
Foam 3	4.2±2.1

Table 8: Pore dimension conclusion of 3 foams

After obtaining the results, it is found that the pore dimension of Foam 1 is the largest and for Foam 2 and 3, the pore dimensions are almost not quite different. This phenomenon is also related to the porosity.

**Porosity** or **void fraction** is a measure of the void (i.e. “empty”) spaces in a material, and is a fraction of the volume of voids over the total volume, between 0 and 1, or as a percentage between 0% and 100%. Strictly speaking, some tests measure the “accessible void”, the total amount of void space accessible from the surface (cf. closed-cell foam). [5]

Examples of the calculation of porosities are reported in *Figures 61-63* for the three foams. Results (mean ± standard deviation) are compared in *Table 9*.

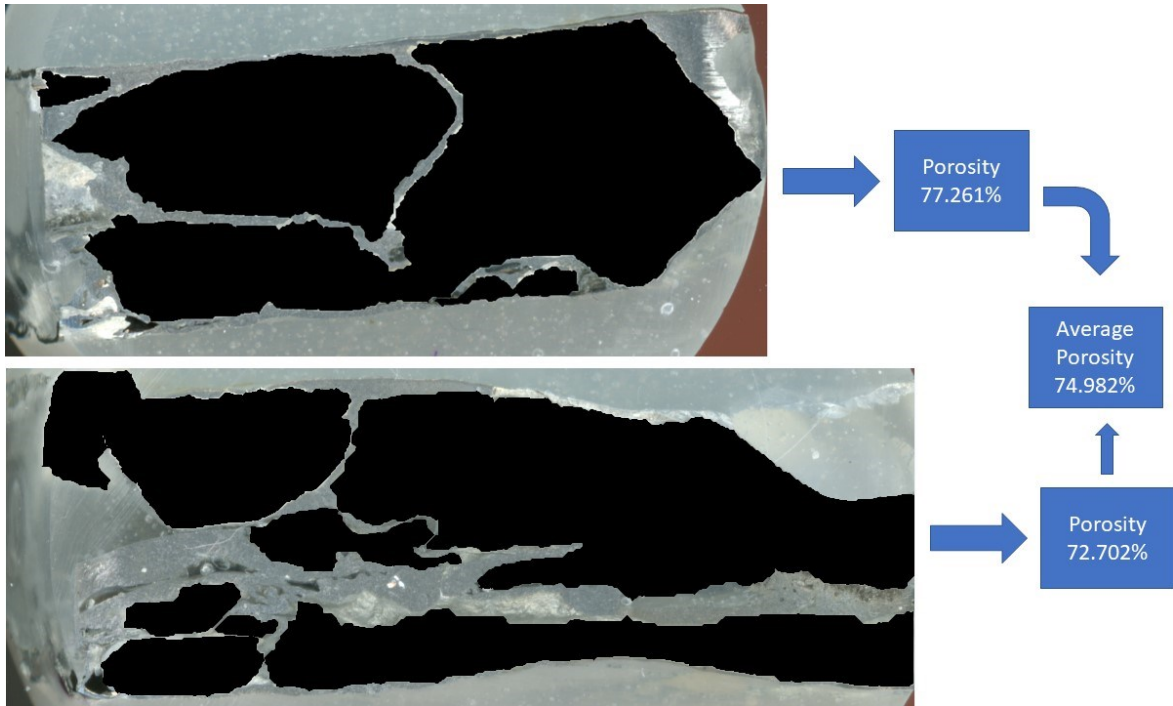


Figure 61: Average porosity of Foam 1 is 75.0%

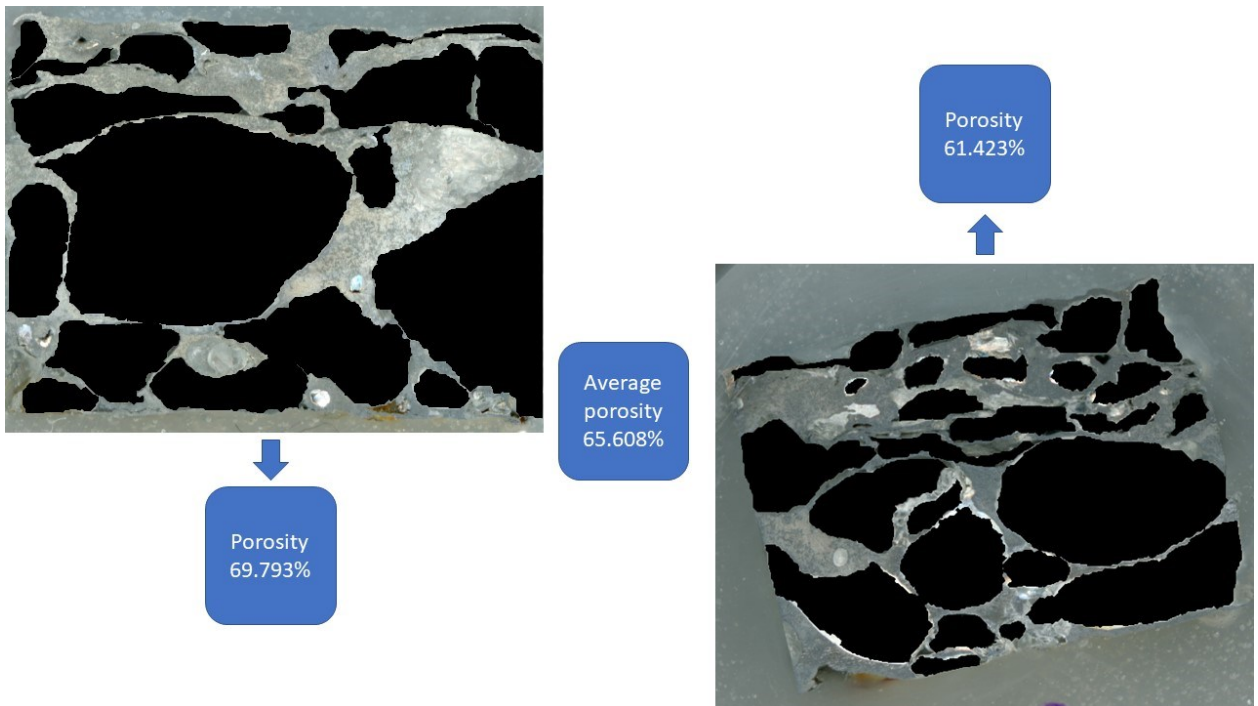


Figure 62: Average porosity of Foam 2 is 65.6%

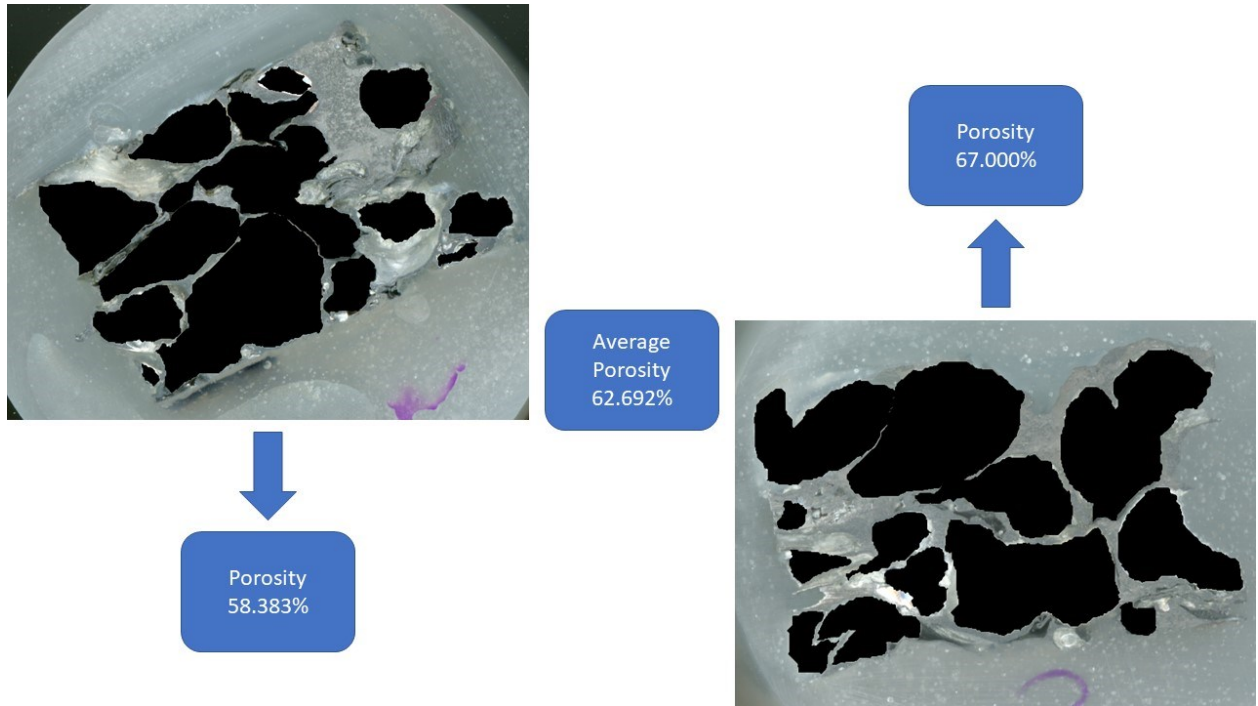


Figure 63: Average porosity of Foam 3 is 62.7%

Foams	Porosity
Foam 1	74.9%
Foam 2	65.6%
Foam 3	62.7%

Table 9: Porosity table for 3 foams

The porosity of Foam 1 is the largest among 3 samples and the pore dimension. So, the relationship between the pore dimension and porosity is positive linear.

#### 4.1.5 FESEM-EDS

Electron images can be obtained under different magnification like 1.00 KX, 5.00 KX or even higher. In this experiment, 5.00 KX magnification is applied for 3 different type of foam.

Usually different zones are analyzed in case of obtaining much more accurate results.

#### Foam 1 EDS results

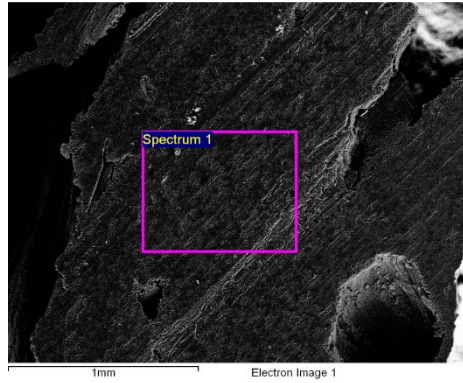


Figure 64: Example of EDS area of analysis

Figure 64 is an example of rectangular zone chosen to analyze on Foam 1. After zone is chosen, the FESEM will analyze the zone automatically.

The EDS spectrum (an example is reported in Figure 65) shows the peaks associated to the emission of X-rays characteristic of the different elements present on the sample surface. Their weight percentages can be calculated.

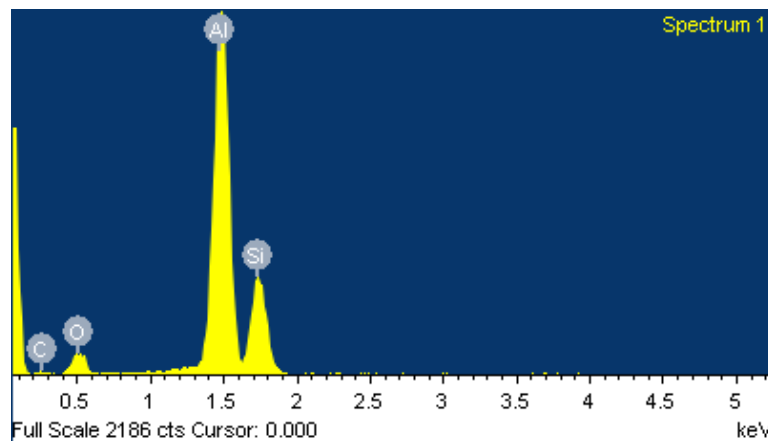


Figure 65: Reflection spectrum for test

At last, after analyzing different zones for Foam 1, an average and deviation values for different elements can be obtained (Table 10):

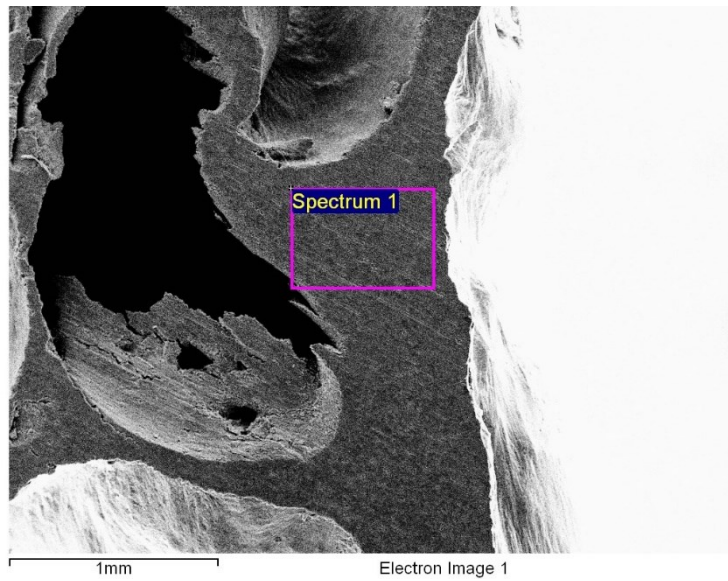
	MEAN(%)	STDEV(%)
<b>C</b>	5.6	2.7
<b>O</b>	16.5	3.2
<b>AL</b>	56.5	10.3
<b>SI</b>	21.4	45.0

Table 10: Foam 1 EDS composition results

### Foam 2 EDS results

The steps to do for foam 2 is same as done in foam 1.

An example image with evidenced the EDS analysis area is reported in *Figure 66*, and the corresponding EDS spectrum in *Figure 67*.



*Figure 66: Example test position for Foam 2*

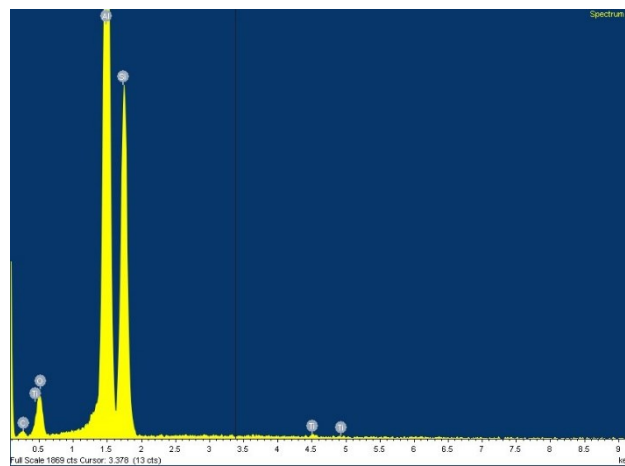


*Figure 67: Example of EDS spectrum for Foam 2*

Same as done in foam 1, after different zones analyzed, the average and deviation of weight percentage is listed in *Table 11*:

	<i>Mean(%)</i>	<i>Stdev(%)</i>
C	9.0	2.8
Si	21.5	6.0
Al	56.8	8.7
O	14.0	2.1

*Table 11: Foam 2 EDS composition*

### Foam 3 EDS results

An example of zone chosen test in foam 3 is in *Figure 68*:

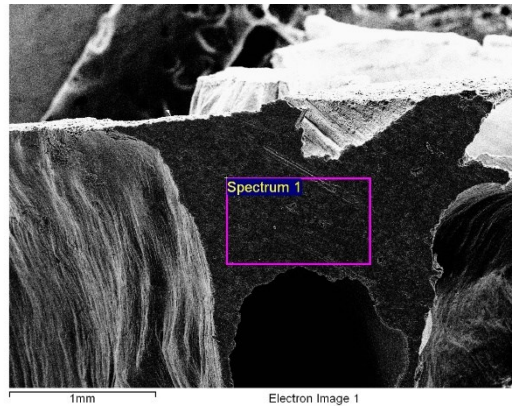


*Figure 68: Example test position of Foam 3*

To follow the steps of foam1 and foam2, the spectrum result for foam 3 is easily obtained in *Figure 69*.

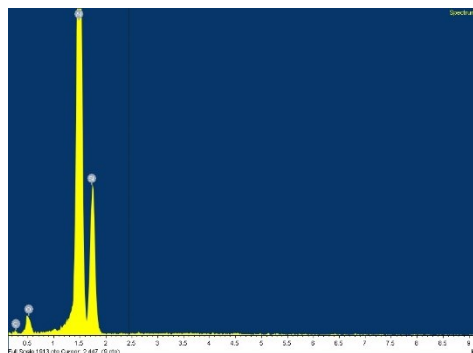


*Figure 69: Example spectrum of Foam 3*

In the last, an average and standard deviation values can be evaluated in *Table 12*:

	<i>Mean(%)</i>	<i>Stdev(%)</i>
C	11.3	1.7
O	15.1	1.8
Al	48.1	4.7
Si	25.5	2.5

*Table 12: Foam 3 EDS composition*

#### 4.1.6 Compression test

Each foam has 3 samples and the experiment is done by 3-time for each foam.

Figures 70-72 report the load-displacement curves obtained for the three foams. For each Foam, 3 curves are reported and they present very similar behavior, so the result is

reproducible. The small differences observed can be attributed to samples inhomogeneities.

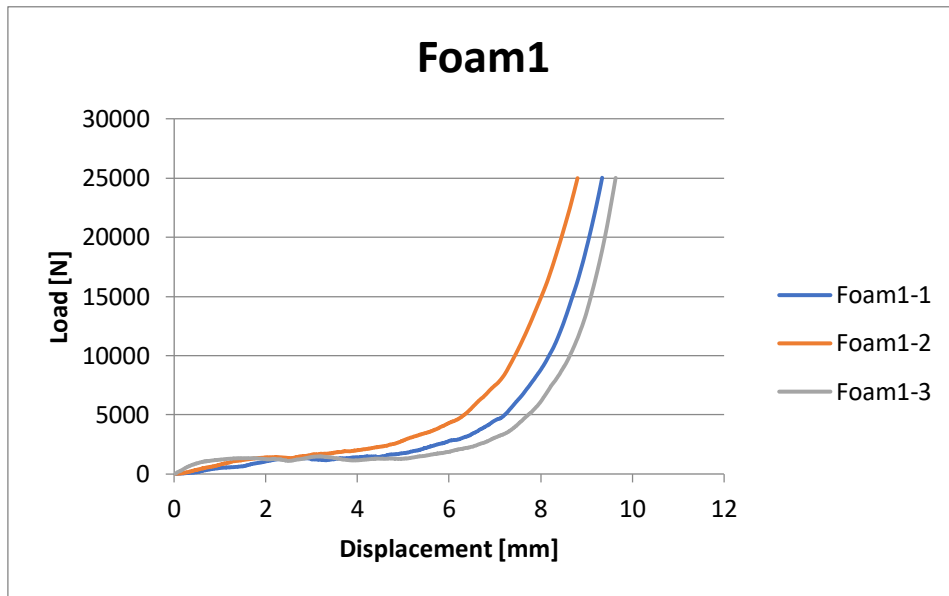


Figure 70: Foam 1 compression test

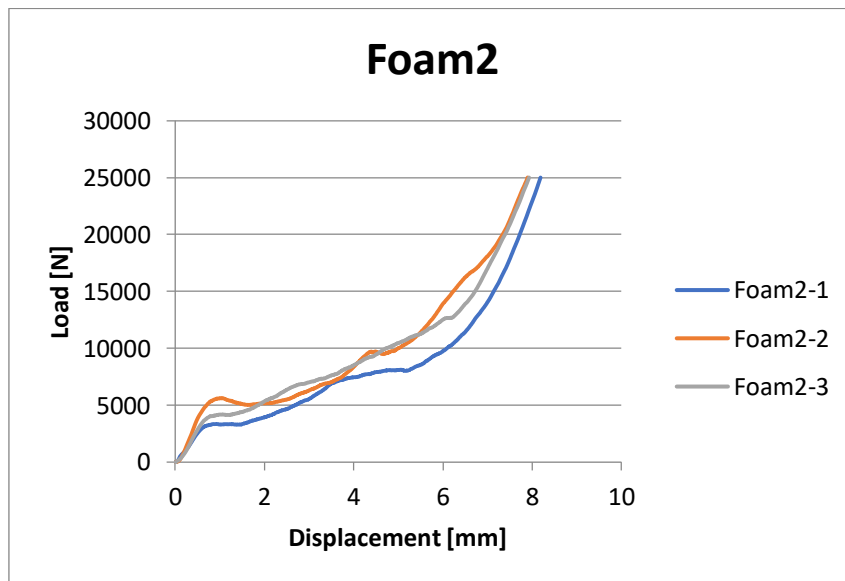


Figure 71: Foam2 compression test

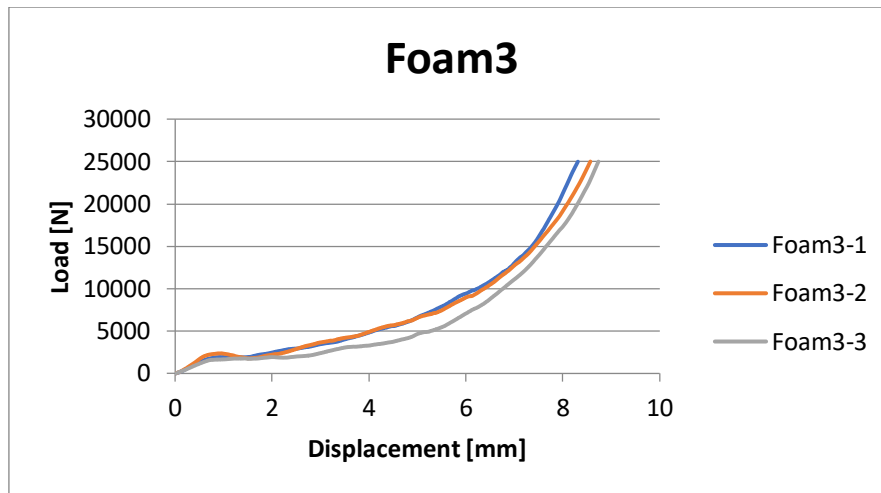


Figure 72: Foam 3 compression test

In all the curves three main zones can be evidenced:

- A linear tract (from 1000 to 5000 N loads) due to the material elastic deformation
- A second zone of plastic deformation at constant loads (plateau)
- A third zone with rapid load increase associated to material progressive collapse and compaction

## 4.2 Foams in casting

### 4.2.1 Macroscopic appearance of foams in casting

Different samples have been obtained from the three cast specimen (S1, S3 and S4 reported in chapter 3). For each specimen 4 samples have been obtained in the 4 different zones:

- dense metal thickness 1
- dense metal thickness 2
- dense metal thickness 1 with foam core
- dense metal thickness 2 with foam core

As described in chapter 3.

The analyzed samples are the following:

1S1- dense metal thickness 1 in cast specimen S1

2S1- dense metal thickness 2 in cast specimen S1

3S1- dense metal thickness 1 with foam core in cast specimen S1

4S1- dense metal thickness 2 with foam core in cast specimen S1

1S3- dense metal thickness 1 in cast specimen S3

2S3- dense metal thickness 2 in cast specimen S3

3S3- dense metal thickness 1 with foam core in cast specimen S3

4S3- dense metal thickness 2 with foam core in cast specimen S3

1S4- dense metal thickness 1 in cast specimen S4

2S4- dense metal thickness 2 in cast specimen S4

3S4- dense metal thickness 1 with foam core in cast specimen S4

4S4- dense metal thickness 2 with foam core in cast specimen S4

As far as samples with foam cores 3S1, 4S1, 3S4 and 4S4 present a significant residual porosity as shown in example images (Figure 73-74). On the other hand sample S3 was totally infiltrated (Figure 73).

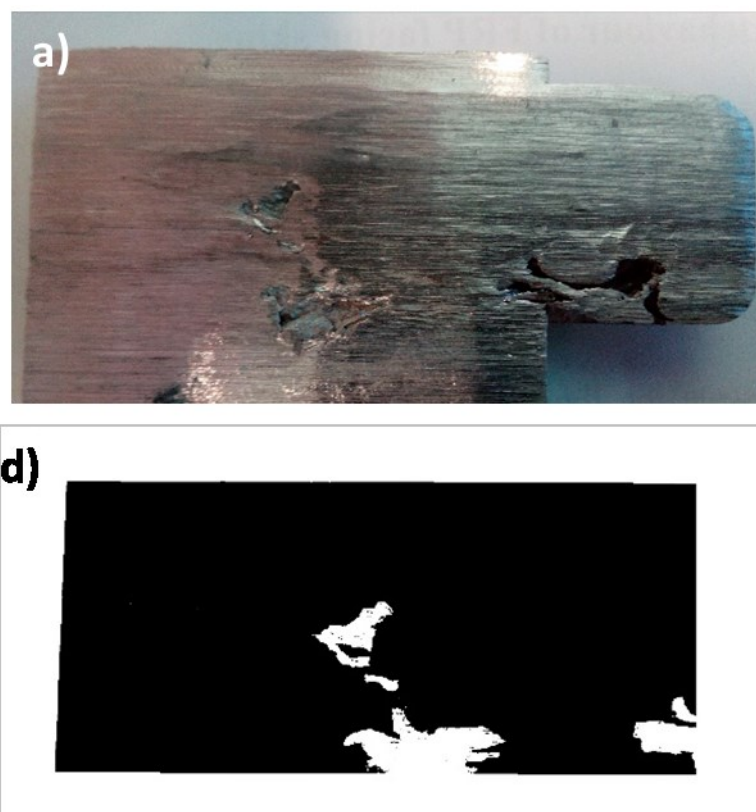


Figure 73: Sample S3 – macroscopic appearance (a) and binary image (d), the foam is totally infiltrated

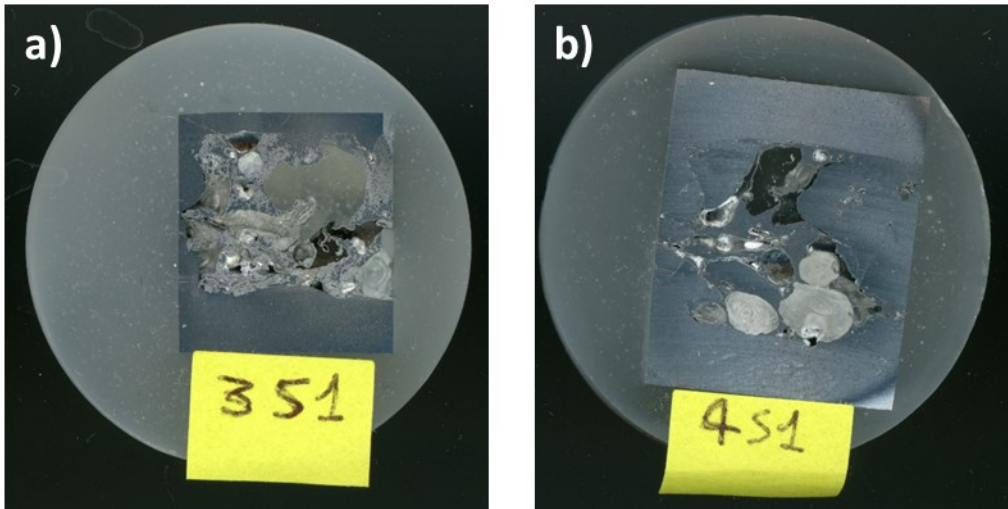


Figure 74: Foams in casting 351 and 451

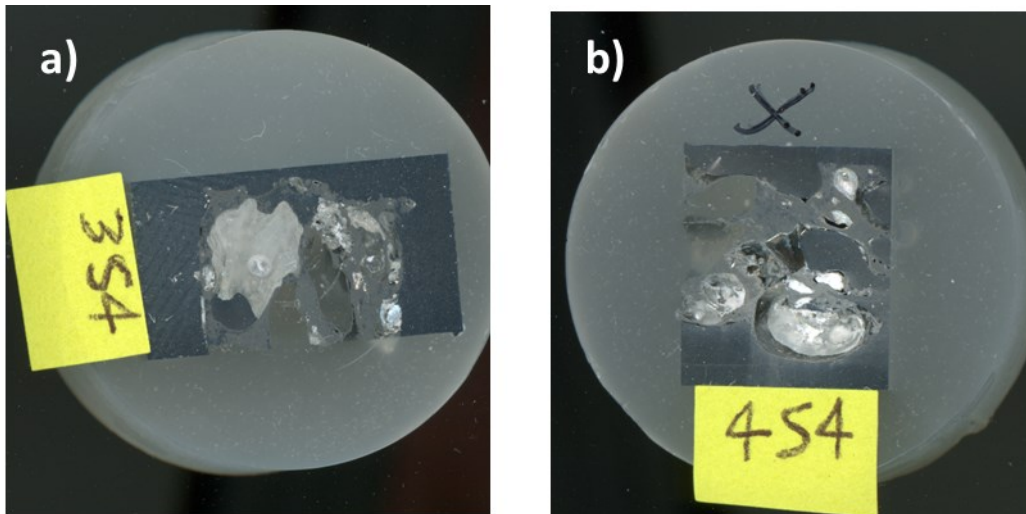
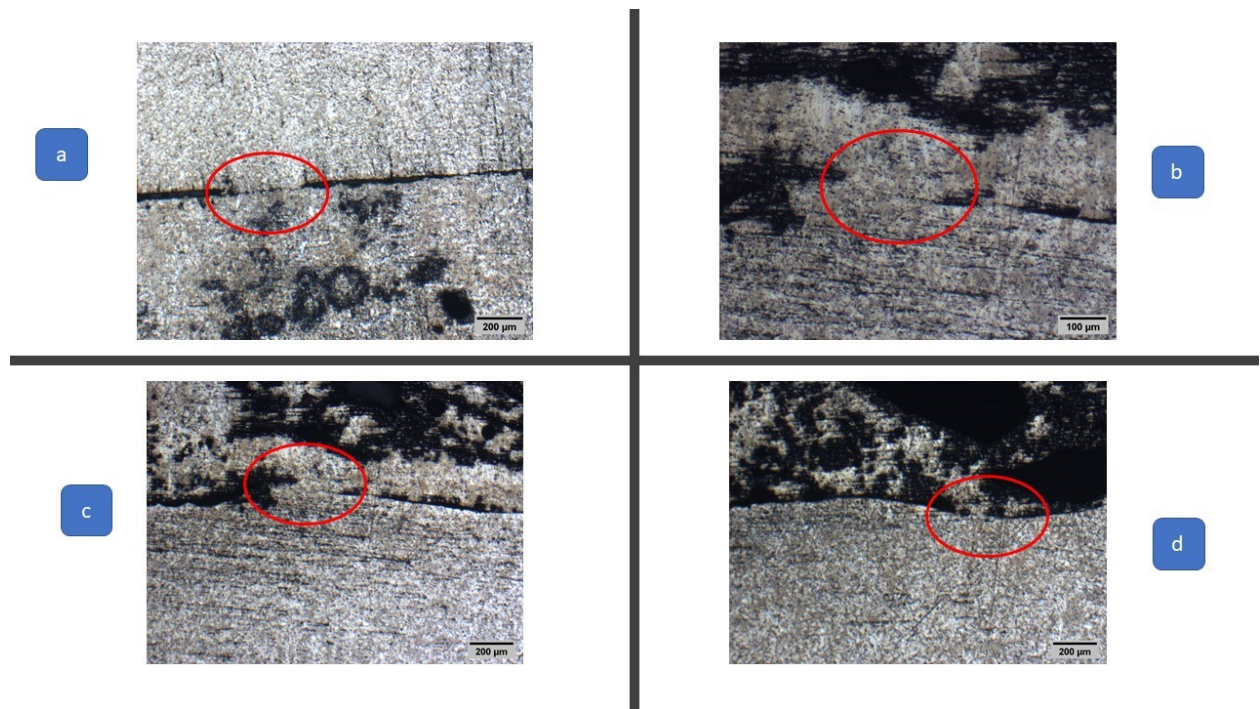


Figure 75: Foams in casting 354 and 454

#### 4.2.2 Optical microscopic analysis and bonding phenomenon

In this experiment, the optical microscopic analysis is under 100X, 200X and 500X magnification. The main issues about foams in casting is the bonding problem. Since it is found that the joining between the dense metal and foam is not quite good which is not wanted. In some industrial application, the bonding is much more important. So, in this chapter, the bonding problem is mostly focused.

In the optical microscopic analysis, it is showed that there are some joining and it depends on 2 aspects: one is in some area, even there are amount of particles, there is showing the bonding; the other case is in some area, it seems only metal joining. The cases will be studied based on figures captured.



*Figure 76: optical images of 3S1 with bonding zones (foam-dense metal) highlighted by red circles*

The *Figure 76* displayed the main types of bonding issues of 3S1. Type a is occurred between 2 straight surfaces. As it can be seen the foam side which is lower side has got black areas. The black areas through higher expose are to be pores of the foam. So here the joining is maybe since the infiltration of the aluminum in dense metal casting.

*Figure 76 b* and *c* are the same type of bonding issue. The joining is quite good. The gain degree in the connecting is almost the same white like in dense metal, not like in the foam full of black particles. This maybe since the melting of the surface is just right. If the melting is going on with foam, it will affect the foam and the joining of the foam and casting will be no meaningful.

*Figure 76 d* is the most type of the joining. It is small with irregular shape and seems not strong connecting. There is black area inside the connection which is introduced to be SiC particles. SiC particles like showed in foams microstructure, they are mostly appeared in the foam solidification.

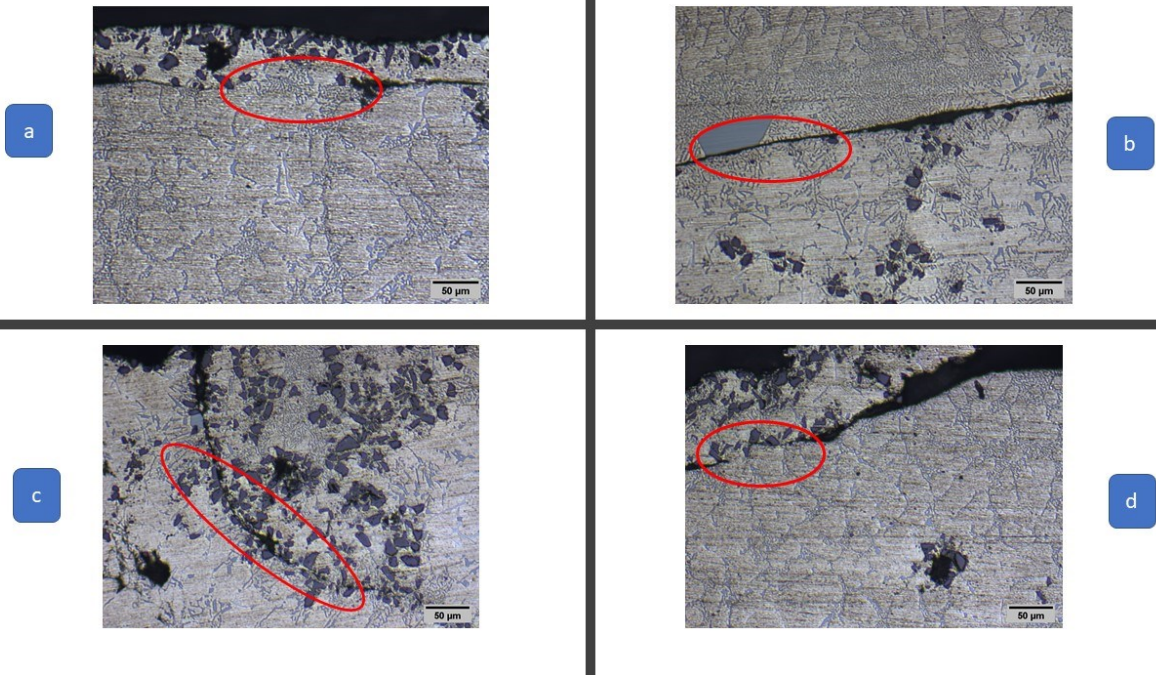
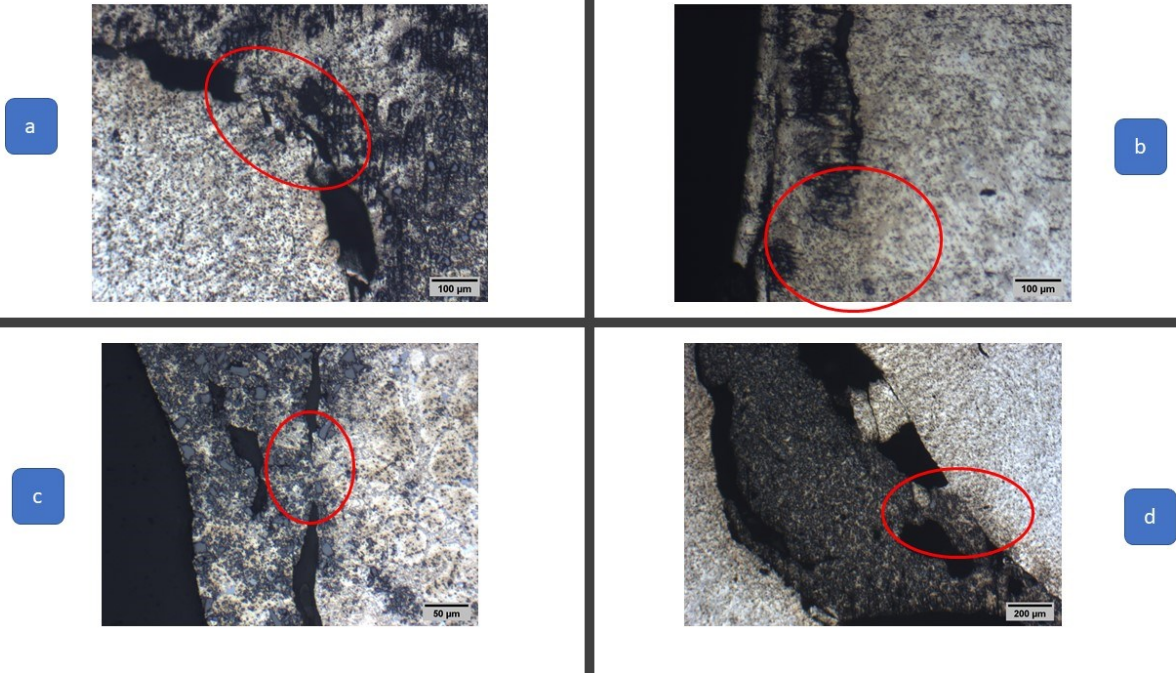


Figure 77: Optical image of S4 with interesting zones (foam- dense and metal) highlighted by red circle

The bonding condition in 4S1 is not like in 3S1. In *Figure 77 a*, the joining area evidence a clear dendritic structure. It maybe since before the solidification, here is already melting together, and results spacing continuous metallurgical structure. *Figure 77 b* shows a clear not connected boundary layer and with the presence of another secondary phase. The color degree of this secondary phases is much lighter that black SiC particles.

For *Figure 77 c* and *d* there are a lot of SiC particles just distributed on the side of the boundary line.



*Figure 78: Optical images of 3S4 with bonding zones (foam-dense metal) highlighted by red circles*

Figure 78 shows 4 types of joining in 3S4 foam in casting. Figure 78 b evidence the most homogenous joining area among the ones reported. Figure 78 a, c and d evidence joining areas in presence of SiC particles.

#### 4.2.3 Porosity

The step to do is the same in foams.

**First to be evaluated is the transverse section of the foams in casting (Figure 79-80):**

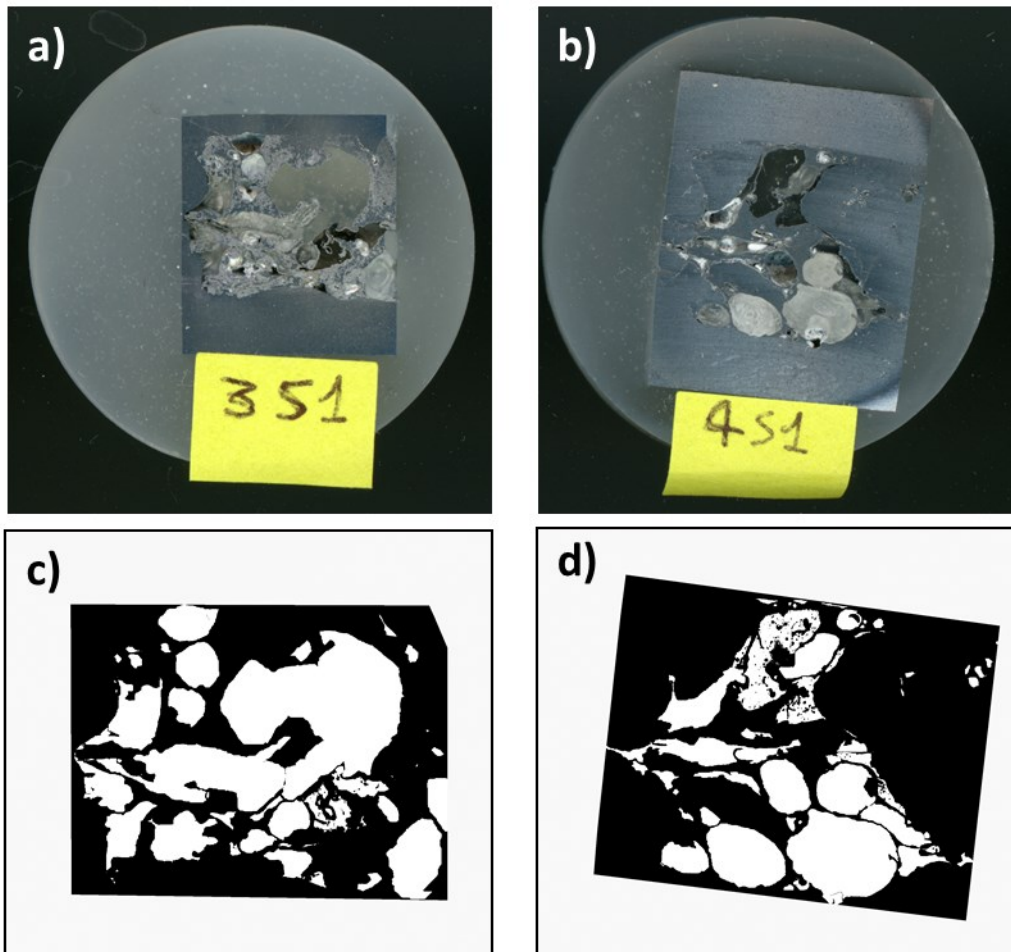


Figure 79: Binary figures of 3S1 and 4S1

The residual porosity calculated for foam in casting 3S1 is 52.1% (Figure 79 a and c), and the residual porosity calculated for foam in casting 4S1 is 30.0% (Figure 79 b and d)

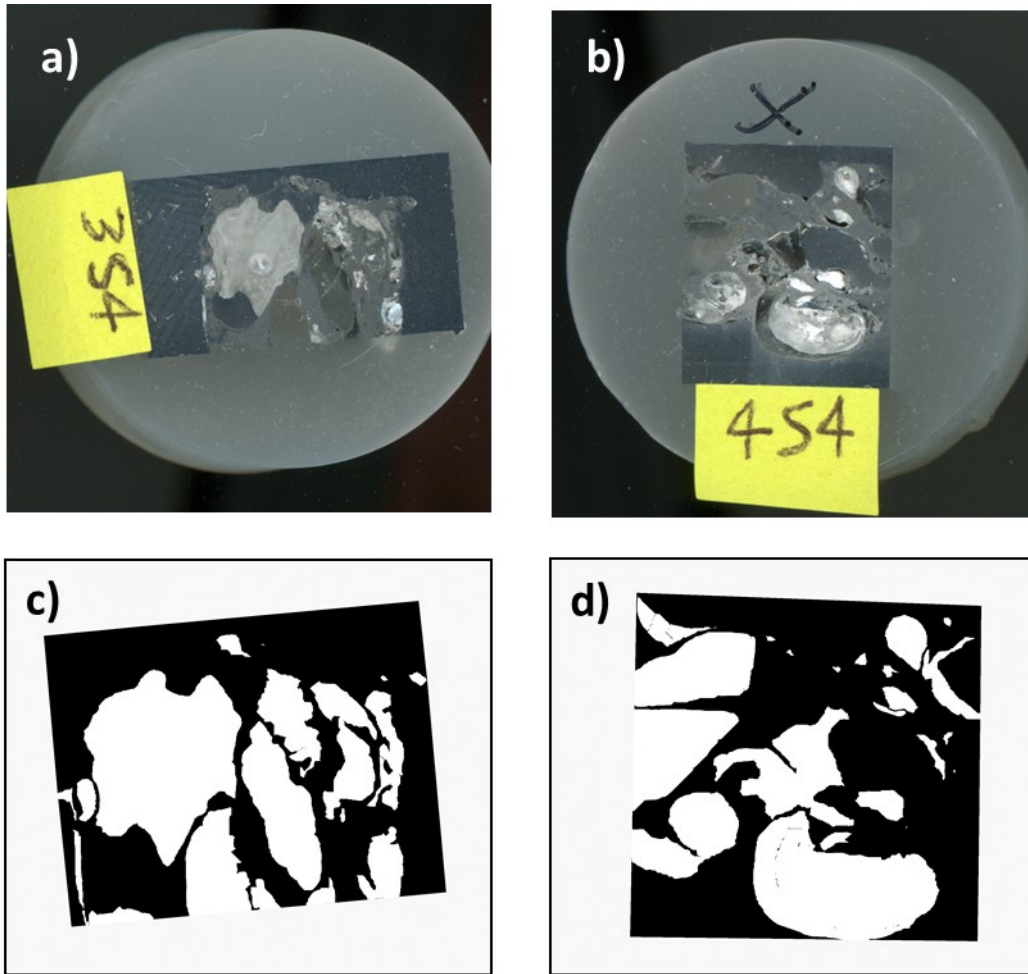


Figure 80: Binary figures of 3S4 and 4S4

The residual porosity calculated for foam in casting 3S4 is 42.8% (Figure 80 a and c), and the residual porosity calculated for foam in casting 4S4 is 40.1% (Figure 80 b and d)

Samples S3 was not analyzed because it was totally infiltrated.

#### Residual porosity for samples with crosscut section

It is needed to measure the residual porosity of each foam in casting since the porosity can affect the solidification of the casting. So, to compare the porosity of the foam in casting and residual porosity is mandatory. The analysis performed crosscut sections (Figure 81-84) can give more representative information because they are referred to wider sample portions.

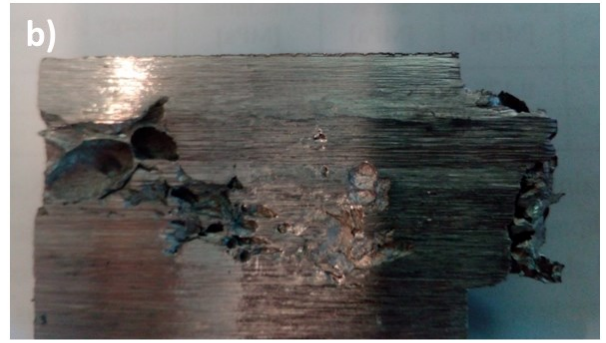
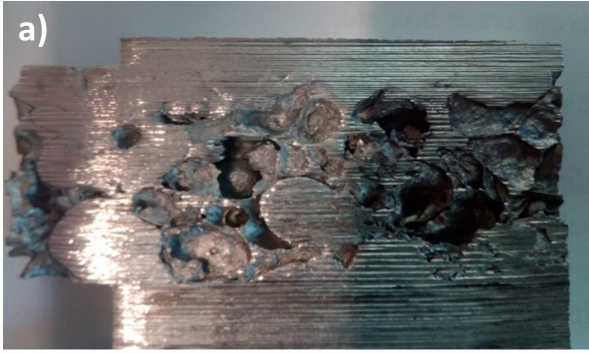


Figure 81: The residual porosity of 3S1 is 36.6%

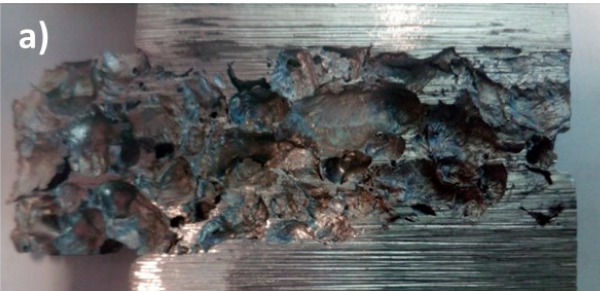


Figure 82: the residual porosity of 4S1 is 69.8%

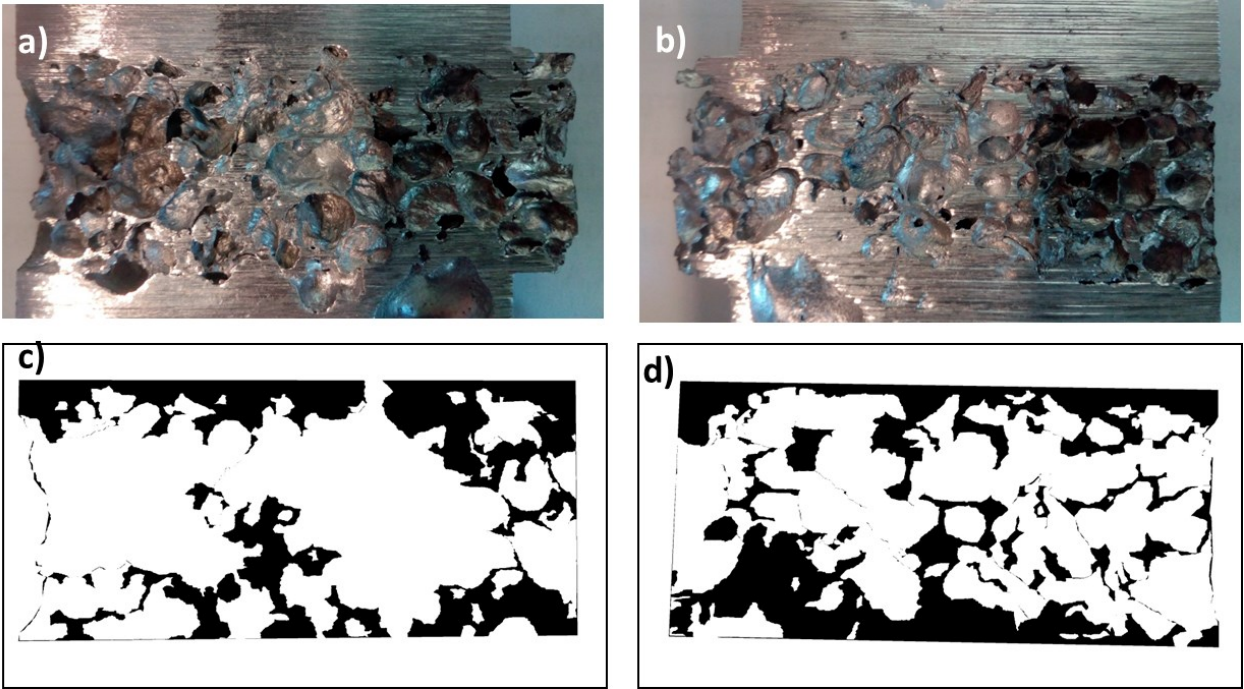


Figure 83: The residual porosity of 3S4 is 56.8%

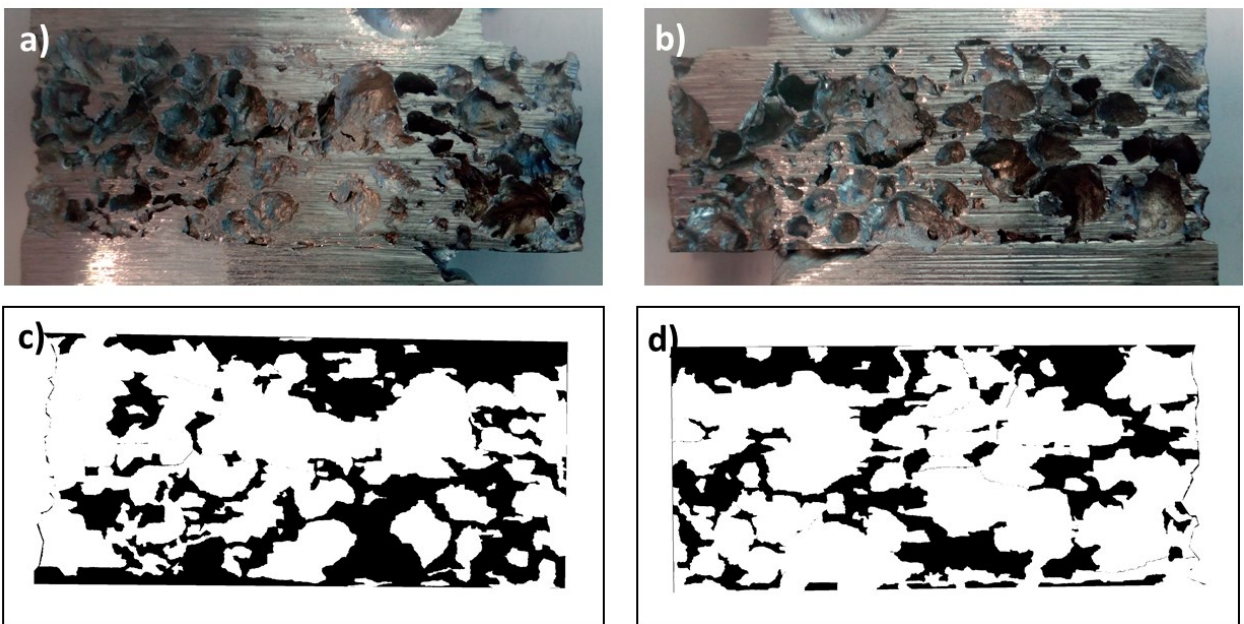


Figure 84: the residual porosity of 4S4 is 44.2%

The analysis of the results are compared in *Table 13*:

<i>Foam in casting</i>	<i>Residual porosity(crosscut section)</i>	<i>Residual porosity(transverse section)</i>
3S1	36.6%	52.1%
4S1	69.8%	30.0%
3S4	56.8%	42.8%
4S4	44.2%	40.1%

Table 13: Porosity comparison of foam in casting

From the table, it is clear that, except 4S4 foam in casting, the other 3 samples all have some infiltration issues since the residual porosity of crosscut section is different from the residual porosity of transverse section.

#### 4.2.4 SDAS measurements results

The secondary dendrite arm spacing can be found mostly in dense metal or denser zones in the foam. In this case, it can be found either in first 2 zones or in last 2 foams in casting. Some examples of the SDAS measurements are reported in Figure 85.

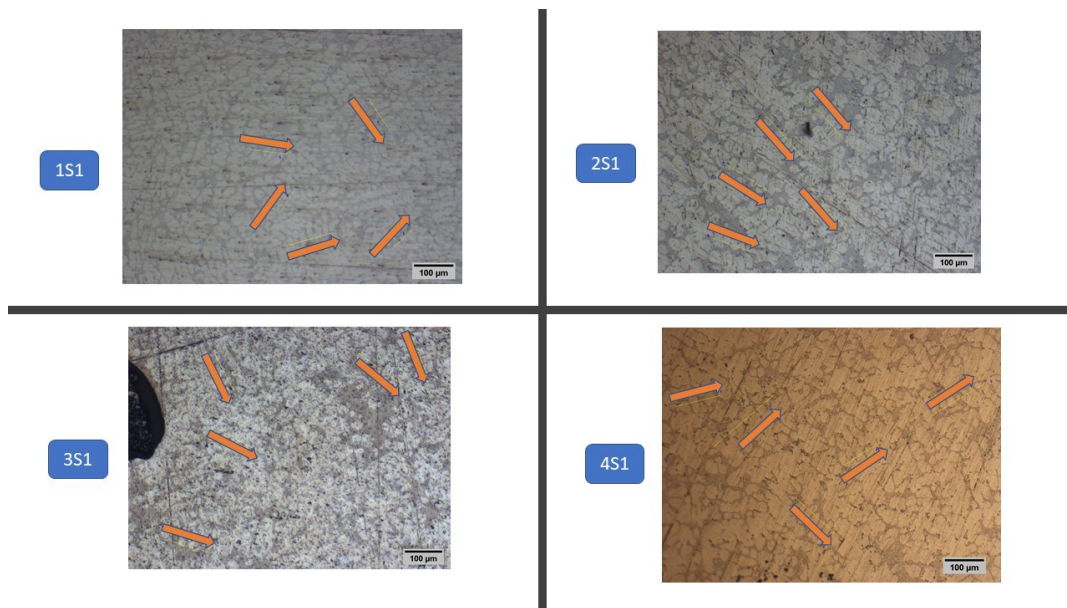


Figure 85: S1 SDAS measurements example

Results are summarized and compared in Table 13:

<i>S1 foam in casting</i>	<i>Mean ± standard deviation(μm)</i>
1S1	33.0 ± 5.4
2S1	29.9 ± 4.9
3S1	33.1 ± 5.6
4S1	30.1 ± 3.8

Table 14: S1 SDAS measurements

For S3 foam in casting, the step is same with S1, an example is reported in Figure 86.

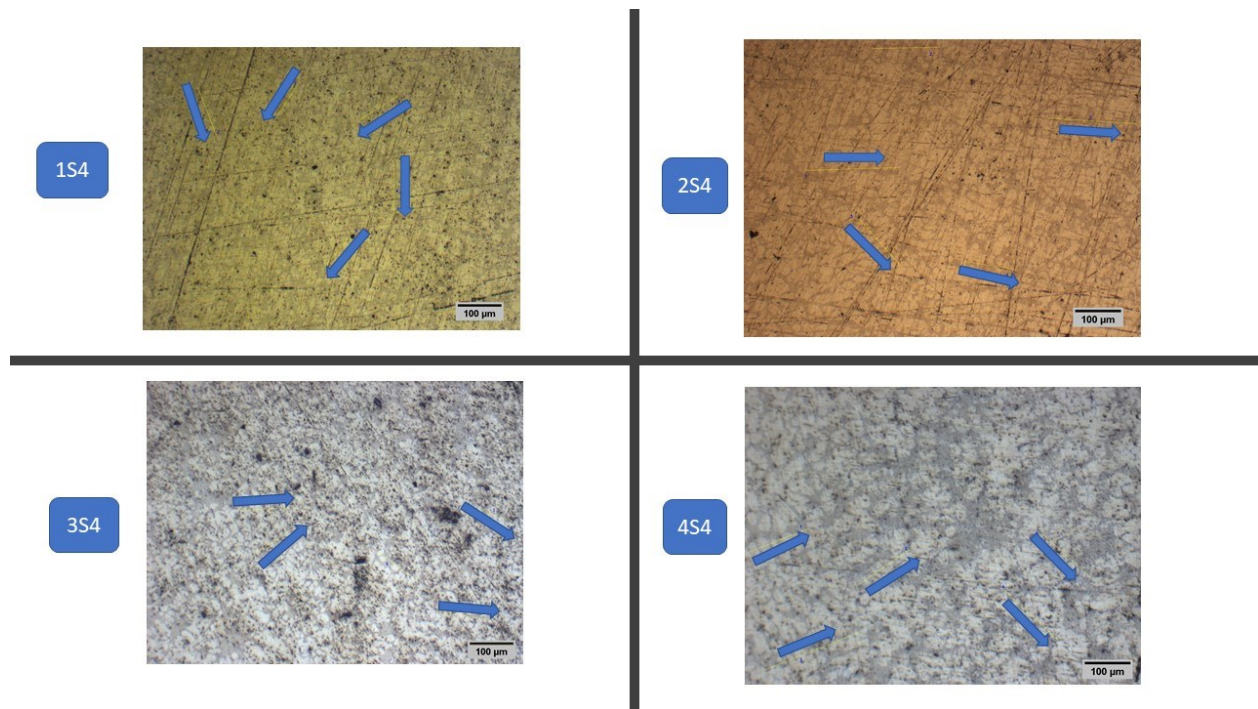


Figure 86: S4 foam in casting measurements example

Results are summarized in Table 14:

<i>S4 foam in casting</i>	<i>Mean ± standard deviation(µm)</i>
1S4	23.4 ± 3.3
2S4	26.3 ± 3.6
3S4	27.0 ± 4.1
4S4	30.0 ± 3.8

Table 15: S4 foam in casting SDAS measurements

Zone 1 of the samples has smaller thickness compared to that of zone 2, so it has a higher cooling rate. With the higher cooling rate of the zone, the SDAS should be lower than that of zone 2. Comparing SDAS of zone 1 and zone 2, the behavior of SDAS can be related to cooling rate. And the higher cooling rate results in lower SDAS results.

In case of zone 3 and zone 4, the behavior is complex since the foam is inserted in it. The foam can affect the casting configuration and the cooling rate so the SDAS not only depends on the thickness but also on the foam presence, then the SDAS trend can not be confirmed.

## 4.3 Coated foams

### 4.3.1 Macro picture of foams



*Figure 87: (from left to right) Uncoated foam, Zirconia coated foam and alumina coated foam*

The macroscopic appearance of the IFAM-FOAMINAL foams (uncoated and coated) is shown in *Figure 87*. From the outside view of 3 different foam core, the outside color is obviously different. The uncoated aluminum core is metal color, while the other 2 foam core is more or less white color.  $ZrO_2$  coated foam has less white than  $Al_2O_3$  coated foam core.

### **4.3.2 Skin and wall thickness**

#### **4.3.2.1 Uncoated Aluminum Foam core**

An example of the measurements for the uncoated foam is reported in *Figure 87*

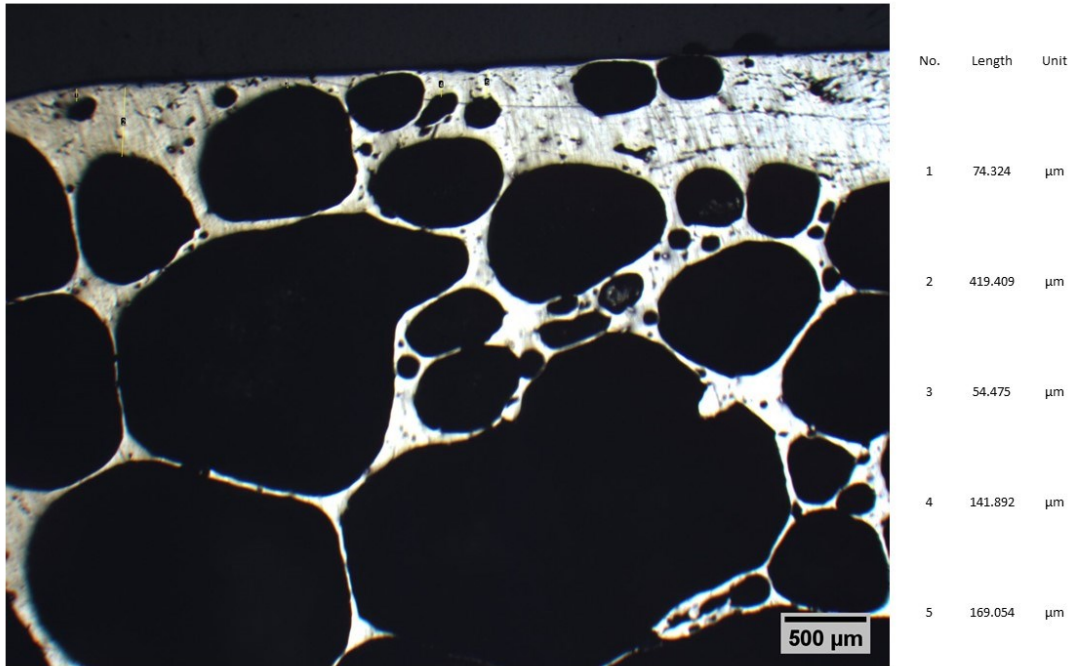


Figure 88: An example of skin thickness measurements for uncoated foam core

After more than 60 measurements, the average and standard deviation of uncoated foam skin thickness is obtained (Figure 88):

$$\text{Uncoated foam skin thickness} = 296.9 \pm 256.1 [\mu\text{m}]$$

An example of wall thickness measurements for uncoated foam core can be reported in Figure 89.

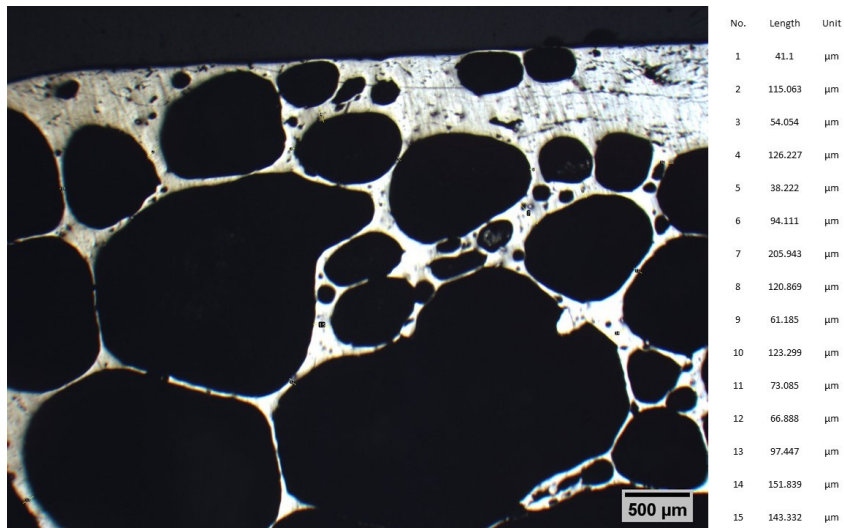


Figure 89: An example of wall thickness measurements for uncoated foam core

The average value and standard deviation can be obtained:

$$\text{Uncoated foam wall thickness} = 104.6 \pm 72.8 [\mu\text{m}]$$

#### 4.3.2.2 Zirconia coated Aluminum Foam core

An example of the measurements for the zirconia coated foam is reported in *Figure 90-91*.

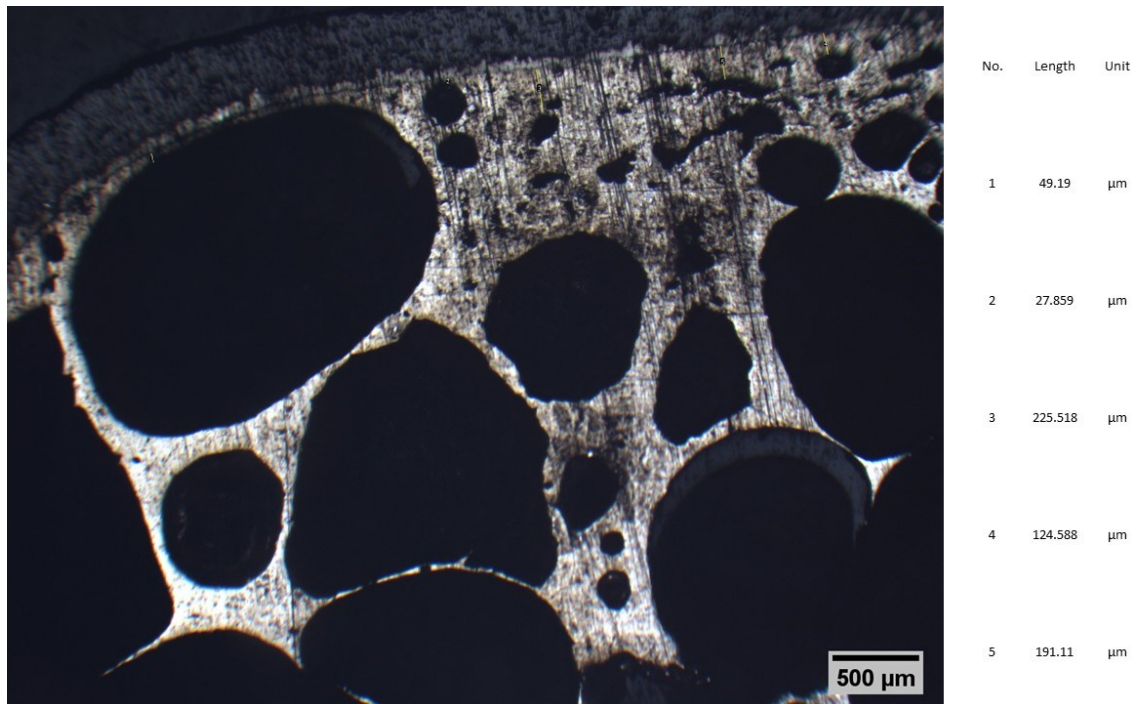


*Figure 90: An example of skin measurements for zirconia coated foam core*

Then the average result and standard deviation can be obtained after several measurements:

$$\text{Zirconia coated foam skin thickness} = 141.9 \pm 94.6 [\mu\text{m}]$$

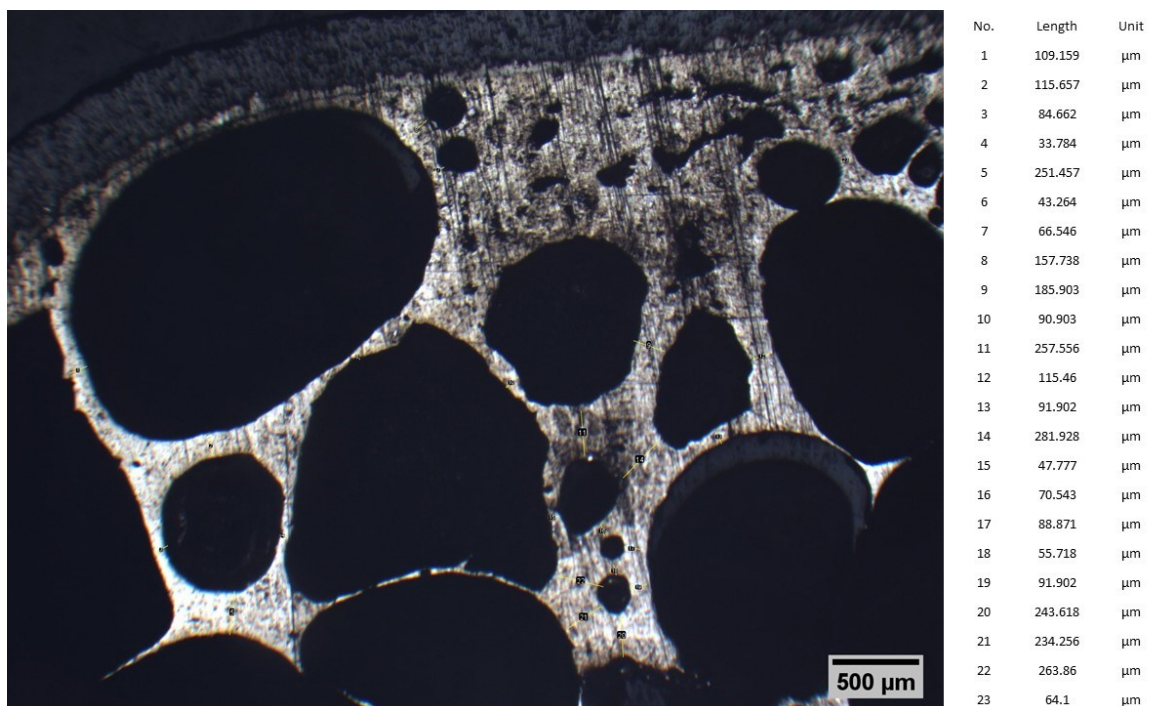


*Figure 91: An example of wall thickness measurements for zirconia foam core*

Then the result after several measurements is found:

$$\text{Zirconia foam wall thickness} = 111.7 \pm 82.7 [\mu\text{m}]$$

#### 4.3.2.3 Alumina coated Aluminum Foam core

An example of the measurements for the alumina coated foam is reported in *Figure 92*

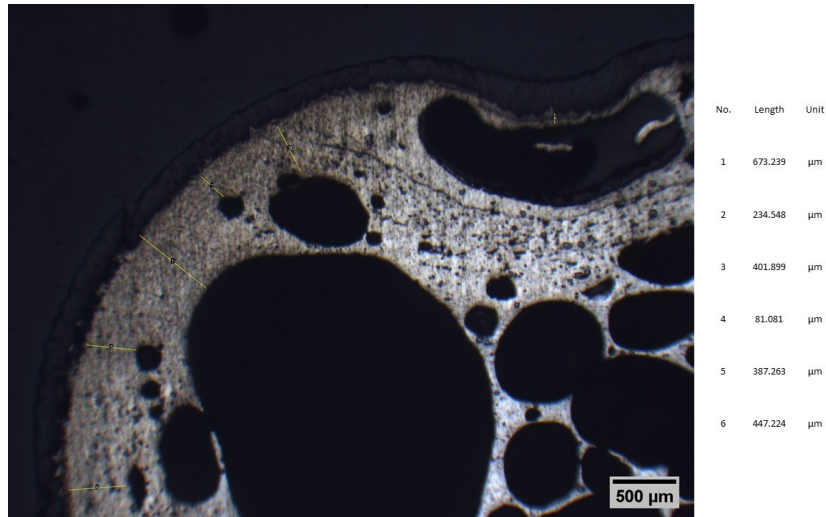


*Figure 92: An example of skin measurements for alumina coated foam core*

The average value and standard deviation results are:

$$\text{Alumina coated foam skin thickness} = 207.1 \pm 161.3 [\mu\text{m}]$$

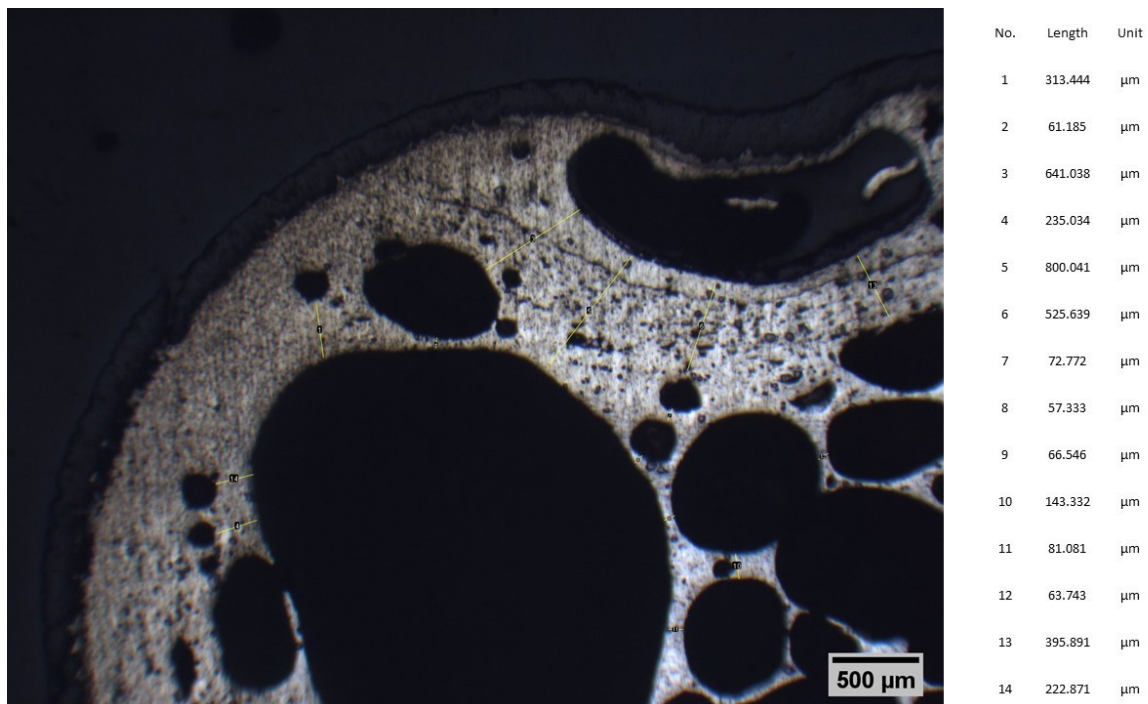


*Figure 93: An example of wall thickness measurements for alumina coated foam core*

The average value and standard deviation are:

$$\text{Alumina coated foam wall thickness} = 102.0 \pm 74.8 [\mu\text{m}]$$

A comparison table for different type of foam core is made:

<i>Foams</i>	<i>Skin thickness</i> [ $\mu\text{m}$ ]	<i>Wall thickness</i> [ $\mu\text{m}$ ]
<i>Uncoated foam</i>	<i>296.9 ± 256.1</i>	<i>104.7 ± 72.7</i>
<i>Zirconia coated foam</i>	<i>141.9 ± 94.6</i>	<i>111.7 ± 82.6</i>
<i>Alumina coated foam</i>	<i>207.1 ± 161.3</i>	<i>102.0 ± 74.7</i>

*Table 16: Comparison of each foam core thickness*

The data present an extremely high dispersion (the standard deviation is in the order of magnitude of the measurement).

Coating thickness for coated foam is reported in *Table 17*:

<i>Coating thickness</i>	<i>Mean ± standard deviation</i> ( $\mu\text{m}$ )
<i>Zirconia coated foam</i>	<i>290.6 ± 114.0</i>
<i>Alumina coated foam</i>	<i>250.6 ± 66.8</i>

*Table 17: Coating thickness*

The thickness is the one of whole coating total. FESEM-EDS analysis (section 4.3.3) will highlight the division of the coating in two different zones with different chemical composition.

### 4.3.3 FESEM-EDS

For each foam core, the EDS results are divided into 2 part: a top view analysis and a section view analysis.

Top view analysis is used to analyze the top composition of the surface which is main the coating. And section view analysis is used to analyze the foam core composition as well as the eventual presence of different coating layers

#### 4.3.3.1 Uncoated foam EDS

For uncoated foam, the composition of top and section are the same since it is not coated by other material except itself.

**Electron Image 1**

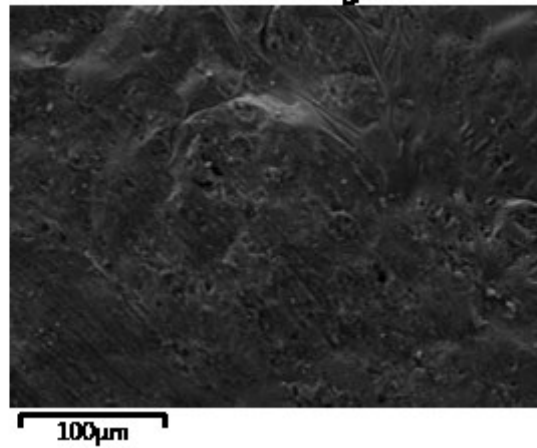


Figure 94: Chosen zone on uncoated foam

In Figure 94 a SEM image is obtained to show the picture on the foam.

An example of EDS spectrum is reported in Figure 95:

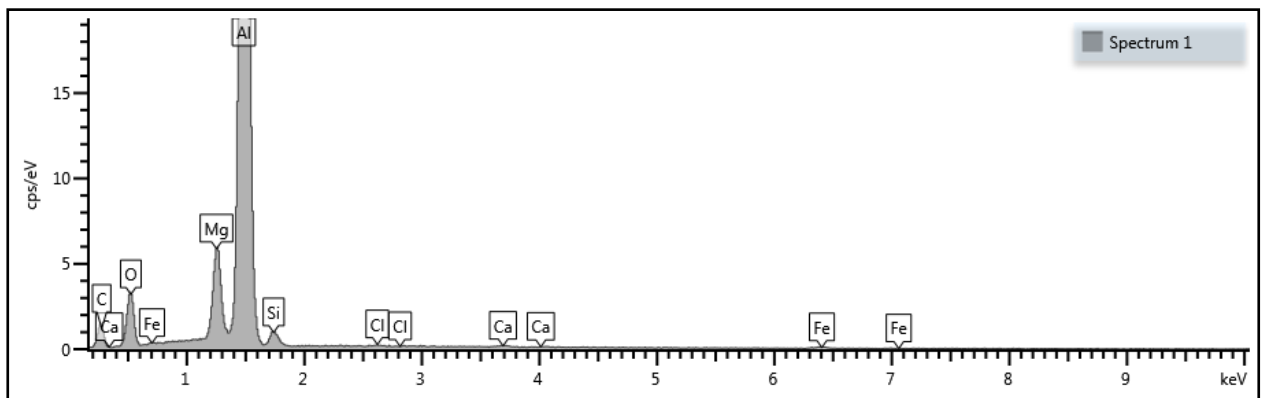


Figure 95: Uncoated foam spectrum

After several zones analyzed, the average weight percentage and standard deviation for different elements are concluded in the Table 18:

Uncoated foam elements	Mean value $\pm$ deviation [%]
C	6.4 $\pm$ 3.3
O	52.7 $\pm$ 4.4
Mg	2.3 $\pm$ 1.9
Al	37.5 $\pm$ 5.5
Si	0.5 $\pm$ 0.2
Ca	0.1 $\pm$ 0.04
Fe	0.3 $\pm$ 0.3
Cl	0.06 $\pm$ 0

Table 18: Composition of uncoated foam core

#### 4.3.3.2 Zirconia coated foam EDS

For Zirconia coated foam, since it is coated by other material, it has to be divided into 2 aspects: top view and section view.

Top view:

Firstly is to choose a zone in the top coating(*Figure 96*)

The top view of the coating highlight the typical morphology of plasma-sprayed coatings.

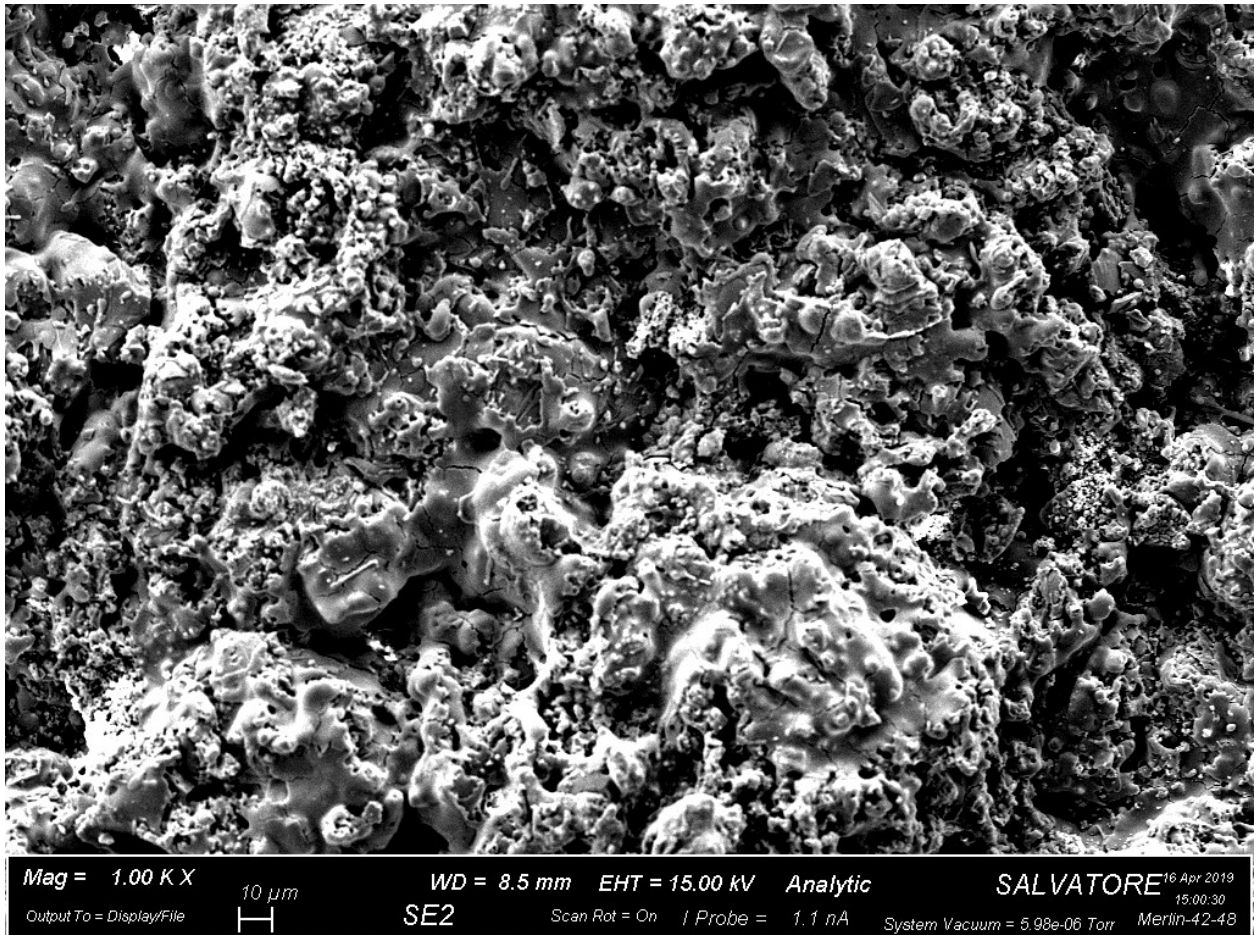


*Figure 96: An top view of zirconia foam under 1K magnification*

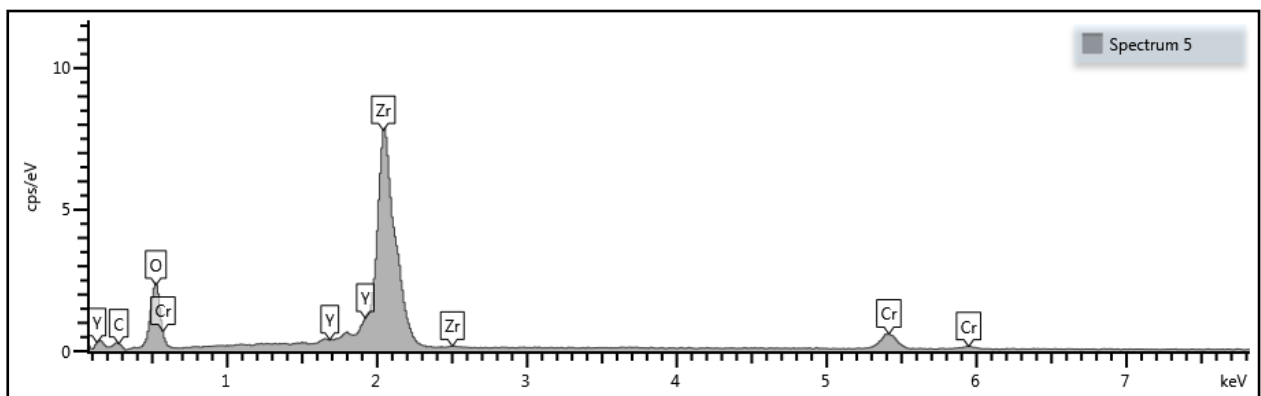


*Figure 97: Top view spectrum of zirconia foam*

Figure 97 reports an example of EDS spectrum on these samples and Table 19 the quantitative calculation of the chemical composition. The analysis indicates that the coating is mainly Yttria-stabilized zirconia.

Zirconia coated foam top view elements	Mean $\pm$ standard deviation[%]
C	8.9 $\pm$ 3.3
O	41.0 $\pm$ 9.0
Y (Yttrium)	3.6 $\pm$ 0.4
Zr	46.3 $\pm$ 2.7

In section view:

Coated foams are different from uncoated foams. It has to be considered into 2 parts to think: one is the same as uncoated foam, inside zone is chosen; the other one is to choose the zone on the boundary. The reason to analyze the boundary is that the boundary is not connected to the foam core, and to solve the question, the very first step is to analyze the chemical composition differences in the boundary or in the foam but near the boundary.

For the foam core analysis, zone chosen is reported in Figure 98:

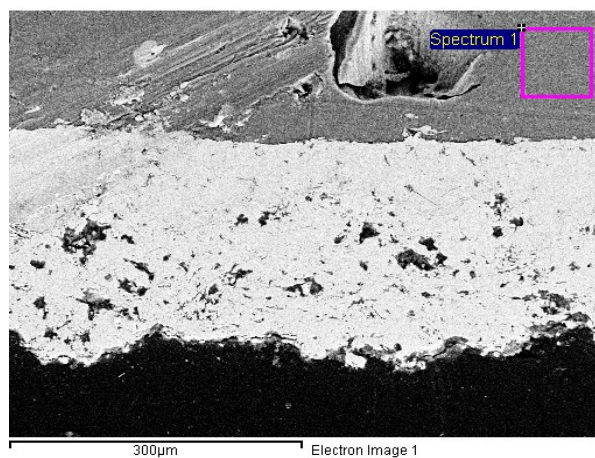


Figure 98: Zone chosen inside the foam

And the spectrum of zirconia coated foam core is obtained(Figure 99):

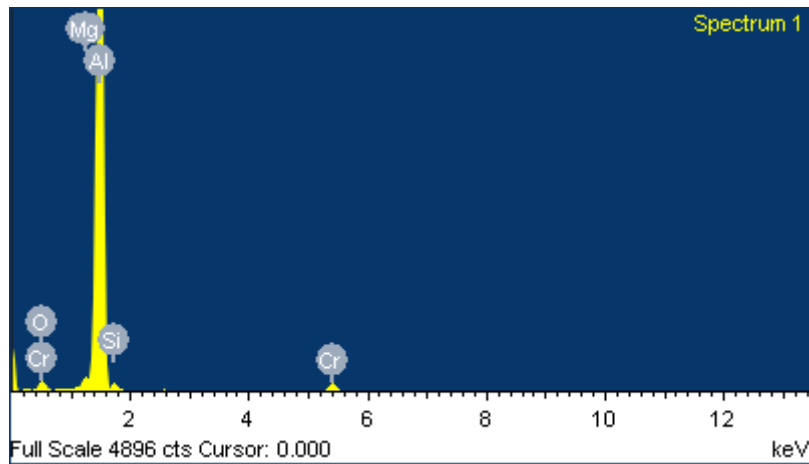


Figure 99: Spectrum of zirconia coated foam core

After several zones analyzing, a table of weight percentage for different elements is listed (Table 20):

Element	Weight%
O	7.9
Mg	0.8
Al	83.6
Si	2.9
Cr	4.7

Table 20: Zirconia coated foam core elements

For the boundary layer zones analysis

3 zones have been chosen to analyze:

- A. Zone inside the foam but near the boundary layer
- B. Zone inside the boundary layer but near the foam
- C. Zone inside the boundary layer but far away from foam

A scheme can be made to explain the 3 zones (Figure 100):

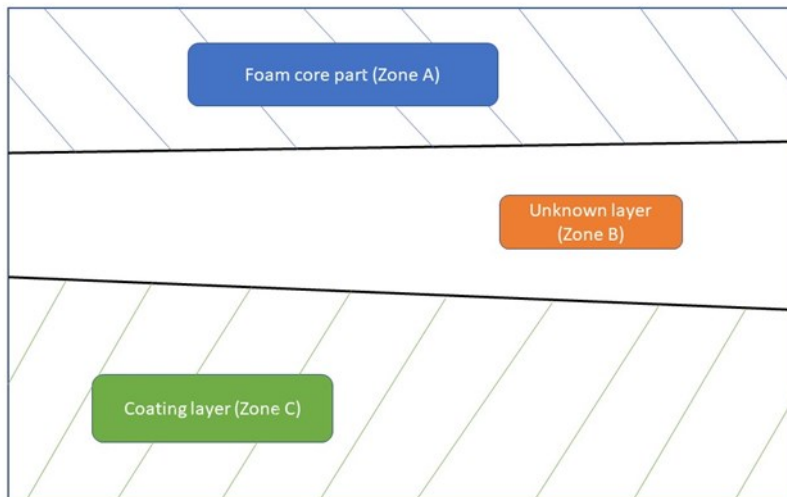


Figure 100: A scheme of zones analyzed

A. Zone inside the foam but near the boundary layer (Figure 101)

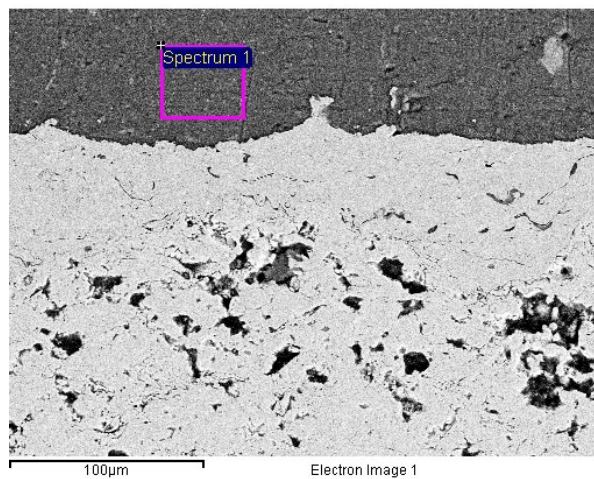


Figure 101: Zone chosen near the boundary layer but inside the foam

And the spectrum is shown(Figure 102):

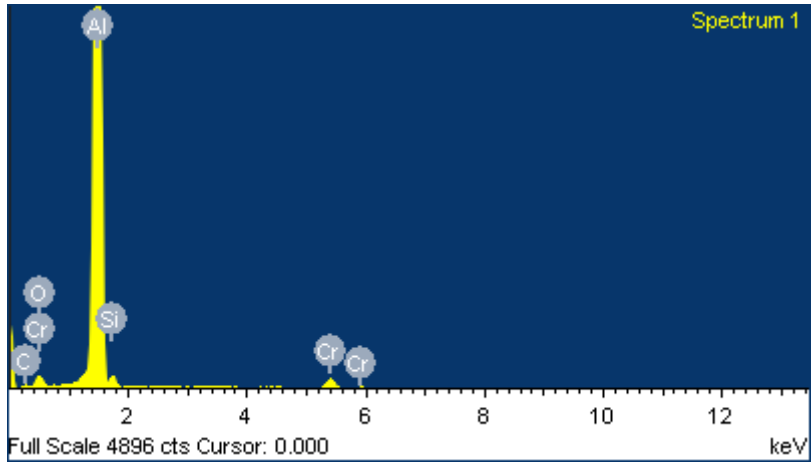


Figure 102: Spectrum for zone A of zirconia coated foam

B. Zone inside the boundary but near the foam (Figure 103)

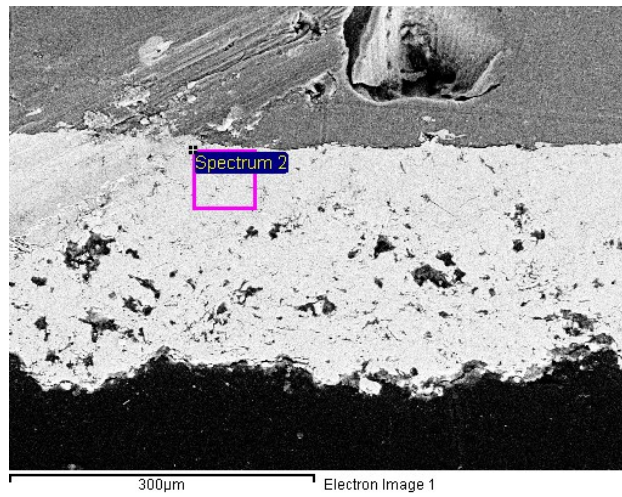


Figure 103: B zone of zirconia coated foam

And the obtained spectrum(Figure 104):

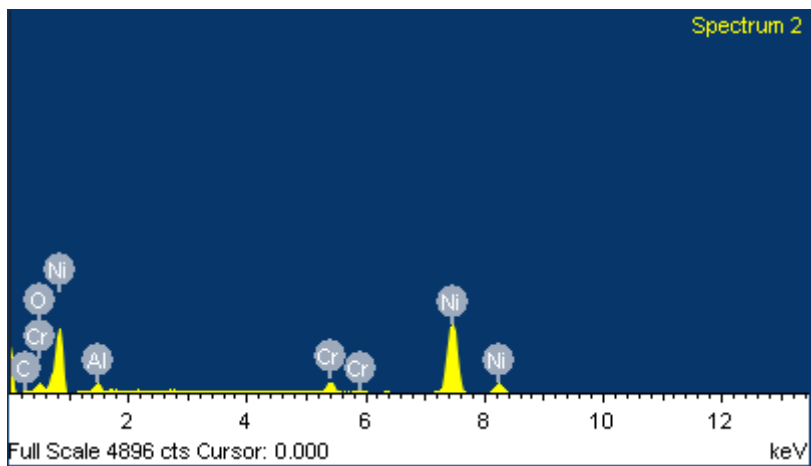


Figure 104: B zone spectrum of zirconia coated foam

C. Zone inside the boundary layer but far away from the foam(Figure 105)

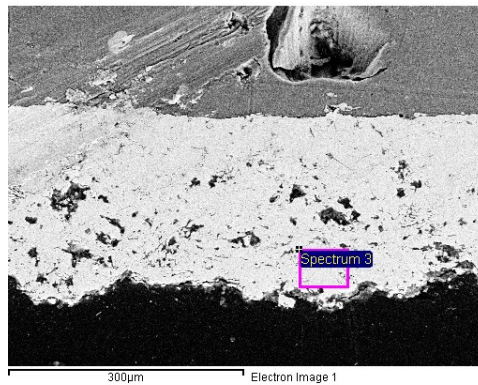


Figure 105: C zone of zirconia coated foam

And the spectrum(Figure 106):

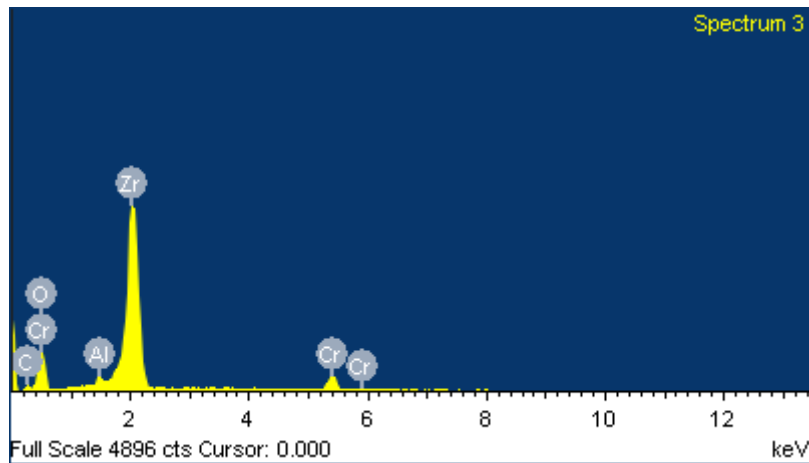


Figure 106: C zone spectrum of zirconia coated foam

A comparison table can be concluded for different elements in 3 zones(Table 21):

Element	Weight%		
	Zone 1	Zone 2	Zone 3
C		3.85	10.28
O	7.94	5.61	32.85
Al	83.55	4.12	0.89
Cr	4.67	5.36	5.53
Mg	0.89		
Si	2.95		
Zr			50.45
Fe		0.69	
Ni		80.38	

Table 21: Zirconia coated foam element

EDS analysis evidenced the presence of a Nickel interlayer in direct contact with foam covered by a zirconia layer on the top surface.

#### 4.3.3.3 Alumina coated foam EDS

Firstly is to analyze the top view of the coating in *Figure 107*:

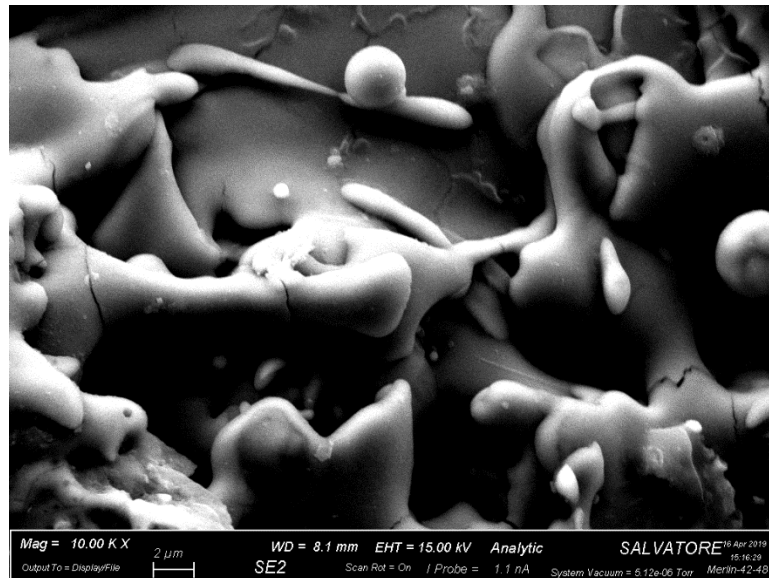


Figure 107: Top view of alumina coating

Then the spectrum is obtained in *Figure 108*:

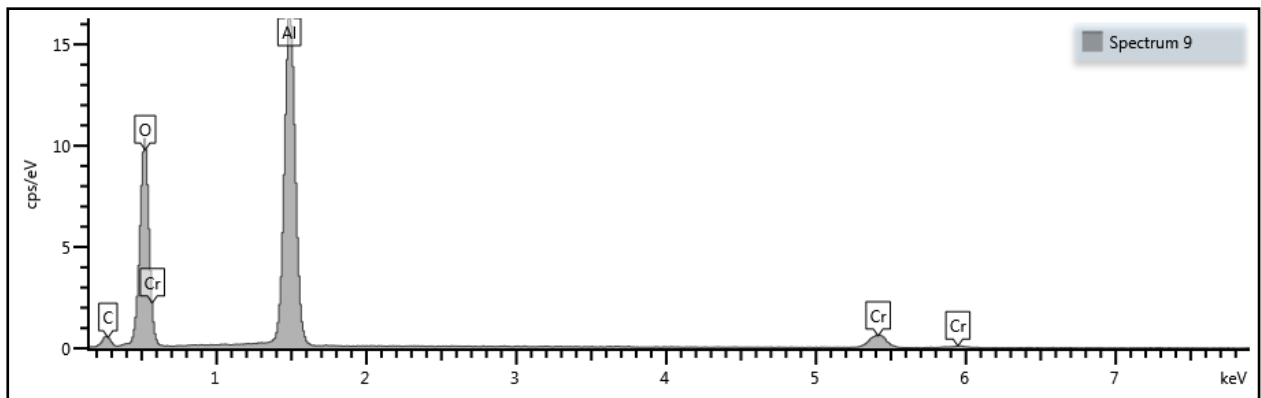


Figure 108: Top view spectrum for alumina foam core

A *Table 22* to control the element of the top view of alumina coated foam core:

Alumina coated foam top view element	Mean $\pm$ standard deviation[%]
C	9.4 $\pm$ 0.9
O	55.9 $\pm$ 2.5
Al	34.5 $\pm$ 1.1

Table 22: Top view element for alumina coated foam

For section view:

As the same as zirconia coated foam, the analysis for alumina coated foam is also divided into 2 parts: one inside the foam; while the other one inside the boundary layer.

But the different thing is, between the alumina coat and the foam core, there is another inter layer is found. Since the layer is unknown, the very first step is also to analyze its chemical composition.

#### 4.3.3.2 For the analysis of the boundary and unknown layer

Here 3 zones are chosen to analyze:

- A. Zone inside the foam near the unknown layer
- B. Zone inside the unknown layer
- C. Zone inside the coating

A scheme of the layers is reported in *Figure 109*:

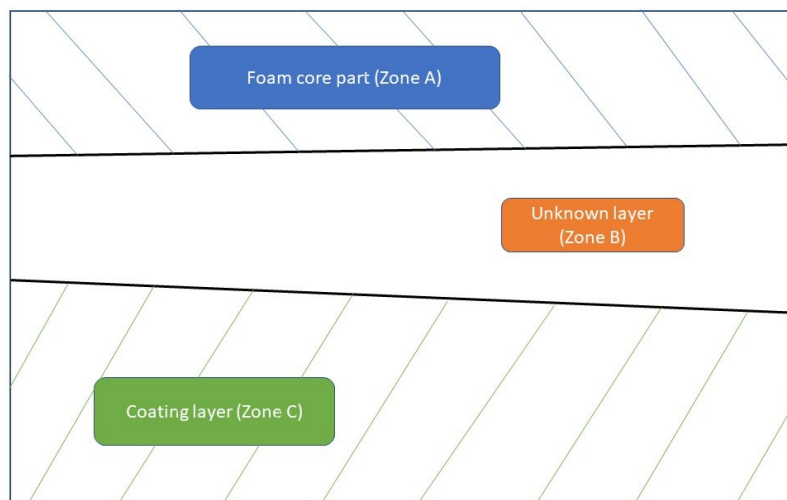


*Figure 109: An example scheme to explain different layers*

#### A. For the zone inside the foam near the unknown layer

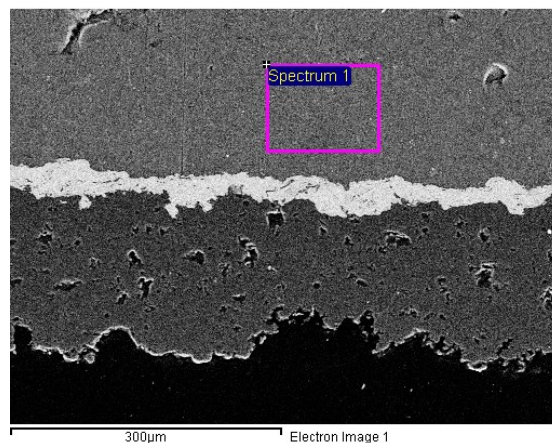


*Figure 110: A zone chosen of alumina coated foam*

The spectrum is obtained:

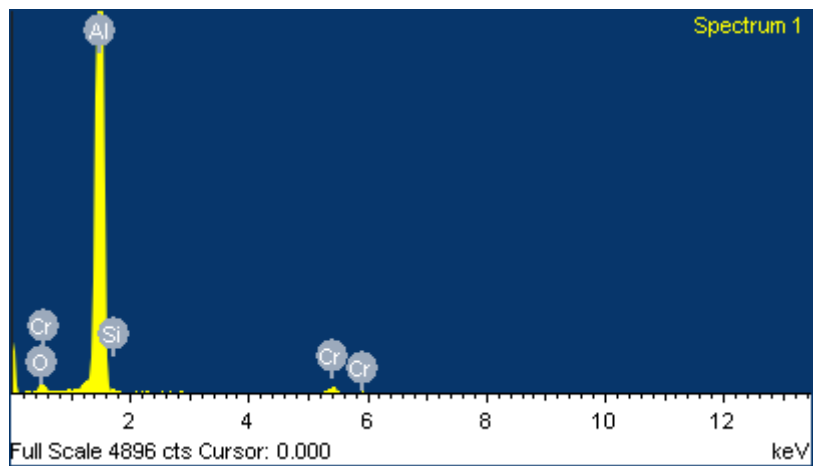


Figure 111: A zone spectrum of alumina coated foam

B. Zone inside the unknown layer

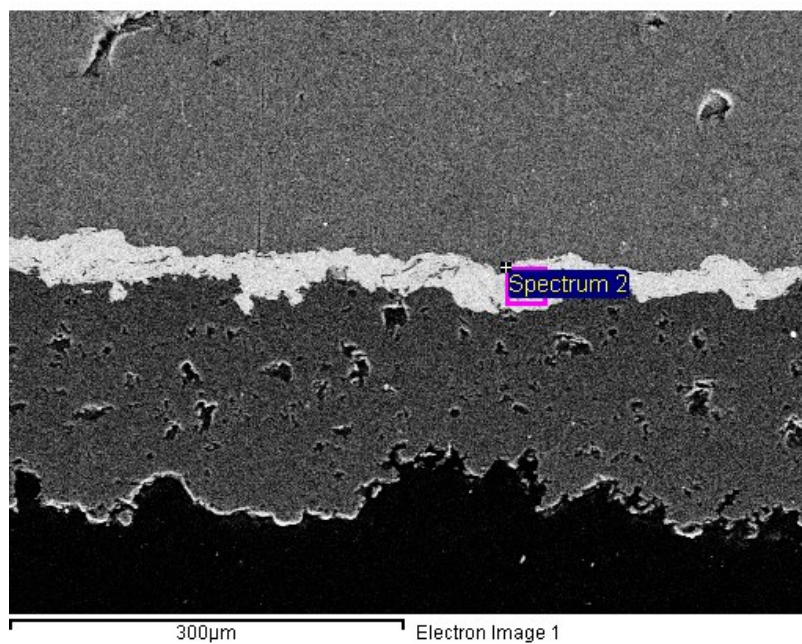


Figure 112: B zone chosen of alumina coated foam

Then the element spectrum can be obtained:

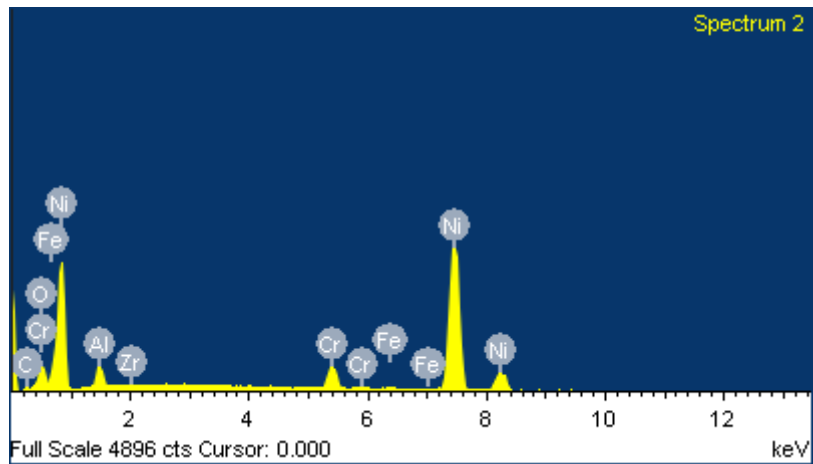


Figure 113: B zone spectrum of alumina coated foam

It seems that the unknown layer is kind of a chemical composition of Nickel. The element weight percentage shows high value for Ni element.

C. Zone inside the coating

The last zone chosen is inside the alumina coating.

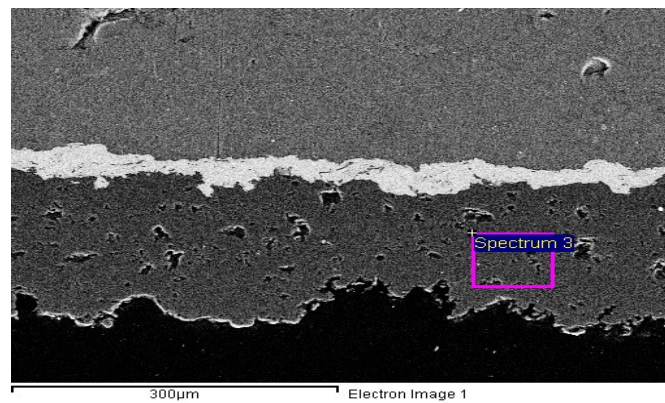


Figure 114: C zone of alumina coated foam

Then the spectrum is listed:

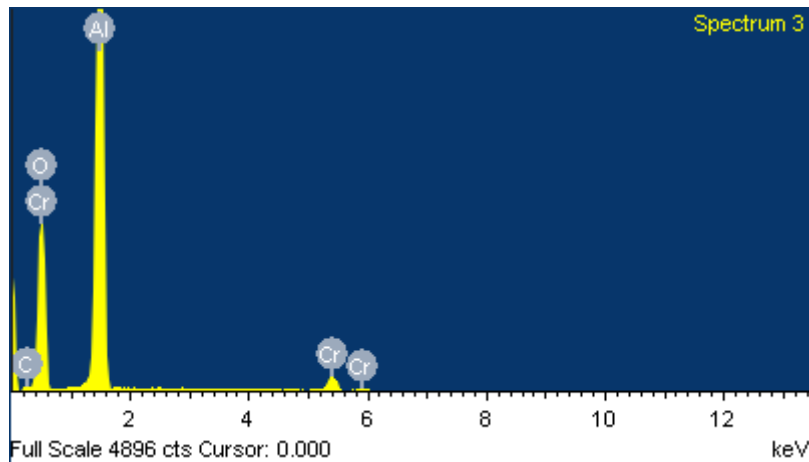


Figure 115: C zone spectrum of alumina coated foam

In the last a comparison table of different elements weight percentage is obtained:

Element	Weight%		
	Zone 1	Zone 2	Zone 3
C			5.34
O	5.67	4.21	47.61
Al	89.31	3.86	43.42
Cr	3.71	4.93	3.63
Si	1.32		
Ni		87.01	

Table 23: Alumina coated foam element

In conclusion also the alumina coating presents a first Nickel interlayer (in contact with the foam surface) covered by an alumina layer. This interlayer seems thinner than the one observed on the zirconia coated foam.

## Chapter 5

### Conclusions

In the present research different Al foams have been characterized. The first set of foams was constituted by Cymat type foams. The 3 foams tested were different for their porosity (pore dimensions and amount of pores). They were fully characterized by means of optical microscopy, compression test and scanning electron microscopy. These foams were used as cores in casting experiments. It was found that it is possible to obtain cast object with foam cores. Depending on the foam characteristics and on the casting parameters different degree of residual porosity and core-shell bonding were obtained. Finally IFAM-FOAMINAL type foams inserts with or without ceramic coatings (alumina or zirconia) were characterized as possible improvement to be used as cores in future casting experiments.

## References

- [1] 2017 Boegger Industrial Limited Website: [www.filter-elements.org](http://www.filter-elements.org)
- [2] 2000 Andrew Kennedy Porous Metals and Metal Foams Made from Powders
- [3] H.Berek, U.ballaschk, C.G.Anezirsis, Katharina Losch, K.Schladitz, The correlation of local deformation and stress-assisted local phase transformations in MMC foams
- [4] John Banhart, Manufacture, characterization and application of cellular metals and metal foams
- [5] Wikipedia <https://en.wikipedia.org>
- [6] Xiaopeng Shi, Yinggang Miao, Shuangyan Liu, Guoxin Lu, Indentation of aluminum foam at low velocity
- [7] Ann. Castro Global foamed metal market insights 2019-2024 : ERG Aerospace Group, Cymat Technologies Ltd, Admiatis Ltd
- [8] Stena Aluminium [www.stenaaluminium.com](http://www.stenaaluminium.com)
- [9] 6013-T4 Aluminum [www.makeitfrom.com](http://www.makeitfrom.com)
- [10] Martin Nosko, Jaroslav Kovacic Sound Absorption Ability of Aluminium Foams
- [11] Branko Bauer, Slobodan Kralj, Matija Basic, Production and application of metal foams in casting technology
- [12] Optical microscope from Alibaba.com
- [13] Ravi Sekhar, Tejinder Paul Singh Mechanisms in turning of metal matrix composites: A review
- [14] L.Y.Zhang, Y.H. Jiang, Z. ma, S.F. Shan, Effect of cooling rate on solidified microstructure and mechanical properties of aliminium -A356 alloy